TRG4580077 ดร. อติพงศ์ นันทพันธุ์

สกว
TRF

FINAL REPORT

Thermal Performance Testing of Finned Tube Producing in Thailand

By

Dr. Atipoang Nuntaphan

Prof. Dr. Tanongkiat Kiatsiriroat

June 2004

Contact No. TRG4580077

Thermal Performance Testing of Finned Tube Producing in Thailand

Researchers	Institutes
Dr. Atipoang Nuntaphan	Electricity Generating Authority of Thailand
Prof. Dr. Tanongkiat Kiatsiriroat	Chiang Mai University

Sponsored by the Thailand Research Fund

ABSTRACT

This research work studies the thermal performance of finned tube heat exchanger which is locally made. The crimped spiral finned tube is selected for this study. This work can be divided into two parts. The first part studies the performance of crimped spiral finned tube under the dry condition and the second part studies the performance under the dehumidifying condition.

A total of 23 cross flow heat exchangers having crimped spiral configurations is studied. The effect of tube diameter, fin spacing, fin height, transverse tube pitch, and tube arrangements are examined. From the experiment, it is found that these parameters play important roles not only on the heat transfer performance but also on the frictional characteristic. Moreover it is found that, in case of the dry surface heat exchanger, the thermal performance and the air stream pressure drop are slightly higher lower than the wet surface.

The empirical correlations for evaluating the heat transfer coefficient and pressure drop of both cases are also developed in this work. It is also found that the correlations can predict the experimental data quite well.

บทคัดย่อ

งานวิจัยนี้ศึกษาสมรรถนะเชิงความร้อนของท่อติดครีบที่ผลิตในประเทศ โดยท่อครีบที่ศึกษาจะเป็นท่อครีบแบบเกลียวชนิดขอบหยัก งานวิจัยนี้แบ่งออกเป็น 2 ส่วน โดยงานวิจัยส่วนแรกจะศึกษาสมรรถนะของกลุ่มท่อครีบในกรณีที่ไม่มีการควบแน่นของไอน้ำในอากาศบนพื้นผิวท่อ และงานวิจัยส่วนที่สองจะศึกษาในกรณีของมีการควบแน่นของไอน้ำในบรรยากาศบนพื้นผิวของท่อครีบ

งานวิจัยนี้ได้ศึกษาเครื่องแลกเปลี่ยนความร้อนแบบไหลตามขาวงที่ใช้ท่อครีบแบบเกลียวชนิดขอบหยักจำนวน 23 แบบ โดยได้ศึกษาผลของขนาดท่อ ระยะห่างระหว่างครีบ ความสูงของครีบ และการจัดเรียงท่อ ซึ่งจากการทดลองพบว่าพารามิเตอร์เหล่านี้ไม่เพียงแต่ส่งผลต่อสมรรถนะการถ่ายเทความร้อนเท่านั้น ยังส่งผลต่อความต้านทานการไหลของอากาศผ่านกลุ่มท่อด้วย และนอกจากนี้ยังพบว่าเครื่องแลกเปลี่ยนที่ไม่มีการควบแน่นของไอน้ำบนผิวท่อมีสมรรถนะเชิงความร้อนสูงกว่า และค่าความดันอากาศตกคร่อมกลุ่มท่อต่ำกว่าเครื่องแลกเปลี่ยนความร้อนที่มีการควบแน่นของไอน้ำบนพื้นผิวเล็กน้อย

งานวิจัยนี้ยังได้พัฒนาสมการสหสัมพันธ์เพื่อใช้คำนวณค่าสัมประสิทธิ์การถ่านเทความร้อนและค่าความดันอากาศตกคร่อมกลุ่มท่อจากงานวิจัยทั้งสองส่วน ซึ่งสมการที่พัฒนาขึ้นสามารถใช้ทำนายผลการทดลองได้เป็นอย่างดี

ACKNOWLEDGEMENTS

The author wishes to express his gratitude and appreciation to his mentor, Professor Dr. Tanongkiat Kiatsiriroat for his valuable guidance and kindly suggestion throughout the research work. A sincere thanks is extended to Dr. Chi-Chuan Wang for his helpful and gives useful comment entire the period of this work.

Acknowledgement is due to the Thailand Research Fund for awarding the scholarship for this work. The author is grateful thank to the Electricity Generating Authority of Thailand for all facilities and accommodations.

Finally, the author wishes to thank to all guidance and encouragement of his parents, which made this work both possible and worthwhile.

CONTENT

LIST OF FIGURES

Figure **Page**

LIST OF TABLES

NOMENCLATURE

A	area (m^2)
A_{min}	minimum free flow area (m^2)
A_o	total surface area (m^2)
$A_{p,i}$	inside surface area of tube (m^2)
$A_{p,m}$	mean surface area of tube (m^2)
$A_{p,o}$	outside surface area of tube (m^2)
b'_p	slope of straight line between the outside and inside tube wall temperature
b'_r	slope of the air saturation curved at the mean coolant temperature
$b'_{w,m}$	slope of the air saturation curved at the mean water film temperature of the external surface
$b'_{w,p}$	slope of the air saturation curve at the mean water film temperature of the primary surface
Cp	specific heat (J/kgK)
$C_{p,a}$	moist air specific heat at constant pressure (J/kgK)
$C_{p,w}$	water specific heat at coolant pressure (J/kgK)
d_f	outside diameter of finned tube (m)
d_i	tube inside diameter (m)
d_o	tube outside diameter (m)
f	friction factor
f_h	fin height (m)
f_i	in-tube friction factor of water
f_s	fin spacing (m)
f_t	fin thickness (m)
F	correction factor
G_c	mass flux of air base on minimum flow area (kg/sm^2)
G_{max}	maximum mass velocity based on minimum flow area

h heat transfer coefficient (W/m^{2}K)

$h_{c,o}$ sensible heat transfer coefficient for wet coil (W/m^{2}K)

h_i inside heat transfer coefficient (W/m^{2}K)

$h_{o,w}$ total heat transfer coefficient for wet external fin (W/m^{2}K)

I_o modified Bessel function solution of the first kind, order 0

I_1 modified Bessel function solution of the first kind, order 1

i air enthalpy (J/kg)

$i_{a,in}$ inlet air enthalpy (J/kg)

$i_{a,out}$ outlet air enthalpy (J/kg)

$i_{r,m}$ saturated air enthalpy at the mean refrigerant temperature (J/kg)

$i_{r,in}$ saturated air enthalpy at the inlet of refrigerant temperature (J/kg)

$i_{r,out}$ saturated air enthalpy at the outlet of refrigerant temperature (J/kg)

$i_{s,p,i,m}$ saturated air enthalpy at the mean inside tube wall temperature (J/kg)

$i_{s,p,o,m}$ saturated air enthalpy at the mean outside tube wall temperature (J/kg)

$i_{s,w,m}$ saturated air enthalpy at the mean water film temperature of the external surface (J/kg)

Δi_m mean enthalpy difference (J/kg)

j the Colburn factor

K_0 modified Bessel function solution of the second kind, order 0

K_1 modified Bessel function solution of the second kind, order 1

k_f thermal conductivity of fin (W/mK)

k_i thermal conductivity of tube side fluid (W/mK)

k_p thermal conductivity of tube (W/mK)

k_w thermal conductivity of water (W/mK)

L length (m)

m parameter

$\dot{m}_a$ air mass flow rate (kg/s)

$\dot{m}_w$ water mass flow rate (kg/s)

n_r	number of tube row
n_t	number of tube in each row
NTU	number of transfer unit
Nu	Nusselt number
P	pressure (Pa)
ΔP	pressure drop (Pa)
Pr	Prandtl number
Q	heat transfer rate (W)
Q_{avg}	mathematical average heat transfer rate (W)
Q_a	air-side heat transfer rate (W)
Q_w	water side heat transfer rate (W)
r_i	distance from the center of the tube to the fin base (m)
r_o	distance from the center of the tube to the fin tip (m)
Re_{Di}	Reynolds number base on inside diameter of bare tube
Re_D	Reynolds number base on outside diameter of bare tube
S_l	longitudinal tube pitch (m)
S_t	transverse tube pitch (m)
S_{min}	minimum flow area (m^2)
T	temperature (°C)
$T_{w,m}$	mean temperature of water film (°C)
$T_{w,in}$	water temperature of at the tube inlet (°C)
$T_{w,out}$	water temperature of at the tube outlet (°C)
$T_{p,i,m}$	mean temperature of the inner tube wall (°C)
$T_{p,o,m}$	mean temperature of the outer tube wall (°C)
$T_{r,m}$	mean temperature of refrigerant coolant (°C)
U	overall heat transfer coefficient (W/m^2K)
$U_{o,w}$	overall heat transfer coefficient (W/m^2K)
V_{max}	maximum velocity (m/s)
x_p	thickness of tube wall (m)

y_w thickness of condensate water film (m)

Greek symbols

ε effectiveness

η efficiency

$\eta_{f,wet}$ wet fin efficiency

μ dynamic viscosity (Pas)

ρ density (kg/m^3)

ρ_i density of inlet air (kg/m^3)

ρ_o density of outlet air (kg/m^3)

ρ_m mean density of air (kg/m^3)

σ contraction ratio of cross sectional area

Subscripts

a Air

b Bare tube

f Fin

i Inlet, tube side

o Outlet, air side

w Water

EXECUTIVE SUMMARY

The thermal performance of locally manufactured finned tube is investigated in this research work. The crimped spiral finned tube, widely used in the industry, is selected in this study. Since there is a very few data about the performance of this finned tube, consequently, this work benefits to the heat exchanger designer.

The method for testing the performance of finned tube follows the ASHRAE and ARI standards. The finned tubes are arranged in a wind tunnel as a cross flow heat exchanger. The water circulates inside the tube while the air stream is flowing outside. By measuring the inlet and the outlet temperatures of the water and the air and also the mass flow rate of both fluids, the performance of the cross flow heat exchanger is evaluated. Note that the performance testing of the heat exchanger covers the heat transfer performance and the frictional characteristic.

This work can be divided into 2 parts. The first part is to study the performances of crimped spiral finned tube under the dry condition and the second part studies the performance under the dehumidifying condition.

For the first part, the approximately 65°C hot water is exchanging heat with the ambient air. While the second part, the cold water is exchanging heat with the approximately 65°C hot air. When the air exchanges heat with the water, the temperature of the air decreases. At the testing condition, the temperature decreasing of the air is designed to lower than the dew point of moisture. Therefore, there is a condensation of moisture from the air stream on the heat exchanger surface. The phenomenon of cooling is more complicated than that of the heating.

For heating and cooling, the heat exchangers have the same dimensions. In this work, the parameters affecting the performance of the heat exchanger are investigated such as tube diameter, fin height, fin spacing and tube arrangement. Note that, the mass flow rate of air is varied in the range of 0.1-0.5 kg/s while the volume flow rate of water is kept constant at 8 l/min. The empirical models for evaluating the heat transfer coefficient and the pressure drop of each part are also developed. The results of the performance testing are as follows:

The heating coil

1. For an inline arrangement, with the rise of tube diameter, the pressure drops increase but the associated heat transfer coefficients decrease with it. The increase of fin height

also gives rise to a considerable increase of the pressure drop but decreases the heat transfer coefficient.

2. For the inline arrangement, the effect of fin spacing on the airside performance varies with the transverse tube pitch. For a larger transverse tube pitch of 71.4 mm, there is an effect on heat transfer coefficient but no detectable influence of the fin spacing on frictional characteristics. It is likely that this phenomenon is related to the considerable airflow bypass between tube rows. On the contrary, at a smaller transverse tube pitch of 50 mm, one can see smaller fin spacing results in higher pressure drops and lower heat transfer coefficients.
3. For the staggered arrangement, the effect of tube diameter on the airside performance is analogous to that of the inline arrangement but to a comparatively small extent. This is because the recirculation zone behind the tube row is much smaller in a staggered arrangement. The effect of the fin height on the pressure drops much smaller than that of inline arrangement due to the major contribution to the pressure drops is from the blockage of the subsequent tube row in a staggered arrangement.
4. The effect of fin spacing on the airside performance for staggered arrangement also varies with the transverse tube pitch. For a smaller transverse tube pitch of 50 mm, there is no appreciable influence of the fin spacing on heat transfer. On the contrary, at a larger transverse tube pitch of 84 mm, one can see smaller fin spacing leads to lower heat transfer coefficients. This is also attributed to the presence of airflow bypass effect.
5 Correlations of the present crimped spiral fins in both staggered and inline arrangement are developed. The proposed correlations give quite good predictive ability against the present test data.

The cooling coil

1. The pressure drop of wet surface heat exchanger increases with the mass flow rate of air and the result is slightly higher or close to that of dry surface because only water condensate can be easily drained in the large fin spacing and individual finned configuration.
2. The heat transfer coefficient of the wet surface is slightly lower than that of the dry surface.
3. The effect of tube diameter on the airside performance is significant. Larger tube diameter not only gives lower heat transfer coefficient but also contributes

significantly to the increase of pressure drops. This phenomenon is applicable in both dry and wet condition.

4. For wet surface, the influence of fin height is negligible whereas there is a small effect in dry surface.
5. The effect of fin spacing on the heat transfer performance is rather small. However, the increasing of fin spacing tends to have a lower heat transfer coefficient.
6. The tube arrangement plays an important role on the heat transfer coefficient, the lower transverse pitch gives the higher heat transfer coefficient.
7. Airside performance in the present study is presented in terms of f and the j factor. The proposed correlations in case of staggered arrangement can predict 75% and 95% of experimental data within ±15%. In case of inline arrangement, the proposed correlations can predict the j and the f factors can estimated about 85.7% and 82.3% of experimental data within ±15% accuracy.

CHAPTER 1
INTRODUCTION

1.1 Statement of Problems and Background

There are many types of heat exchanger applicable to the recovery of waste heat such as shell-and-tube, plate, and cross-flow heat exchangers. Among them, the cross flow type is especially suitable for recovering heat from high temperature air. Normally, the liquid always flows inside the tube whereas the gas flows across the tube bank. Because the dominant resistance occurs on the airside, it is a common practice to employ fins (such as circular fins) on the tube bundle to increase the gas side performance. For circular fin geometrics, there are many empirical correlations available in the literature [1-5]. However, circular fin implemented in typically industrial application is usually in the form of crimped spiral fin as shown in Figure 1.1. Unfortunately, there is no airside data reported in the literature especially the finned tube manufactured in Thailand. In this regard, it is the objective of this study to present relevant airside data of the crimped spiral fins produced from Thai industry. Furthermore, relevant important geometric parameters such as tube diameter, fin spacing, fin height, and tube spacing influencing the airside performance are also investigated. Moreover the empirical correlations for evaluating the airside performance are also developed.

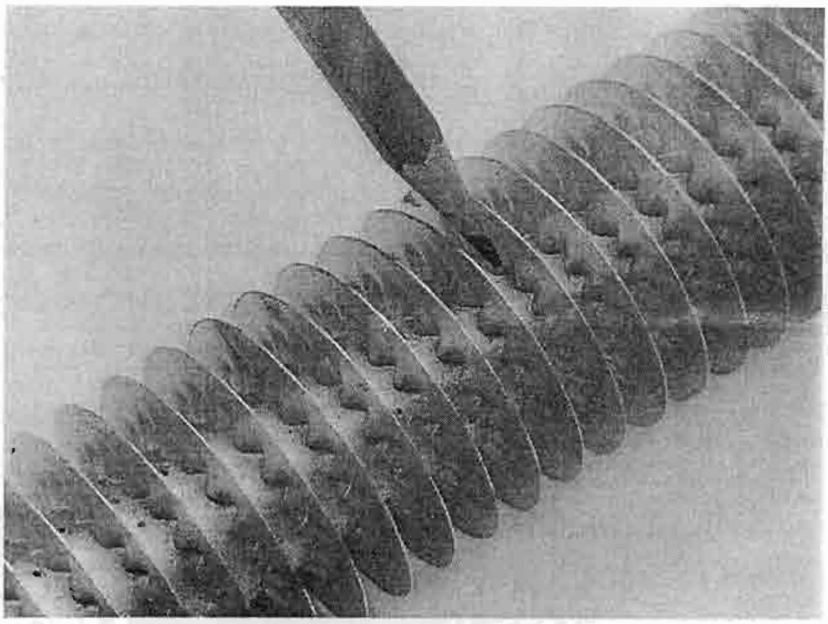

Figure 1.1 Schematic of the crimped spiral fin geometry.

The first part of this work is dealing with the performance testing of the heat exchanger operating under no condensation of moisture from the air stream on the heat exchanger surface. Actually, for practical waste heat recovery system, the heat exchanger may accompany with condensation of moisture air on the heat exchanger surface. Although the designers try to avoid this situation due to considerably corrosive problem associated with it, condensation may still takes place from time to time. This is commonly encountered if the load is not constant such as small boilers where the steam consumption varies with time and the the flue gas temperature fluctuates in a wide range. In that regard, the airside performance in the presence of dehumidification is rather important. Unfortunately, there are simply no data reported for the crimped spiral finned heat exchangers. Hence, it is the objective of the second part of this work. The heat transfer and friction characteristic of cross flow heat exchanger using crimped spiral fin in the presence of dehumidification are reported. Moreover, the heat transfer and friction correlations are also developed in this part.

1.2 Research Objectives

1. Develop the correlation for predicting the heat transfer coefficient of cross flow heat exchanger using crimped spiral fin under no condensation of moisture from the air stream and dehumidifying conditions.
2. Develop the correlation for predicting the air stream pressure drop of cross flow heat exchanger using crimped spiral fin under no condensation of moisture from the air stream and dehumidifying conditions.

1.3 Scope of Work

The aim of this work is to correlate the heat transfer and frictional characteristic of the cross flow heat exchanger using crimped spiral finned tube which are locally manufactured. The dimensions of finned tube are the same size as using in the industry. The dimensions and the testing conditions of this research are as follow:

1. Dimensions of finned tube

Outside diameter of tube	17.3, 21.7, 27.2 mm.
Fin spacing	2.85, 3.85, 6.10 mm.
Fin height	10, 15 mm.
Fin thickness	0.4 mm.
Tube arrangement	Inline, Staggered

2. Testing conditions

Part 1. No condensation of moisture from the air stream.

Inlet temperature of air	25 °C (approx.)
Inlet temperature of hot water	65 °C
Frontal velocity of air	0.5-2 m/s
Mass flow rate of water	0.12 kg/s

Part 2. Dehumidifying condition.

Inlet temperature of hot air	65 °C
Inlet temperature of water	25 °C
Frontal velocity of air	0.5-2 m/s
Mass flow rate of water	0.12 kg/s
Relative humidity of air	50% RH (approx.)

1.4 Methodology

1. Design the test rig for testing the performance of a cross flow heat exchanger using crimped spiral fin.
2. Calibrate all of the instrument by follow the standard method [6-9]
3. Performance testing of a cross flow heat exchanger under no condensation of moisture of air stream on heat exchanger surface and construct the empirical model for evaluating the heat transfer coefficient and the air stream pressure drop.
4. Performance testing of a cross flow heat exchanger under dehumidifying condition and construct the empirical model for evaluating the heat transfer coefficient and the air stream pressure drop.

1.5 Expected Benefits

The results from this research can help the heat exchanger designer select the suitable size of the heat exchanger using the crimped spiral finned tubes.

CHAPTER 2
EXPERIMENTAL SET-UP

2.1 Overview of the Experimental Apparatus

As mention in the previous chapter, this research work divides into two parts. The first part is to study the performance of the cross flow heat exchanger using crimped spiral finned tube operating under the condition having no condensation of moisture from the air stream on heat exchanger surface. Normally the heat exchanger operating under this condition is called heating coil. The second part investigates the performance in case of dehumidifying condition that having condensation of moisture on the heat exchanger surface. This heat exchanger is called cooling coil.

Therefor the experimental set-up of this work can be divided into two parts follow the testing conditions. The experimental apparatus is designed to support the testing conditions and the schematic sketch of the apparatus is shown in Figure 2.1. Note that this apparatus is designed and calibrated by following the ASHRAE and ARI standards [6-9]. The apparatus shown in Figure 2.1 is the wind tunnel. The cross flow heat exchanger is mount in this tunnel. This heat exchanger exchanges heat between the air stream and the water. The next sections will describe the operating methods and the testing conditions of this test rig. Figures 2.2-2.10 show the images of the experimental apparatus.

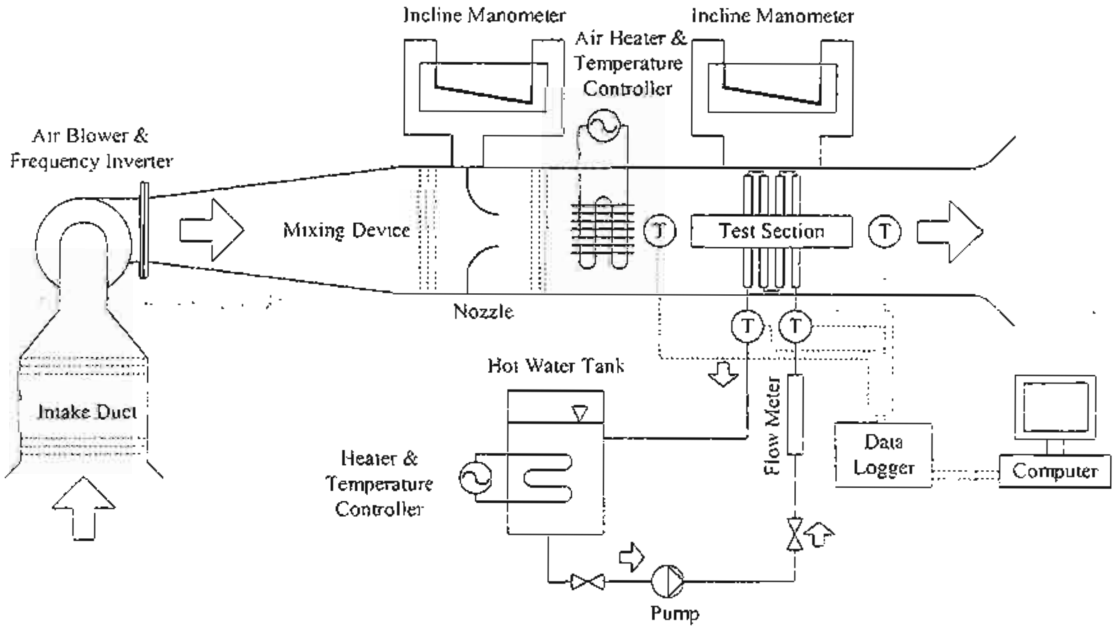

Figure 2.1 Schematic sketch of the experimental apparatus.

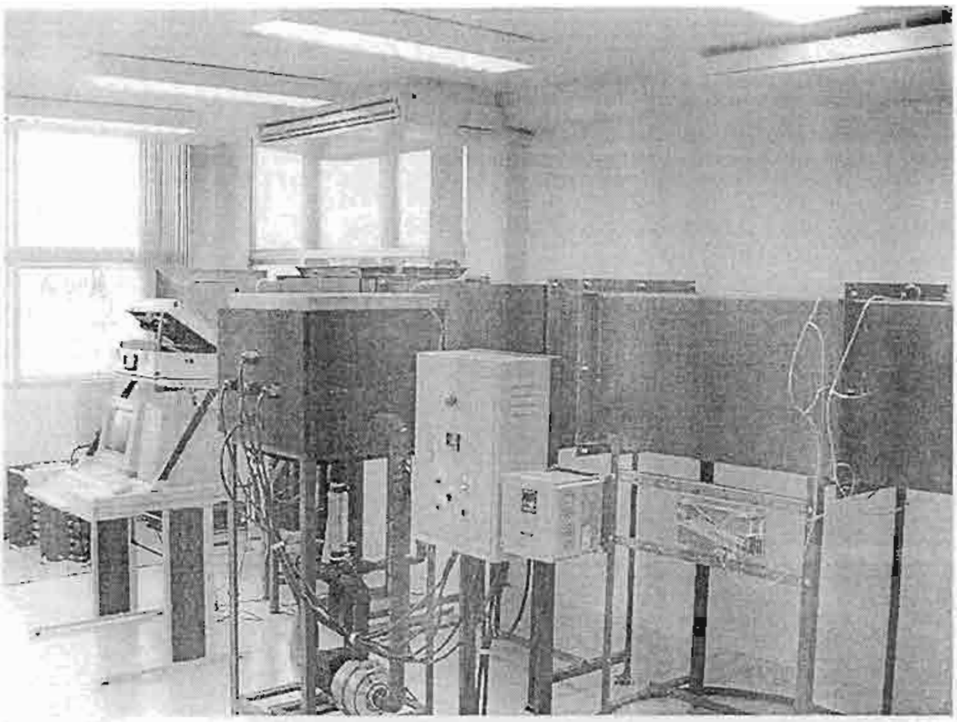

Figure 2.2 The front view of the apparatus.

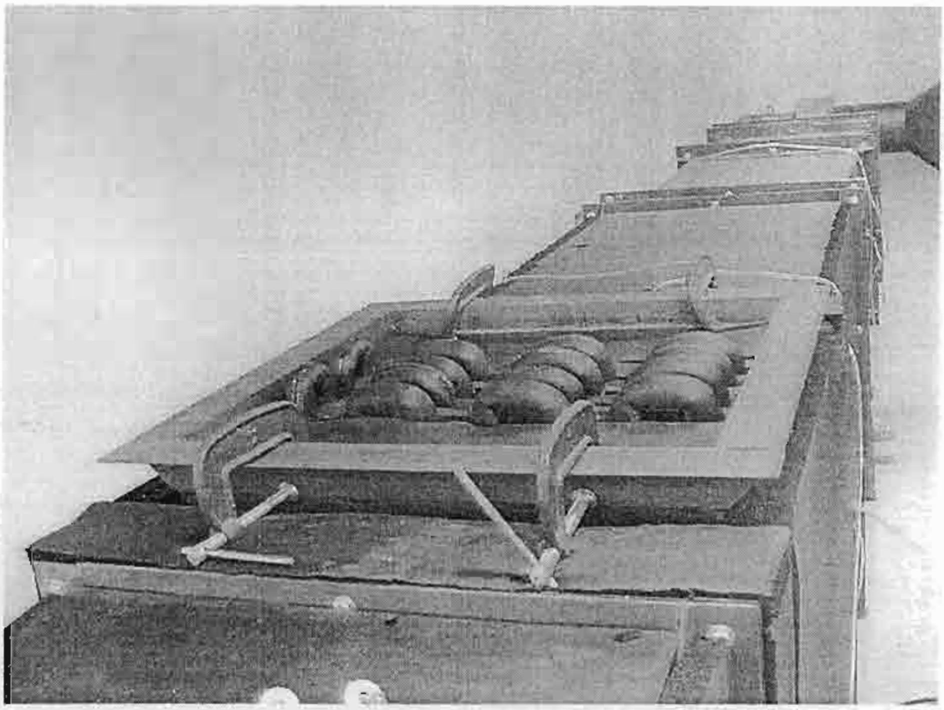

Figure 2.3 The top view of the apparatus at testing section.

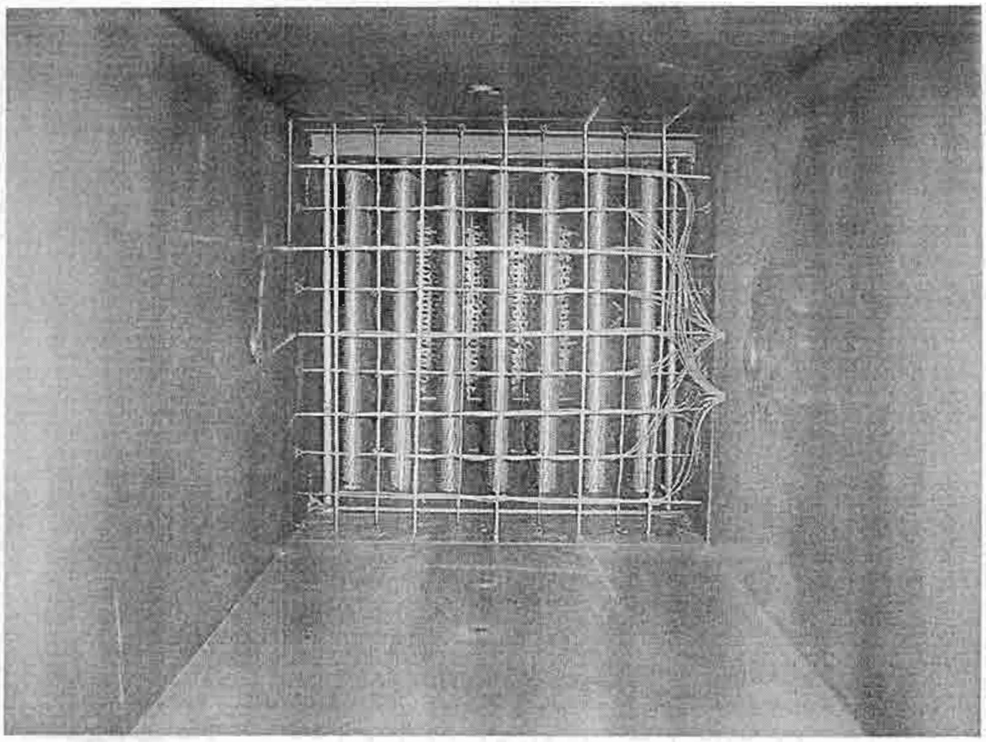

Figure 2.4 The cross flow heat exchanger setting in the wind tunnel.

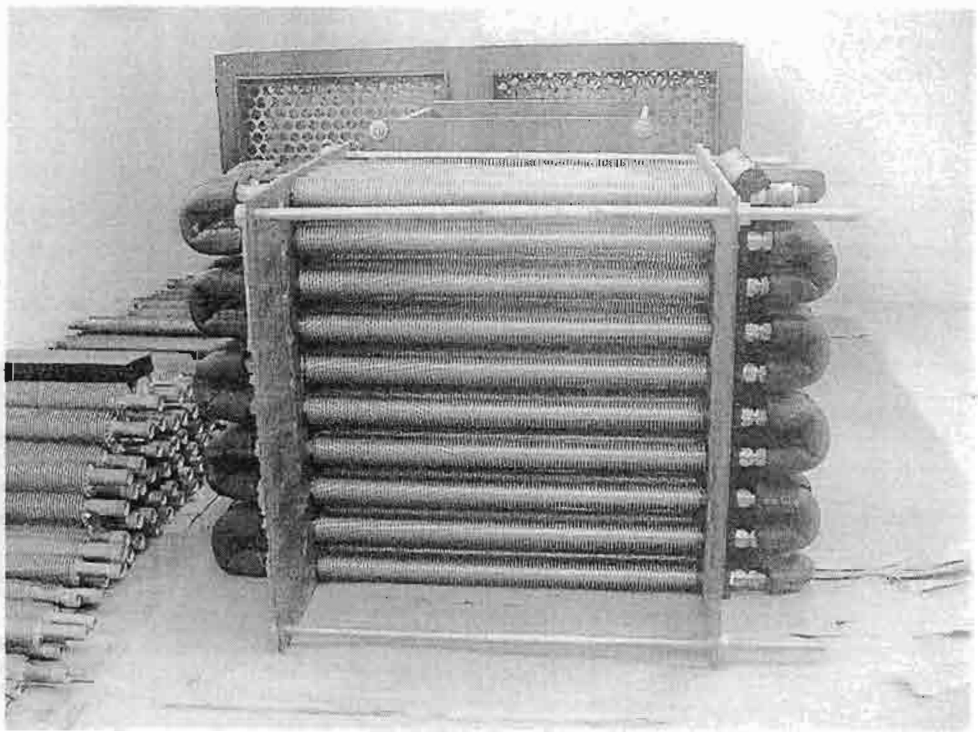

Figure 2.5 The testing specimen before mount in the wind tunnel.

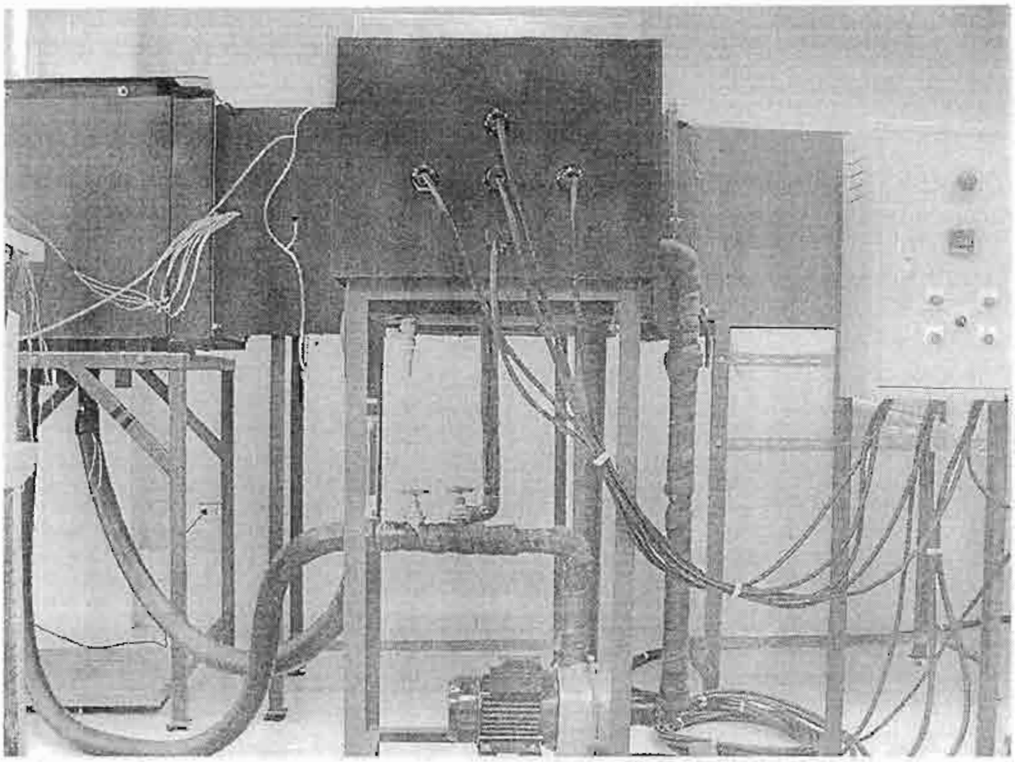

Figure 2.6 Hot water tank.

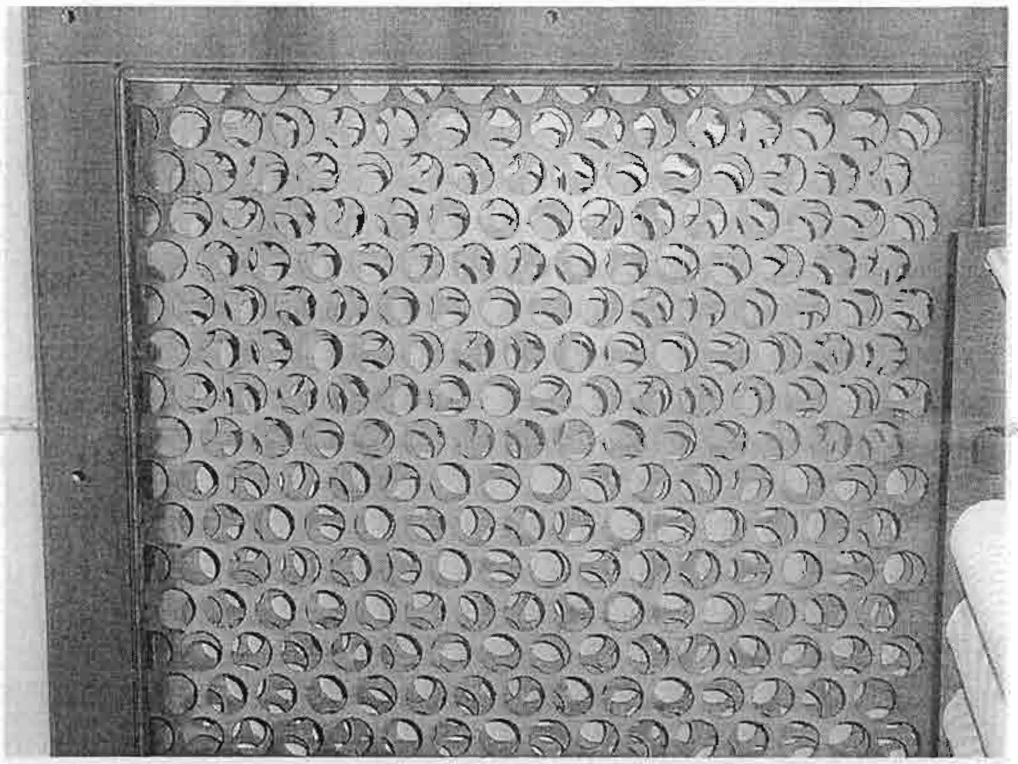

Figure 2.7 The mixing device.

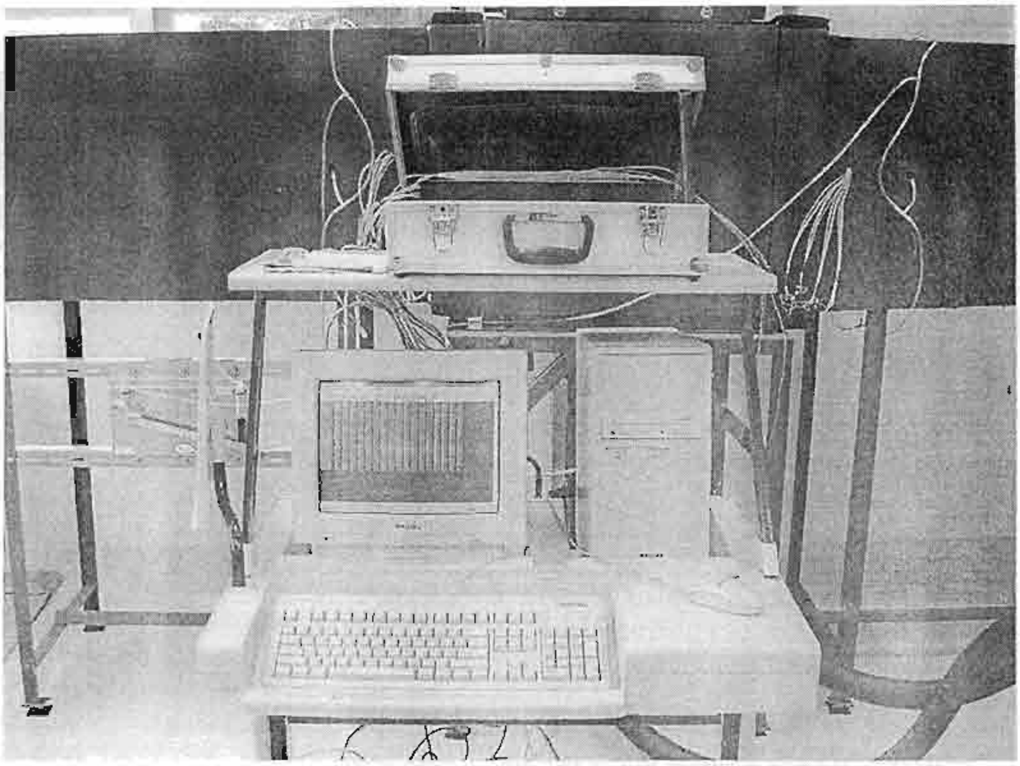

Figure 2.8 Temperature data logger and computer controller.

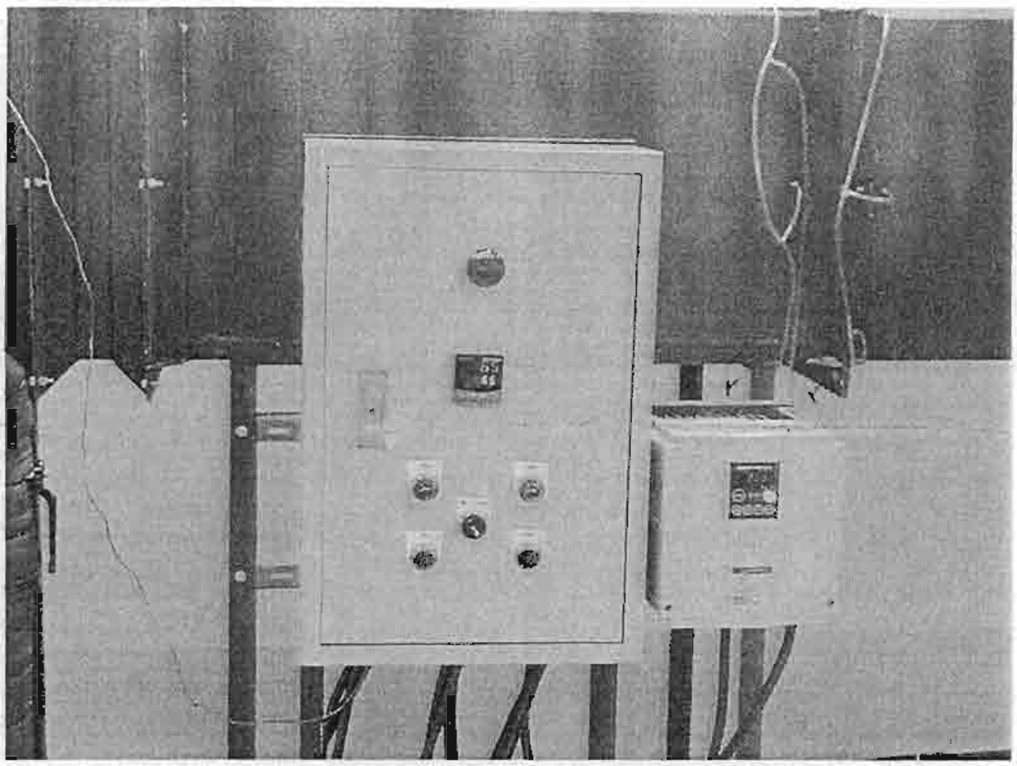

Figure 2.9 Control panel of the wind tunnel.

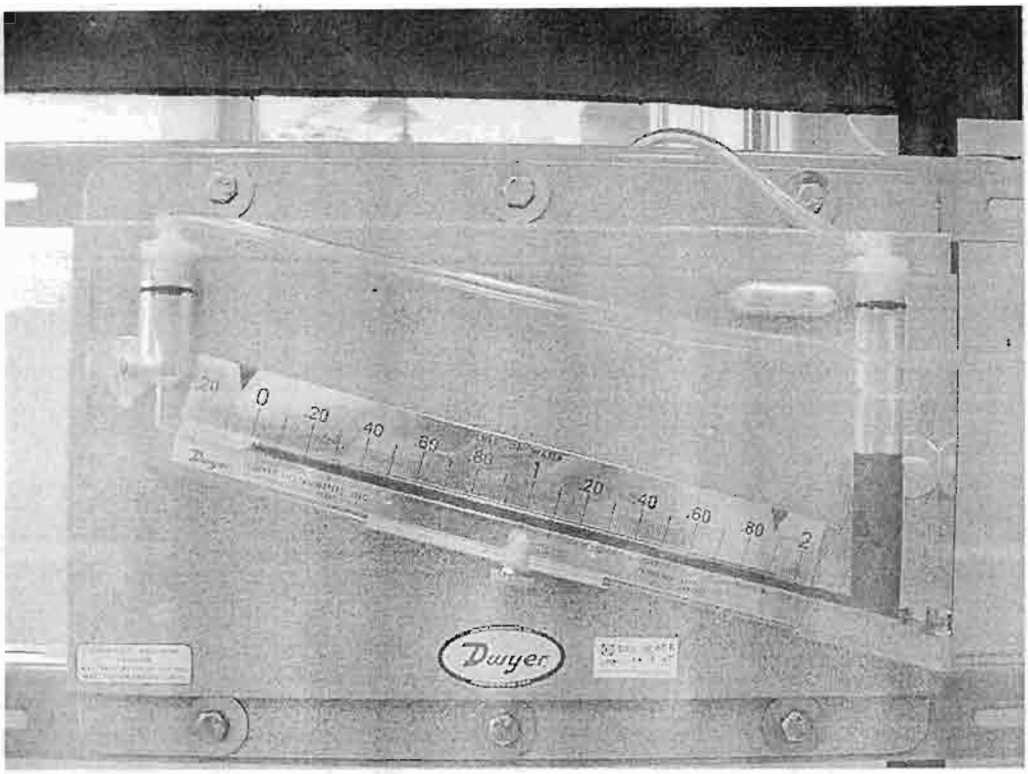

Figure 2.10 Inclined manometer for measuring the pressure drop.

2.2 The Experimental Set-up of the First Part

As mention in the previous section, the first part is to study the performance of the cross flow heat exchanger using crimped spiral finned tube operating under the condition having no condensation of moisture from the air stream on heat exchanger surface.

From Figure 2.1, the air stream at room temperature flows through the tube bank with hot water circulating inside the tubes. In this experiment, the water flow rate is kept at a constant flowrate of 8 L/min. An accurate flowmeter is used for the measurement with a precision of ±0.1 L/min. The inlet temperature of water is maintained at 65°C. Both of the inlet and outlet temperatures of water are measured by a set of calibrated K-type thermocouples and the signals are recorded by a temperature data logger.

The airflow across the heat exchanger is generated by a 1.5 kW centrifugal air blower with the controllable range of 0.1-0.5 kg/s by using a frequency inverter. The mass flow rate of air stream is measured by a standard nozzle and an inclined manometer with ±0.5 Pa accuracy. The inlet and the outlet temperatures of air stream are also measured by another set of K-type thermocouple mesh. The inlet and outlet temperature measuring meshes consist of 16 and 41 thermocouples, respectively. Note that all of thermocouples have been calibrated to ±0.1 °C accuracy. The pressure drop across the heat exchanger is also measured by the inclined manometer with ±0.5 Pa accuracy.

A total of 23 crimped spiral fin heat exchangers having various geometric parameters are tested in this study. Table 2.1 lists the details of the tested samples. Relevant definitions of the geometrical parameters can be also shown in Figure 2.11. Notice that both inline and staggered arrangements are tested in this study. The effects of tube diameter, fin height, fin spacing, fin thickness, and tube arrangement on the airside performance are examined accordingly.

Table 2.1 Geometric dimensions of cross flow heat exchanger.

No	d_o (mm)	d_i (mm)	f_s (mm)	f_h (mm)	f_t (mm)	S_t (mm)	S_l (mm)	n_r	n_t	arrangement
1	17.3	13.3	6.10	10.0	0.4	50.0	50.0	4	10	inline
2	21.7	16.5	6.10	10.0	0.4	71.4	50.0	4	7	inline
3	21.7	16.5	6.10	10.0	0.4	50.0	50.0	4	10	inline
4	21.7	16.5	3.85	10.0	0.4	71.4	50.0	4	7	inline
5	21.7	16.5	3.85	10.0	0.4	50.0	50.0	4	10	inline
6	21.7	16.5	2.85	10.0	0.4	71.4	50.0	4	7	inline
7	21.7	16.5	2.85	10.0	0.4	50.0	50.0	4	10	inline
8	21.7	16.5	3.85	15.0	0.4	71.4	50.0	4	7	inline
9	27.2	21.6	3.85	10.0	0.4	50.0	50.0	4	10	inline
10	21.7	16.5	6.10	10.0	0.4	72.0	36.0	4	6	staggered
11	21.7	16.5	3.85	10.0	0.4	72.0	36.0	4	6	staggered
12	21.7	16.5	2.85	10.0	0.4	72.0	36.0	4	6	staggered
13	21.7	16.5	6.10	10.0	0.4	84.0	24.2	4	5	staggered
14	21.7	16.5	3.85	10.0	0.4	84.0	24.2	4	5	staggered
15	21.7	16.5	2.85	10.0	0.4	84.0	24.2	4	5	staggered
16	21.7	16.5	6.10	10.0	0.4	50.0	43.3	4	9	staggered
17	21.7	16.5	3.85	10.0	0.4	50.0	43.3	4	9	staggered
18	21.7	16.5	2.85	10.0	0.4	50.0	43.3	4	9	staggered
19	21.7	16.5	6.10	10.0	0.4	55.6	48.2	4	8	staggered
20	21.7	16.5	3.85	10.0	0.4	55.6	48.2	4	8	staggered
21	21.7	16.5	2.85	10.0	0.4	55.6	48.2	4	8	staggered
22	21.7	16.5	3.85	15.0	0.4	55.6	48.2	4	8	staggered
23	27.2	21.6	3.85	10.0	0.4	50.0	43.3	4	9	staggered

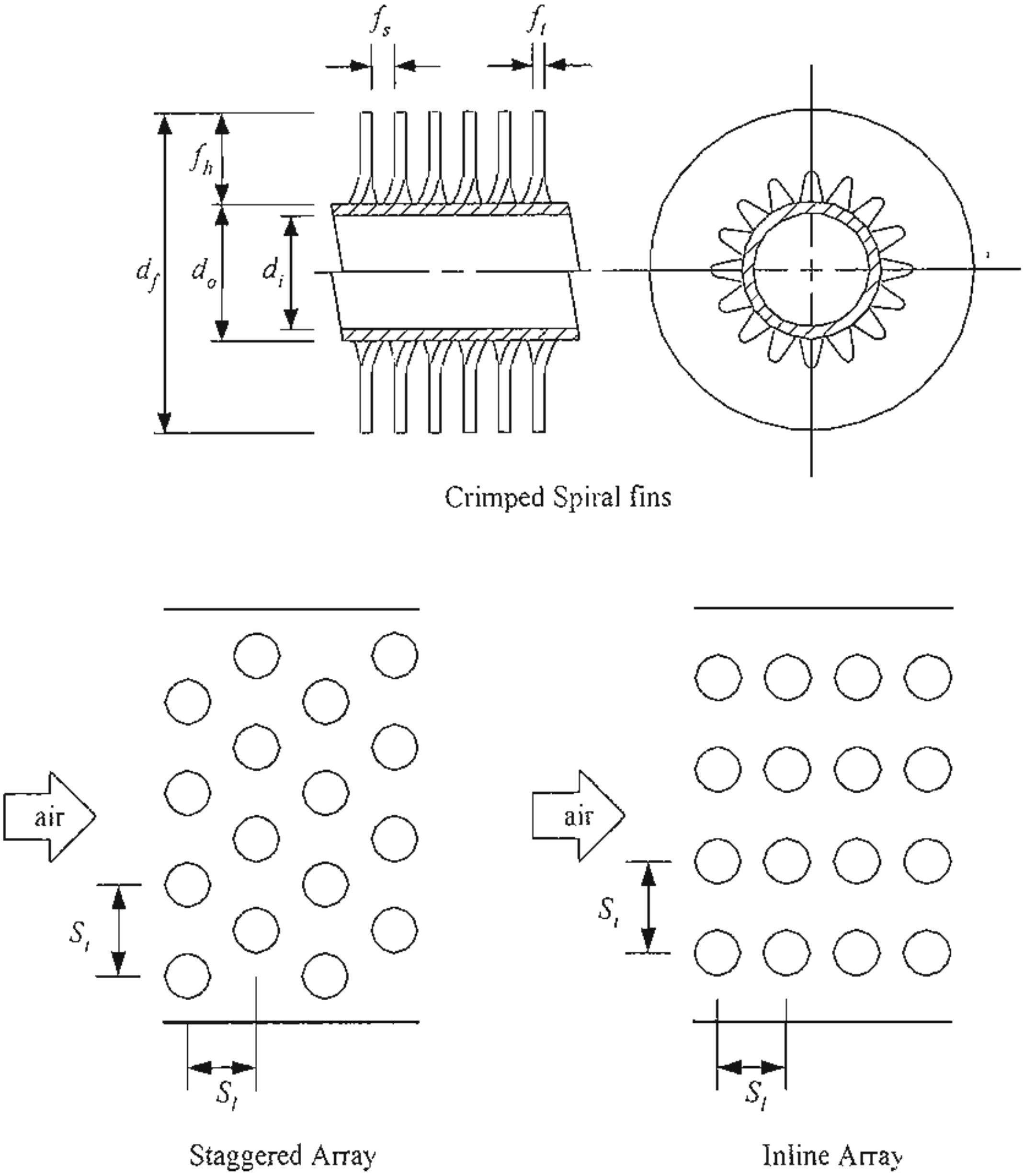

Figure2.11 Details of crimped spiral fins geometry and tube arrangements.

2.3 The Experimental Set-up of the Second Part

The second part is to study the performance of the cross flow heat exchanger using crimped spiral finned tube operating under dehumidifying condition. In this part, the hot air stream flows through the tube bank and the water at room temperature circulates inside the tubes. In this experiment, the water flow rate is kept constant at 8 L/min. An accurate water flow meter is used for the measurement with a precision of ±0.1 L/min. The inlet temperature of water is approximately 30°C. Both the inlet and outlet temperatures of water are measured by a set of calibrated K-type thermocouples and a temperature data logger records these signals.

A 1.5 kW centrifugal air blower accompanied with a frequency inverter having a controllable range of 0.1-0.5 kg/s air is used to conduct flowing air across the heat exchanger. A standard nozzle and an inclined manometer are adopted to measure the mass flow rate of air stream. The uncertainty of the inclined manometer is ±0.5 Pa accuracy. The inlet temperature of air stream is kept constant at 65 °C by the set of heaters and the temperature controller. The inlet and the outlet dry bulb temperatures of air stream are also measured by another set of two meshes of K-type thermocouples. The inlet and the outlet wet bulb temperatures of air stream are also measured. Note that all of thermocouples have been calibrated to ±0.1 °C accuracy. The pressure drop across the heat exchanger is measured by another set of inclined manometer with calibrated uncertainty of ± 0.5 Pa accuracy.

A total of 10 crimped spiral fin heat exchangers having various geometric parameters are tested in this study. The details of the tested samples is the same as shown in Table 2.1. Relevant definitions of the geometrical parameters can be also shown in Figure 2.11. The effects of tube diameter, fin height, fin spacing, fin thickness, and tube arrangements on the airside performance are examined accordingly.

CHAPTER 3

AIR-SIDE PERFORMANCE OF HEAT EXCHANGER USING CRIMPED SPIRAL FINS, A CASE STUDY OF HEATING COIL

3.1 Introduction

This chapter describes the performance testing of cross flow heat exchanger using crimped spiral fins producing from Thai industry. Actually, there are many reports about the performance of this kind of heat exchanger, especially in case of circular fin. Briggs and Young [1] developed the air side heat transfer coefficient of the staggered tube bank in term of Colburn j factor as:

$$j = 0.134\,\mathrm{Re}_D^{-0.319}\left(\frac{f_s}{f_h}\right)^{0.2}\left(\frac{f_s}{f_t}\right)^{0.11} . \tag{3.1}$$

Note that the above correlation is valid for four or more tube rows and applicable to the following ranges: $1100 \le \mathrm{Re}_D \le 18000$, $1.0 \le f_s/f_t \le 6.6$, $0.09 \le f_h/d_o \le 0.69$, $0.01 \le f_t/d_o \le 0.15$, and $15 \le S_t/d_o \le 8.2$. The standard deviation of the Briggs and Young correlation is 5.1%.

Robinson and Briggs [2] provided the frictional performance termed as the Fanning friction factor for the circular fin tube bank having staggered arrangement:

$$f = 9.47\,\mathrm{Re}_D^{-0.316}\left(\frac{S_t}{d_o}\right)^{-0.927}\left(\frac{S_t}{S_d}\right)^{0.515} . \tag{3.2}$$

Equation (2) is based on isothermal air flow with data from 17 staggered tube banks. Its applicable range is $2{,}000 \le \mathrm{Re}_D \le 50{,}000$, $0.15 \le f_s / f_h \le 0.19$, $3.8 \le f_s / f_t \le 6.0$, $0.35 \le f_h / d_o \le 0.56$, $0.01 \le f_t / d_o \le 0.03$ and $1.9 \le S_t / d_o \le 4.6$. The standard deviation of Equation (2) is 7.8%.

Rabas et al. [3] developed the Colburn j factor and friction factor for circular finned tube bank having low fin height and small fin spacing:

$$j = 0.292\,\mathrm{Re}_D^{\,n}\left(\frac{f_s}{d_o}\right)^{1.12}\left(\frac{f_s}{f_h}\right)^{0.26}\left(\frac{f_t}{f_s}\right)^{0.67}\left(\frac{d_f}{d_o}\right)^{0.47}\left(\frac{d_f}{f_t}\right)^{0.77} , \tag{3.3}$$

$$n = -0.415 + 0.0346\left(\frac{d_f}{f_s}\right), \tag{3.4}$$

$$f = 3.805\,\mathrm{Re}_D^{-0.234}\left(\frac{f_s}{d_o}\right)^{0.25}\left(\frac{f_s}{f_h}\right)^{0.76}\left(\frac{d_o}{d_f}\right)^{0.73}\left(\frac{d_o}{S_t}\right)^{0.71}\left(\frac{S_t}{S_l}\right)^{0.38} . \tag{3.5}$$

Equations (3.3)-(3.5) are also valid with 4 or more rows of tube bank. The applicable range are $5{,}000 \le \mathrm{Re}_D \le 25{,}000$, $1.3 \le f_s / f_h \le 1.5$, $0.01 \le f_s / f_t \le 0.06$, $f_h / d_o \le 0.1$, $0.01 \le f_t / d_o \le 0.02$ and $1.3 \le S_t / d_o \le 1.5$. These equations could predict 94% and 90% of the experimental *j* and *f* data within ±15%.

ESDU [4] recommended a correlation for heat transfer performance of high fin geometry:

$$Nu = 0.242\,\mathrm{Re}_D^{\;0.658}\left(\frac{f_s}{f_h}\right)^{0.297}\left(\frac{S_t}{S_l}\right)^{-0.091}\mathrm{Pr}^{0.333}. \tag{3.6}$$

This correlation is also valid for air-cooled heat exchanger with four or more tube rows and the suitable ranges for application are $2{,}000 \le \mathrm{Re}_D \le 40{,}000$, $0.13 \le f_s / f_h \le 0.57$, $1.15 \le S_t / S_l \le 1.72$.

The preceding correlations were developed with the cross flow heat exchanger having staggered arrangement. In case of inline arrangement, despite of its comparatively low heat transfer performance, its lower pressure drop and high reliability (easy to maintain and clean) are very attractive in very severe environment. For the heat transfer performance, Schmidt [5] recommended a correlation for inline arrangement with high fin,

$$Nu = 0.30\,\mathrm{Re}_D^{\;0.625}\left(\frac{A}{A_t}\right)^{-0.375}\mathrm{Pr}^{0.333}. \tag{3.7}$$

Where A and A_t are the total surface area and that of bare tube. Range of applicability for Equation (3.7) is $5{,}000 \le \mathrm{Re}_D \le 100{,}000$ and $5 \le A / A_t \le 12$.

However, circular fin implemented in typically industrial application is usually in the form of crimped spiral fin. Unfortunately, there is no airside data reported in the literature especially the crimped spiral fin producing from Thai industry. In this regard, it is the objective of this study to present relevant airside data of the crimped spiral fins. Furthermore, relevant important geometric parameters such as tube diameter, fin spacing, fin height, and tube spacing influencing the airside performance are also investigated. Moreover the empirical correlations capable of evaluating the airside performance are also developed.

3.2 Data Reduction

During the experiment, hot water flowing inside the tube bank transfers heat to the outside air and the the heat transfer rate (Q) can be calculated as

$$Q = \dot{m}_a Cp_a \left(T_{ao} - T_{ai}\right), \tag{3.8}$$

$$Q = \dot{m}_w Cp_w \left(T_{wi} - T_{wo}\right), \tag{3.9}$$

Where $\dot{m}_a$ is the mass flow rate of air, $\dot{m}_w$ is the mass flow rate of water, T_{ai}, T_{ao} are the inlet and outlet temperatures of air stream, T_{wi}, T_{wo} are the inlet and outlet temperature of water, and Cp_a, Cp_w are the specific heat of air and water, respectively.

The performance of the heat exchangers is analyzed by conventional ε-NTU technique, the effectiveness is defined as

$$\varepsilon = \frac{Q}{Q_{\max}}, \tag{3.10}$$

or

$$\varepsilon = \frac{Q}{\left(\dot{m}Cp\right)_{\min} \Delta T_{\max}}, \tag{3.11}$$

The relationship of the effectiveness and the number of transfer unit (NTU) for the present 4-tube configuration is as follow (ESDU [10]);

$$\varepsilon = \frac{1}{C^*}\left\{1 - e^{-4KC^*}\left[1 + C^* K^2\left(6 - 4K + K^2\right) + 4\left(C^*\right)^2 K^4 \left(2 - K\right) + \frac{8\left(C^*\right)^3 K^6}{3}\right]\right\}, \tag{3.12}$$

$$K = 1 - e^{-NTU/4}, \tag{3.13}$$

$$NTU = \frac{UA}{\left(\dot{m}Cp\right)_{\min}}, \tag{3.14}$$

$$C^* = \frac{\left(\dot{m}Cp\right)_{\min}}{\left(\dot{m}Cp\right)_{\max}}, \tag{3.15}$$

Once the overall resistance is obtained from Equations (3.12-3.14), the heat transfer coefficients can be obtained from the following overall resistance equation:

$$\frac{1}{UA} = \frac{1}{\eta_o h_o A_o} + \frac{\ln\left(d_o / d_i\right)}{2\pi k L} + \frac{1}{h_i A_i}, \tag{3.16}$$

Where h is the heat transfer coefficient, A is the surface area, d is tube diameter, L is total tube length, k is thermal conductivity of tube material, η_o is surface efficiency and the subscripts o, i denote the air side and the tube side, respectively. The tube side heat transfer coefficient can be calculated from Gnielinski correlation [11] as

$$h_i = \left(\frac{k}{d}\right)_i \frac{(\mathrm{Re}_{Di}-1000)\mathrm{Pr}(f_i/2)}{1+12.7\sqrt{f_i/2}\left(\mathrm{Pr}^{2/3}-1\right)}, \tag{3.17}$$

$$f_i = [1.58\ln(\mathrm{Re}_{Di}) - 3.28]^{-2}, \tag{3.18}$$

Where Re_{Di} is the tube-side Reynolds number. The relation of the surface efficiency in Equation (3.16) and the fin efficiency η is

$$\eta_o = 1 - \frac{A_f}{A_o}(1-\eta), \tag{3.19}$$

$$A_o = A_f + A_b, \tag{3.20}$$

Where A_o is the total surface area of finned tube, A_f is surface area of fin, A_b is the surface area of the bare tube. The fin efficiency η can be approximated from the Schmidt approximation [12]:

$$\eta = \frac{\tanh(mr\phi)}{mr\phi}, \tag{3.21}$$

where

$$m = \sqrt{\frac{2h_o}{k_f f_t}}, \tag{3.22}$$

$$\phi = \left(\frac{R_{eq}}{r} - 1\right)\left[1 + 0.35\ln\left(\frac{R_{eq}}{r}\right)\right], \tag{3.23}$$

$$\frac{R_{eq}}{r} = 1.27\frac{X_M}{r}\left(\frac{X_L}{X_M} - 0.3\right)^{1/2}, \tag{3.24}$$

$$X_L = \frac{\sqrt{(S_t/2)^2 + S_L}}{2}, \tag{3.25}$$

$$X_M = 0.5S_t, \tag{3.26}$$

where k_f is thermal conductivity of the fin. S_t and S_L are transverse and longitudinal pitches of the tube bank and f_t is fin thickness.

The total surface area of finned tube and the total surface area of the fin can be estimated by assuming equal to that of the circular fin as [13];

$$A_o = \frac{nL\pi}{f_s + f_t}\left(0.5\left(d_f^2 - d_o^2\right) + d_f f_t + d_o f_s\right), \tag{3.27}$$

$$A_f = \frac{nL\pi}{f_s + f_t}\left(0.5\left(d_f^2 - d_o^2\right) + d_f f_t\right), \tag{3.28}$$

where n is the total number of tube, d_f is outer diameter of finned tube, f_s is spacing between adjacent fin and f_t is fin thickness.

In this study, the pressure drop across tube bank is in the form of Fanning friction factor. The relation of the friction factor including the entrance and exit pressure loss [14] relative to the measured pressure drop ΔP is

$$f = \frac{A_c \rho_i}{A_o \rho_m}\left[\frac{2\rho_i \Delta P}{G_c^2} - \left(1+\sigma^2\right)\left(\frac{\rho_i}{\rho_o} - 1\right)\right], \quad (3.29)$$

where A_c is the minimum flow area, σ is the contraction ratio, G_c is the mass flux of air flow based on the minimum flow area and the subscripts i, o, m represent the inlet, outlet, and mean value, respectively.

3.3 Results and Discussion

3.3.1 Inline Arrangement

In the case of inline arrangement, there are nine samples of inline arrangement as shown in Table 3.1. Figure 3.1 shows the effect of tube diameter on the airside performance. Results are termed as heat transfer coefficient and the pressure drop vs. frontal velocity. In this comparison, the fin spacing (3.85 mm), fin thickness (0.4 mm), and the fin height (10 mm) are all the same. The transverse and the longitudinal tube pitches are 50 mm. As expected, the pressure drop rises with the tube diameter. However, it is interesting to note that the heat transfer coefficient increases with the reduction of tube diameter. It is likely that this phenomenon is attributed to the ineffective area behind the tube increases with the tube diameter. The ineffective are is especially pronounced for an inline arrangement. Wang et al. [14] performed flow visualizations via dye injection technique for fin-and-tube heat exchangers having inline arrangement. Their visual results unveil a very huge flow circulation behind the tube row. Consequently this huge recirculation not only contributes to the decrease of heat transfer coefficient but also to the rise of pressure drop. In addition, the huge recirculation may also block the subsequent tube row and degrade the heat transfer performance hereafter.

Figure 3.2 shows the effect of fin height on the airside performance for inline arrangement. In this comparison, the associated fin heights are 10 and 15 mm and the fin spacing and the tube diameter are 3.85 mm and 21.7 mm with the transverse and the longitudinal pitches are 71.4 and 50 mm, respectively. As seen in the figure, the influence of fin height shows tremendous influence on the heat transfer performance and the pressure drop. Although the increase of fin height is only 50%, the corresponding increase of fin surface area is roughly 53% that eventually leads to a dramatic increase of pressure drop (roughly 100%). Unlike those of pressure drops, the heat transfer coefficients are dropped drastically with the increase of fin height. This is probably due to the airflow bypass effect. Actually the airflow is prone to flowing the portion where the flow resistance is small. In case of f_h = 15 mm, the airflow resistance around fin tube is larger than f_h = 10 mm. Therefore, part of the directed airflow just bypass the tube row without effective contribution to the heat transfer and lower heat transfer coefficient is obtained.

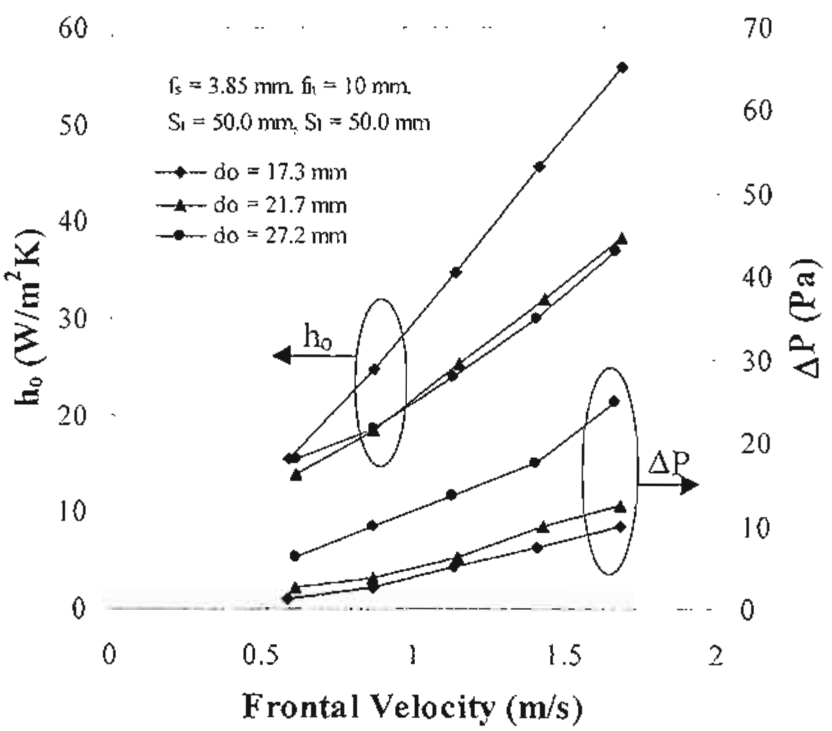

Figure 3.1 Effect of tube diameter on the airside performance for the inline arrangement.

The effects of the fin spacing on the airside performance at different transverse tube pitch (50 and 71.4 mm) are shown in Figure 3.3. At a larger transverse tube pitch of 71.4 mm, one can see the effect of fin spacing on pressure drops is rather small. Surprisingly, the reduction of the fin spacing does not give rise to the pressure drops. This may be related to the presence of the bypass airflow between the tubes. Since the bypass airflow does not increase the pressure drops, therefore no detectable change of pressure drops is seen at a very large transverse tube pitch of 71.4 mm. On the contrary, the reduction of fin spacing give rise to pressure drops at a smaller transverse tube pitch of S_l = 50 mm. This is due to the significant decrease of bypass airflow and the reduction of the associated hydraulic diameter. From Figure 3.3, it is also found that the increase of fin spacing give rise to heat transfer coefficient. An explanation of this phenomenon is the same as the effect of fin height that the result comes from airflow bypass effect. As is known, the corresponding pressure drop rises with the decrease fin spacing. Therefore, lower fin spacing gets higher bypass airflow and the heat transfer coefficient is decreased at smaller fin spacing.

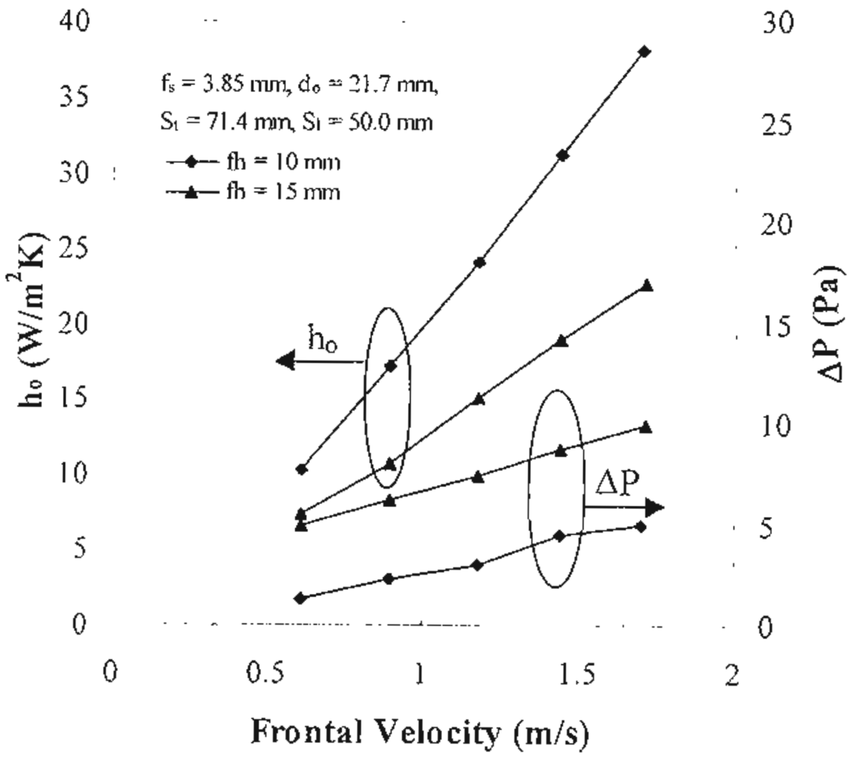

Figure 3.2 Effect of fin height on the airside performance for the inline arrangement.

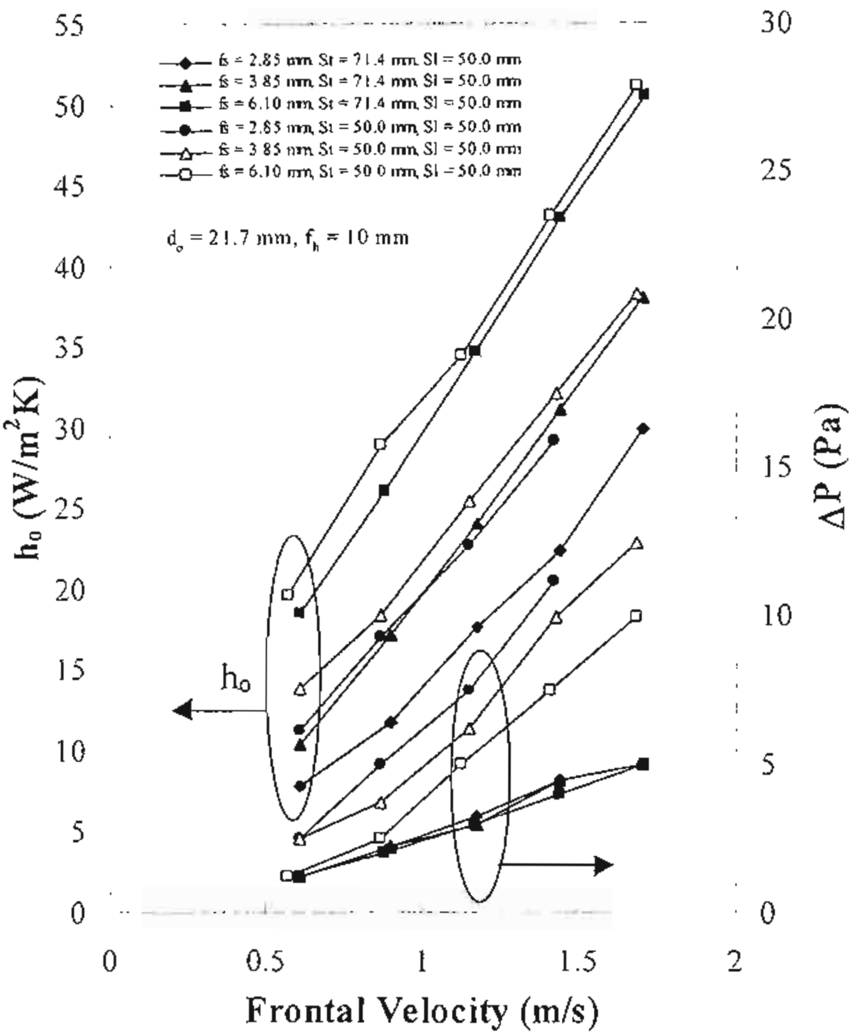

Figure 3.3 Effect of fin spacing and tube arrangement on the airside performance for the inline arrangement.

3.3.2 Staggered Arrangement

For staggered arrangement. Figure 3.4 shows effect of tube diameter on the air side performance. The geometrical parameters of fin spacing, fin height, transverse pitch and longitudinal pitch are 3.85 mm, 10 mm, 50 mm and 4.33 mm, respectively. Analogous to that of inline arrangement but the influence is comparatively less to some extent, the heat transfer coefficient and the pressure drop decrease with the tube diameter. Explanation of this phenomenon is the same as that of inline arrangement. However, the recirculation region for staggered arrangement behind the tube is much smaller than that of the inline arrangement due to the airflow across the adjacent tubes is directed by the subsequent tube row. The directed oblique airflow will reduce the recirculation area behind the tube. This phenomenon can be also made clear from the flow visualization experiment by Wang et al. [15] in staggered arrangement. Their visualization indicated a much smaller recirculation area of the staggered arrangement than that of inline arrangement.

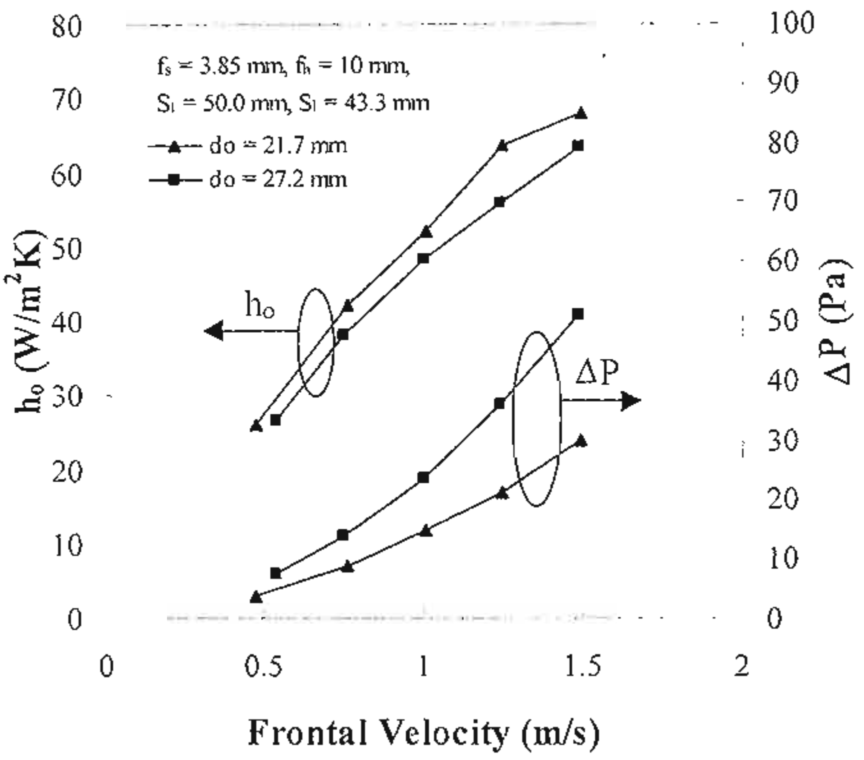

Figure 3.4 Effect of tube diameter on the airside performance for the staggered arrangement.

The effect of fin height on the airside performance is shown in Figure 3.5. It is found that the heat transfer coefficients of f_h = 10 mm are slightly higher than those of f_h = 15 mm and the explanation is similar to that of inline arrangement. However, the pressure drops for both fin height are about the same irrespective of the fin area of f_h = 15 mm are approximately 53% higher than that of f_h = 10 mm. The results are quite different from those of inline arrangement in which one can see an approximately two times increase of pressure drops for f_h = 15 mm relative to that of f_h = 10 mm. Explanation of this phenomenon can be made clear as follows. For the same fin height of f_h = 10 mm, one can see a dramatic increase of pressure drops of six times for staggered arrangement relative to that of inline arrangement. This implies the major contribution to the total pressure drops comes from the type of arrangement. For staggered arrangement, the airflow is directed by the subsequent tube row in which most of the pressure loss is generated. On the contrary, since the air flow across the inline arrangement is not directed by the subsequent tube row. The pressure drop is mainly affected by the friction caused by the fins and the recirculation area behind the tube. Thus one can see a very small increase of the pressure drop with the rise of fin height for staggered arrangement.

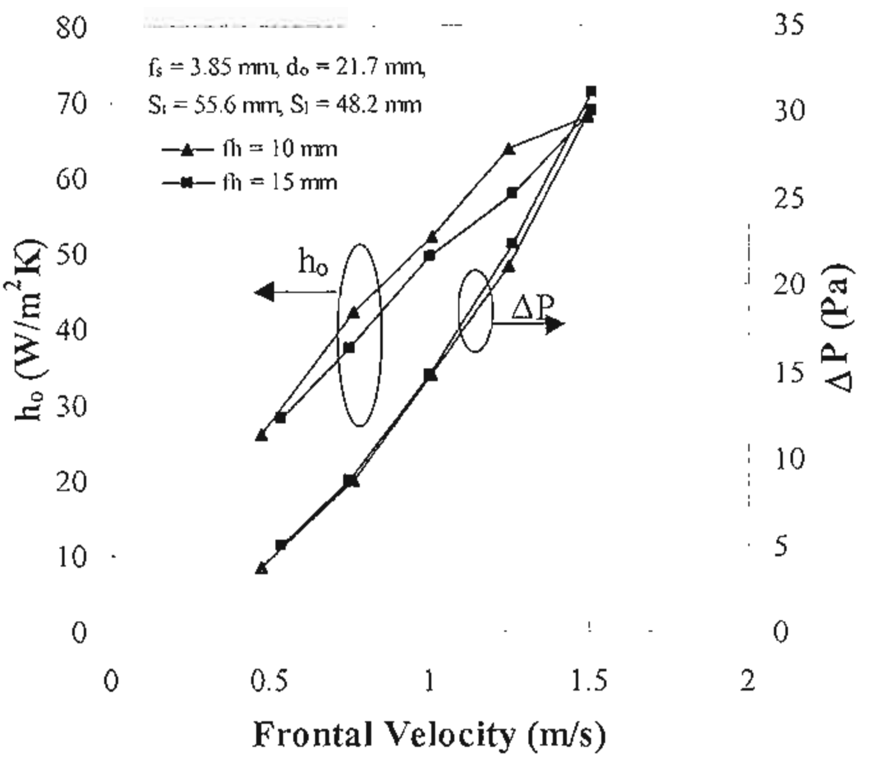

Figure 3.5 Effect of fin height on the airside performance for the staggered arrangement.

Figure 3.6 shows the effect of fin spacing, and S_t on the airside heat transfer coefficients and pressure drops. The tube diameter is 21.7 mm and the fin height is 10 mm. From Figure 3.5, it can be concluded that higher fin spacing gives lower pressure drops. For a smaller transverse tube pitch (S_t = 50 mm), one can see the effect of fin spacing on the heat transfer coefficients is negligible. This result is analogous to that of continuous fin geometry as reported by Rich [16] and Wang et al. [17]. However, for a larger transverse pitch of 84 mm, the heat transfer coefficients decrease with the decrease of fin spacing. Again explanation of this phenomenon may arise from the influence of airflow bypass effect. As is known, the corresponding pressure drop rises with the decrease fin spacing. As a consequence, although the airflow is directed by the tube row, the airflow is prone to flowing the portion where the flow resistance is smaller. For a very large of transverse tube pitch of 84 mm, part of the directed airflow just bypass the tube row and fin without effective contribution to the heat transfer, thereby causing a drop of heat transfer coefficients at smaller fin spacing. This flow bypass phenomenon becomes much where the transverse tube pitch is reduced. Therefore, one can see no appreciable change of heat transfer coefficients for S_t = 50 mm.

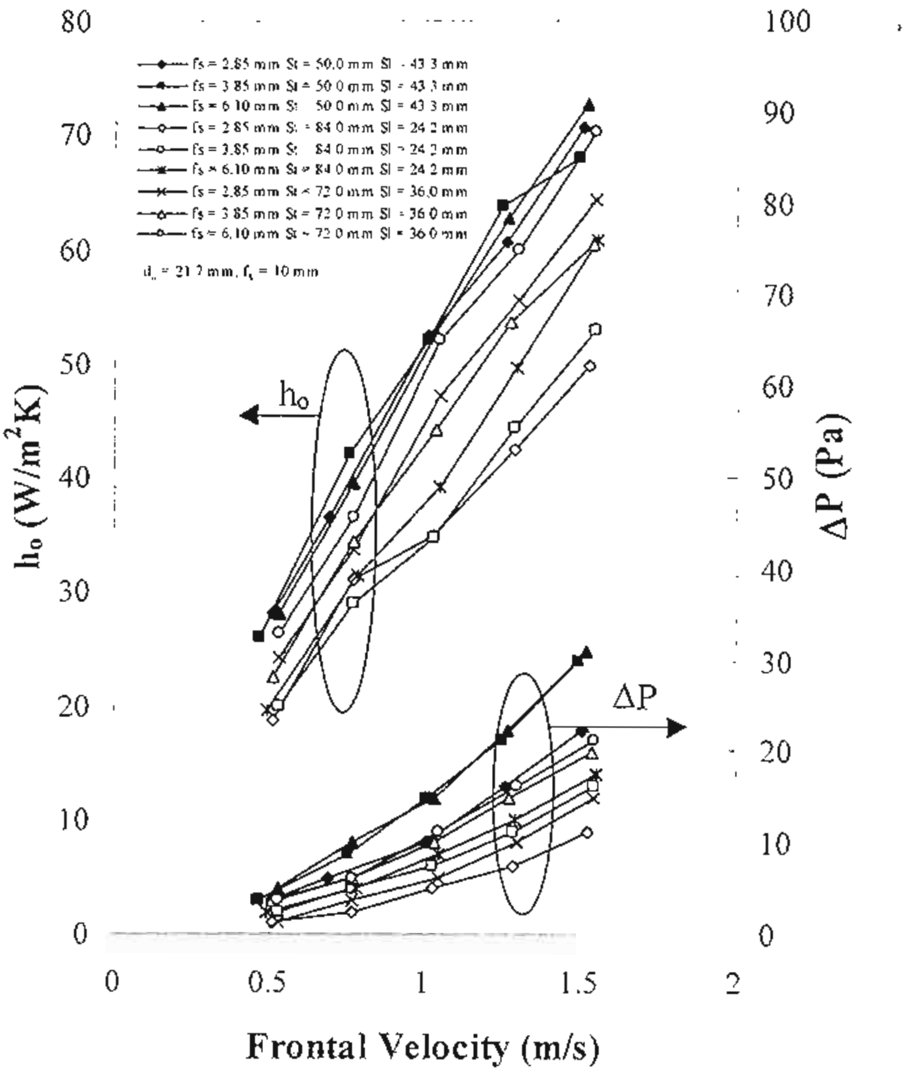

Figure 3.6 Effect of fin spacing and tube arrangement on the airside performance for the staggered arrangement.

3.3.3 <u>Empirical Correlations</u>

Based on the previous discussions, it is obvious from the test data that no single curve can be expected to describe the complex behaviors about the heat transfer and frictional characteristics in both inline and staggered arrangements. For easier engineering calculations, we had performed multiple linear regression technique to obtain the relevant correlations. The corresponding correlations are given as follows:

Correlation of the heat transfer performance of the inline arrangement:

$$j = 3.9048\times10^{-4}\,\mathrm{Re}_D^{\,0.0637}\left(\frac{f_t}{f_s}\right)^{-0.8363}\left(\frac{S_l}{S_t}\right)^{1.9926}\left(\frac{S_t}{d_o}\right)^{2.2810}\left(\frac{d_f}{d_o}\right)^{-2.1720} \tag{3.30}$$

Correlation of the heat transfer performance of the staggered arrangement:

$$j = 0.1970\,\mathrm{Re}_D^{\,-0.1295}\left(\frac{f_t}{f_s}\right)^{-0.1452}\left(\frac{S_l}{S_t}\right)^{1.1874}\left(\frac{S_t}{d_o}\right)^{0.8238}\left(\frac{d_f}{d_o}\right)^{0.0010} \tag{3.31}$$

Correlation of the frictional performance of the inline arrangement:

$$f = 0.1635\,\mathrm{Re}_D^{\,-0.4172}\left(\frac{f_t}{f_s}\right)^{-0.5215}\left(\frac{S_l}{S_t}\right)^{-1.2235}\left(\frac{S_t}{d_o}\right)^{-0.6334}\left(\frac{d_f}{d_o}\right)^{1.2000} \tag{3.32}$$

Correlation of the frictional performance of staggered arrangement:

$$f = 2.1768\,\mathrm{Re}_D^{\,-0.2679}\left(\frac{f_t}{f_s}\right)^{-0.2468}\left(\frac{S_l}{S_t}\right)^{1.8680}\left(\frac{S_t}{d_o}\right)^{0.3011}\left(\frac{d_f}{d_o}\right)^{-0.4470} \tag{3.33}$$

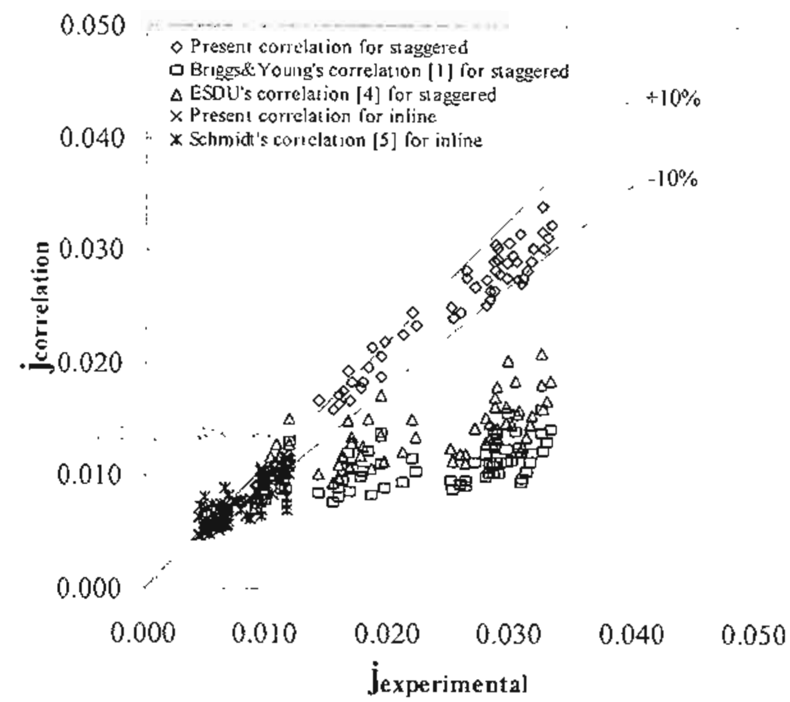

Figure 3.7 Comparison of the heat transfer correlations with experimental data.

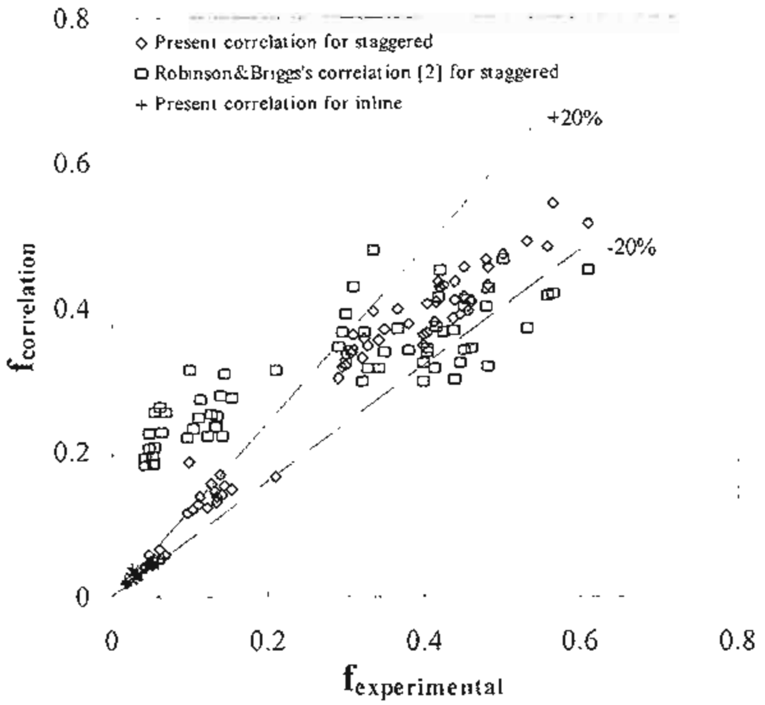

Figure 3.8 Comparison of the frictional correlations with experimental data.

Figures 3.7-3.8 show the comparison of j and f of the experimental results with the proposed correlations. For the heat transfer correlations, Equations (3.30)-(3.31) can predict 89.7% and 88.4% of the experimental data with ±10% and the friction factor correlations, Equations (3.32)-(3.33) give a predictive ability of 79.6% and 91.3% of the experimental data within ±20%. The standard deviation of the correlations Equations (3.30)-(3.33) are 7.90%, 7.15%, 16.70%, and 13.7%, respectively.

The comparison of the proposed correlations and the previous correlations are also investigated. In case of the inline arrangement, it is found that Schmidt's correlation [5] can predicts 71.8% of the experimental data with in ±30%. This result comes from the lower Reynolds number of air stream of the experimental. Moreover, Schmidt's correlation did not include the effect of the geometrical of finned tube. Therefore, lower accuracy is obtained.

In case of the staggered arrangement, the correlations of Briggs and Young [1] and ESDU [4] give approximately 30% lower than the present correlation. The explanation of this result is the shape of the crimped spiral finned tube differs from that of the circular finned tube and the effect of crimped edge pronounce the heat transfer rate of the heat exchanger. The friction factor correlation of Robinson and Briggs [2] gives over predicting of the experimental value at low friction factor. However, at higher friction factor, the accuracy is close to that of the present correlation.

3.4 Conclusion

The present experimental study reports the airside performance of the crimped spiral fin heat exchanger. The effects of tube diameter, fin spacing, transverse tube pitch, and tube arrangements are examined. On the basis of previous discussions, the following conclusions are made:

5. For an inline arrangement, the pressure drops increase with the rise of tube diameter but the associated heat transfer coefficients decrease with it. The increase of fin height also gives rise to considerable increase of pressure drop but decrease of heat transfer coefficient.
6. For the inline arrangement, the effect of fin spacing on the airside performance varies with the transverse tube pitch. For a larger transverse tube pitch of 71.4 mm, there is an effect on heat transfer coefficient but no detectable influence of the fin spacing on frictional characteristics. It is likely that this phenomenon is related to the considerable airflow bypass between tube rows. On the contrary, at a smaller transverse tube pitch of 50 mm, one can see smaller fin spacing results in higher pressure drops and lower heat transfer coefficients.
7. For the staggered arrangement, the effect of tube diameter on the airside performance is analogous to that of inline arrangement but to a comparatively small extent. This is because the recirculation zone behind the tube row is much smaller in a staggered arrangement. The effect of the fin height on the pressure drops is much smaller than that of inline arrangement due to the major contribution to the pressure drops is from the blockage of the subsequent tube row in a staggered arrangement.
8. The effect of fin spacing on the airside performance for staggered arrangement also varies with the transverse tube pitch. For a smaller transverse tube pitch of 50 mm, there is no appreciable influence of the fin spacing on heat transfer. On the contrary, at a larger transverse tube pitch of 84 mm, one can see smaller fin spacing leads to lower heat transfer coefficients. This is also attributed to the presence of airflow pass effect.

6 Correlations of the present crimped spiral fins in both staggered and inline arrangement are developed. The proposed correlations give fairly good predictive ability against the present test data.

CHAPTER 4

AIR-SIDE PERFORMANCE OF HEAT EXCHANGER USING CRIMPED SPIRAL FINS, A CASE STUDY OF COOLING COIL

4.1 Introduction

For practical waste heat recovery system, the heat exchanger may accompany with condensation of moisture air on the heat exchanger surface. Although the designers try to avoid this situation due to considerably corrosive problem associated with it, condensation may still take place from time to time. This is commonly encountered if the load is not constant such as small boilers where the steam consumption varies with time and the flue gas temperature fluctuates in wide range. In that regard, the airside performance in the presence of dehumidification is rather important. Unfortunately, there are simply no data reported for the crimped spiral finned heat exchangers. Hence, it is the objective of this work is to report the heat transfer and friction characteristic of cross flow heat exchanger using crimped spiral fin in the presence of dehumidification. Moreover, the heat transfer and friction correlations are also developed in this work.

4.2 Data Reduction

The heat transfer rate of cross flow heat exchanger under dehumidifying condition can be calculated as follows:

$$Q_a = \dot{m}_a\left(i_{a,in} - i_{a,out}\right), \quad (4.1)$$

$$Q_w = \dot{m}_w C_{pw}\left(T_{w,out} - T_{w,in}\right). \quad (4.2)$$

Note that Equation (4.1) and Equation (4.2) denote heat transfer rate in the air-side and the tube-side, respectively. In this study, the mathematical average of the heat rate is used, i.e.,

$$Q_{avg} = 0.5(Q_a + Q_w). \quad (4.3)$$

The average heat transfer rate is related to the rate equation given in the following (enthalpy based potential),

$$Q_{avg} = U_{o,w} A_o F \Delta i_m . \quad (4.4)$$

Where F is the correction factor of unmixed/unmixed configuration.

The log-mean enthalpy potential Δi_m is (Threlkeld [18])

$$\Delta i_m = \frac{(i_{a,in} - i_{r,out}) - (i_{a,out} - i_{r,in})}{\ln\left(\dfrac{i_{a,in} - i_{r,out}}{i_{a,out} - i_{r,in}}\right)}. \tag{4.5}$$

Myers [19] derived the enthalpy-based overall heat transfer coefficient ($U_{o,w}$) to individual resistance as

$$\frac{1}{U_{o,w}} = \frac{b'_r A_o}{h_i A_{p,i}} + \frac{b'_p x_p A_o}{k_p A_{p,m}} + \frac{1}{h_{o,w}\left(\dfrac{A_{p,o}}{b'_{w,p} A_o} + \dfrac{A_f \eta_{f,wet}}{b'_{w,m} A_o}\right)}, \tag{4.6}$$

where

$$h_{o,w} = \frac{1}{\dfrac{C_{p,a}}{b'_{w,m} h_{c,o}} + \dfrac{y_w}{k_w}}. \tag{4.7}$$

Note that the ratio of water film thickness and thermal conductivity of water (y_w / k_w) is very small compared to other terms [20] and it is neglected in this study.

The tube side heat transfer coefficient can be calculated from Gnielinski correlation [11] as

$$h_i = \frac{(f_i/2)(\mathrm{Re}_{Di} - 1000)\mathrm{Pr}}{1.07 + 12.7\sqrt{f_i/2}\left(\mathrm{Pr}^{2/3} - 1\right)}\left(\frac{k_i}{d_i}\right), \tag{4.8}$$

where

$$f_i = \frac{1}{(1.58 \ln \mathrm{Re}_{Di} - 3.28)^2}. \tag{4.9}$$

The four quantities in Equation 4.7 can be estimated follow the method of Wang et al. [20] base on the enthalpy-temperature ratios. b'_r and b'_p, they can be calculated as

$$b'_r = \frac{i_{s,p,i,m} - i_{r,m}}{T_{p,i,m} - T_{r,m}}, \tag{4.10}$$

$$b'_p = \frac{i_{s,p,o,m} - i_{s,p,i,m}}{T_{p,o,m} - T_{p,i,m}}. \tag{4.11}$$

The quantity $b'_{w,p}$ is the slope of saturated enthalpy curve evaluated at the outer mean water film temperature at the base surface and can be approximated at the slope of saturated enthalpy curve evaluated at the base surface temperature of tube [20]. However, the quantity $b'_{w,m}$, which defines as the slope of saturated enthalpy curve evaluated at the outer mean water film temperature at the fin surface, can not be calculated directly.

Consequently, a trial and error procedure of iteration is needed (Wang et al. [20]) Detailed procedures are in the following:

1. Assume a value of $T_{w,m}$ and calculate the quantity $b'_{w,m}$
2. Calculate $h_{o,w}$ from Equation 4.6
3. Calculate the quantity $i_{s,w,m}$ by this following relation

$$i_{s,w,m} = i - \frac{C_{p,a} h_{o,w} \eta_{f,wet}}{b'_{w,m} h_{c,o}} \times \left(1 - U_{o,w} A_o \left[\frac{b'_r}{h_i A_{p,i}} + \frac{x_p b'_p}{k_p A_{p,m}}\right]\right)\left(i - i_{r,m}\right). \tag{4.15}$$

4. Determine the new $T_{w,m}$ at $i_{s,w,m}$ and repeat the procedure again until the torrance is met.

The wet fin efficiency is calculated as (Wang et al [20]):

$$\eta_{f,wet} = \frac{2r_i}{M_T\left(r_o^2 - r_i^2\right)} \times \left[\frac{K_1(M_T r_i) I_1(M_T r_o) - K_1(M_T r_o) I_1(M_T r_i)}{K_1(M_T r_o) I_o(M_T r_i) + K_o(M_T r_i) I_1(M_T r_o)}\right], \tag{4.16}$$

where

$$M_T = \sqrt{\frac{2h_{o,w}}{k_f f_t}} = \sqrt{\frac{2h_{c,o}}{k_f f_t}} \sqrt{\frac{b'_w}{C_{p,a}}}. \tag{4.17}$$

In this research work, the sensible heat transfer coefficient ($h_{c,o}$) and the pressure drop of air stream across tube bank are presented in terms of the Colburn factor (j) and the friction factor (f) factors,

$$j = \frac{h_{c,o}}{G_{max} C_{p,a}} \Pr^{2/3}, \tag{4.18}$$

$$f = \frac{A_{min}}{A_o} \frac{\rho_i}{\rho_m} \left[\frac{2\rho_i \Delta P}{G_c^2} - \left(1 + \sigma^2\right)\left(\frac{\rho_i}{\rho_o} - 1\right)\right]. \tag{4.19}$$

4.3 Results and Discussion

4.3.1 Staggered Arrangement

4.3.1.1 Pressure Drop

The associated pressure drops for all the test samples are shown in Figures 4.1-4.4. In Figure 4.1, the influence of tube diameter is examined. As seen in the figure, the pressure drops for wet condition is only slightly higher than that of dry condition. This is because the fin spacing in this figure is comparatively large (3.85 mm). In that respect, the condensate can easily drain without adhering to the interspacing of fins, thereby giving only a slight increase of pressure drops of the wet surface relative to dry conditions. However, one can find a considerable influence of tube size on the total pressure drop. For the same frontal velocity of 1.5 m/s, the associated pressure drop for d_o = 27.2 mm is roughly 2.5 times higher that of d_o = 17. 3 mm.

The effect of fin height on the total pressure drops is shown in Figure 4.2. The pressure drops increase with fin height because of more fin surface is provided. The effective surface area of f_h = 0.015 m is roughly 30% higher than that of f_h = 0.01 m and the corresponding increase of pressure drop is also around 30~40% which indicate a linear relationship of the fin height and total pressure drop. Conversely, one can go back to Figure 4.1 where the effective surface area increase caused by the tube size is less than 10% because the surface area is dominated by secondary surface (fins). However, the pressure drops is greatly increased with the tube size. The excess pressure drop are attributed to (1) large form drag of the large tube; and (2) ineffective flow separation zone behind the tube which may increase its influence to further downstream and results in more pressure drops associated with it. This phenomenon is analogous to the continuous fin pattern reported by Wang et al. [21].

The effect of fin spacing on the pressure drops is shown in Figure 4.4. Notice that there is very small difference between dry and wet conditions since the tube diameter and fin height is relatively small which in term helps to drain the water condensate. Again smaller fin spacing increases the effective surface area and correspondingly higher pressure drops. In essence, the pressure drop increases with tube diameter (d_o), fin height (f_h) and decrease with it for a smaller fin spacing (f_s). Among them, the influence of tube diameter is most pronounced. The effect of tube arrangement is also found in Figure 4.3-4.4. Higher transverse pitch of tube bank (S_t) gives rise to lower pressure drop. Again this is also attributed to the increase of surface area. The relevant influences of geometric parameters on the friction characteristics are correlated in terms of friction factor, and is given as,

$$f = 17.02\,\mathrm{Re}_D^{-0.5636}\left(\frac{d_o}{S_t}\right)^{0.3956}\left(\frac{f_t}{f_s}\right)^{-0.3728}\left(\frac{S_l}{S_t}\right)^{1.2804}\left(\frac{d_o}{d_f}\right)^{-0.1738} \qquad (4.20)$$

From Figure 4.5, one can see the proposed friction factor correlation can predict 75% of the experimental data within ±15% accuracy.

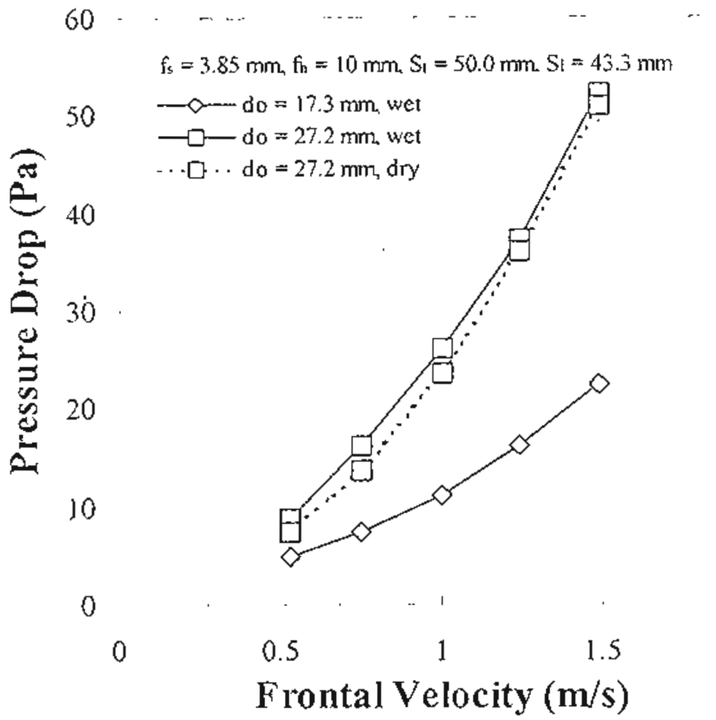

Figure 4.1 Comparisons of the pressure drop in dry and wet condition in case of different tube diameter.

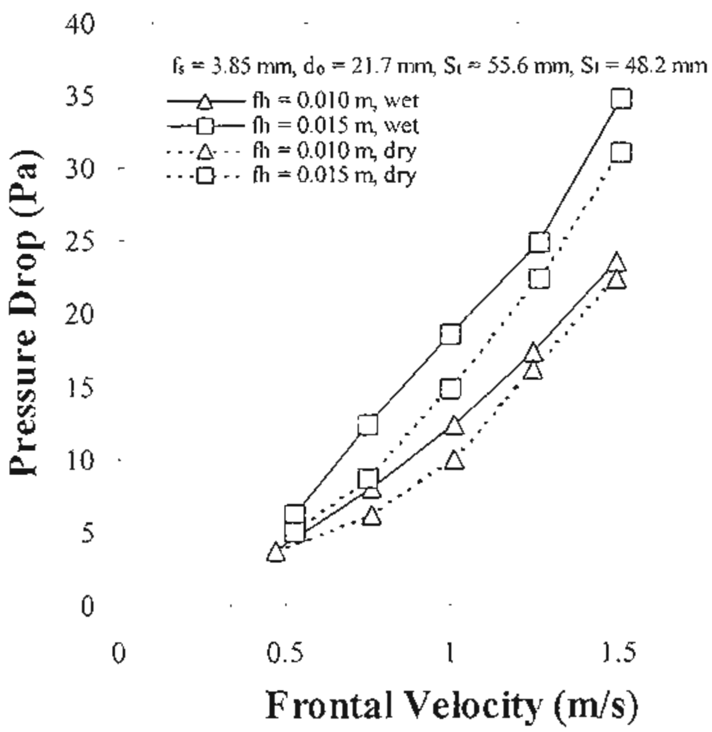

Figure 4.2 Comparisons of the pressure drop in dry and wet condition in case of different fin height.

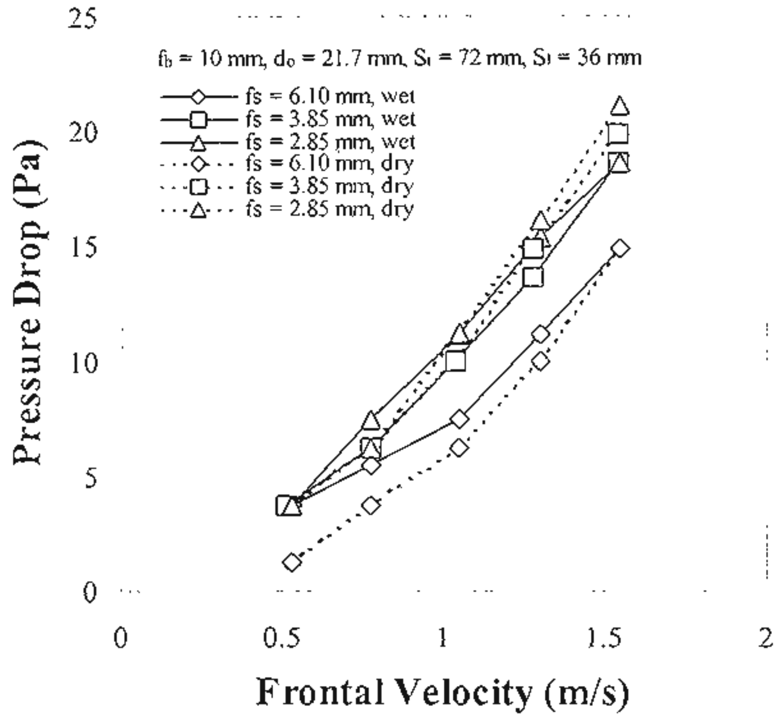

Figure 4.3 Comparisons of the pressure drop in dry and wet condition in case of different fin spacing at S_t = 72 mm and S_l = 36 mm.

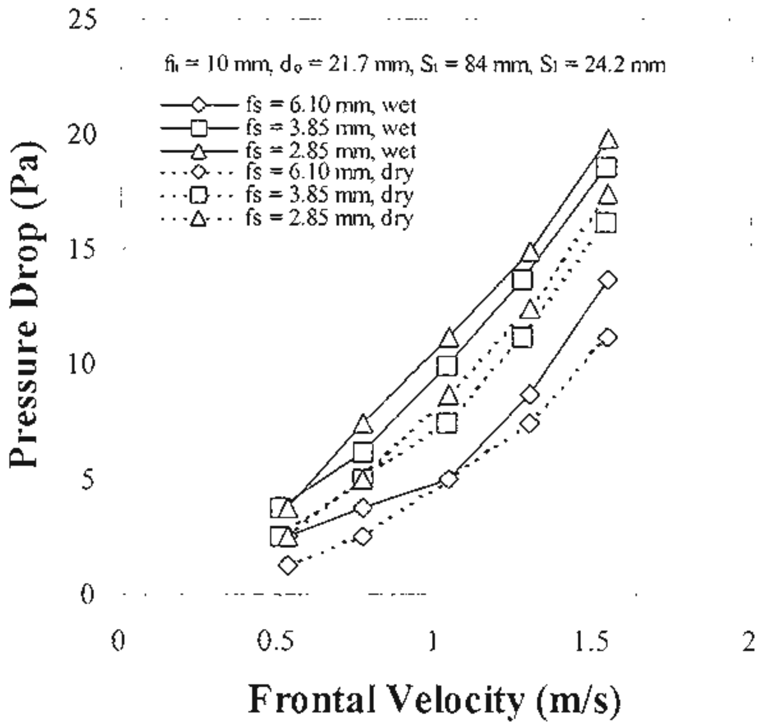

Figure 4.4 Comparisons of the pressure drop in dry and wet condition in case of different fin spacing at S_t = 84 mm and S_l = 24.2 mm.

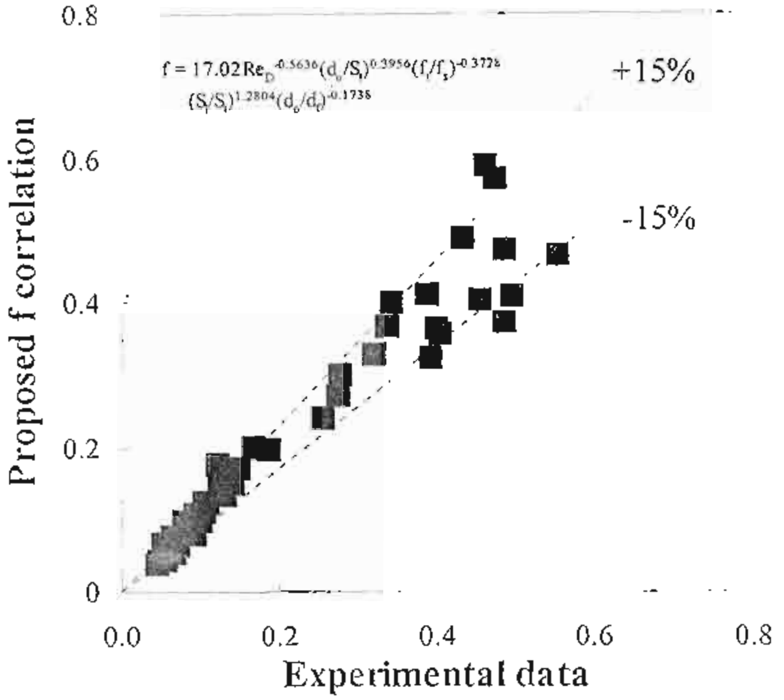

Figure 4.5 Comparison of the frictional data with the proposed correlation.

4.3.1.2 Sensible heat transfer coefficient

The related heat transfer coefficients vs. frontal velocity for all the test samples are shown in Figures 4.6-4.10. For comparison purpose, the relevant heat transfer coefficient in dry condition is also shown in the figure. It is found that the heat transfer coefficient of wet surface is slightly lower than that of dry surface. Actually, there are many studies showing the comparison of the heat transfer coefficients between wet and dry surface heat exchanger. Some studies indicated that the heat transfer coefficient is augmented in wet surface conditions, such as Myers [19], Elmahdy [22] and Eckels and Rabas [23] who reported results for the continuous plate finned tube. These investigators argued that the presence of water condensate may roughen the heat transfer surface, leading to higher heat transfer coefficient. However, some of the studies showed a drop of heat transfer coefficient of wet surface, such as the wavy finned tube heat exchanger by Mirth and Ramadhyani [24] who reported about 17-50% decreasing of heat transfer coefficient of wet surface. One possible cause of the degradation is due to water film resistance and condensate blocking. Moreover Wang et al. [20] shows the decreasing of the Colburn j factor of plate finned tube heat exchangers when the Reynolds number lower than 2,000. However, at the higher Reynolds number, the j factor of wet surface is slightly higher than that of dry surface. The present results are generally in agreement with the trend of Wang et al. [20].

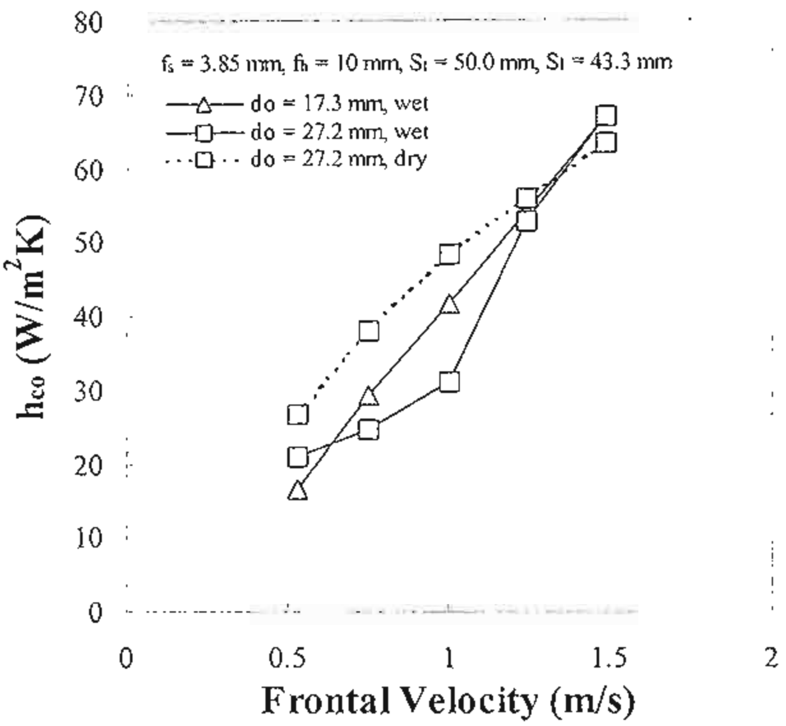

Figure 4.6 Comparisons of the heat transfer coefficient in dry and wet condition in case of different tube diameter.

The effect of tube diameter on the heat transfer performance is shows in Figure 4.6, it is found that the larger tube diameter (d_o = 27.2 mm) has a lower heat transfer coefficient than that of the small one (d_o = 17.3 mm). This phenomenon is attributed to the ineffective area behind the tube increases with the tube diameter. Wang et al. [15] performed flow visualizations via dye injection technique for fin-and-tube heat exchangers having inline arrangement. Their visual results unveil a very huge flow circulation behind the tube row. Consequently this huge recirculation not only contributes to the decrease of heat transfer coefficient but also to the rise of pressure drop as shown in the preceding discussions. In addition, the huge recirculation may also block the subsequent tube row and degrade the heat transfer performance hereafter.

Figure 4.7 shows the effect of fin height on the heat transfer coefficient. As seen in the figure, the influence of the fin height is negligible in wet condition. For the fully dry case, the previous chapter reports the 15 mm fin height gives lower heat transfer coefficient than that of 10 mm. This result comes from the airflow by pass effect. Actually the airflow is prone to flowing the portion where the flow resistance is small. In case of f_h = 15 mm, the airflow resistance across the finned tube portion is larger than that of f_h = 10 mm. Therefore, part of the directed airflow just bypass the tube row without effective contribution to the heat transfer, hence showing a lower heat transfer coefficient. However, in case of wet surface, the condensate of water vapor covering the surface of heat exchanger become dominant and it increases the airflow resistance around tube. Therefore the effect of fin height is comparatively reduced.

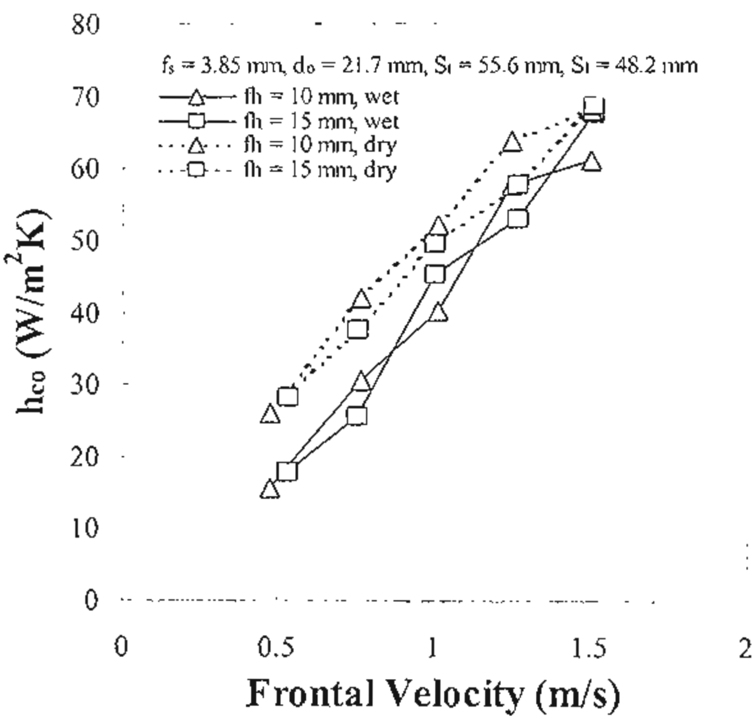

Figure 4.7 Comparisons of the heat transfer coefficient in dry and wet condition in case of different fin height.

The effect of fin spacing shown in Figures 4.8 and 4.9. As seen in the figure, the effect of fin spacing is small. However, small fin spacing tends to have lower heat transfer coefficient, and this is particularly pronounced in Figure 4.9 where S_t = 84 mm and S_l = 24.2 mm. This result may be related to the water condensate effect. The presence of water condensate increases the air flow resistances into the heat exchanger, thereby causing more airflow to bypass. This phenomenon becomes more significant with S_t = 84 mm because more bypass airflow. In that regard, one can see a moderately decrease of heat transfer coefficient at smaller fin spacing. The reports of McQuiston [25,26] also show the decreasing of sensible heat transfer coefficient when the fin density is higher than 10 fins per inch.

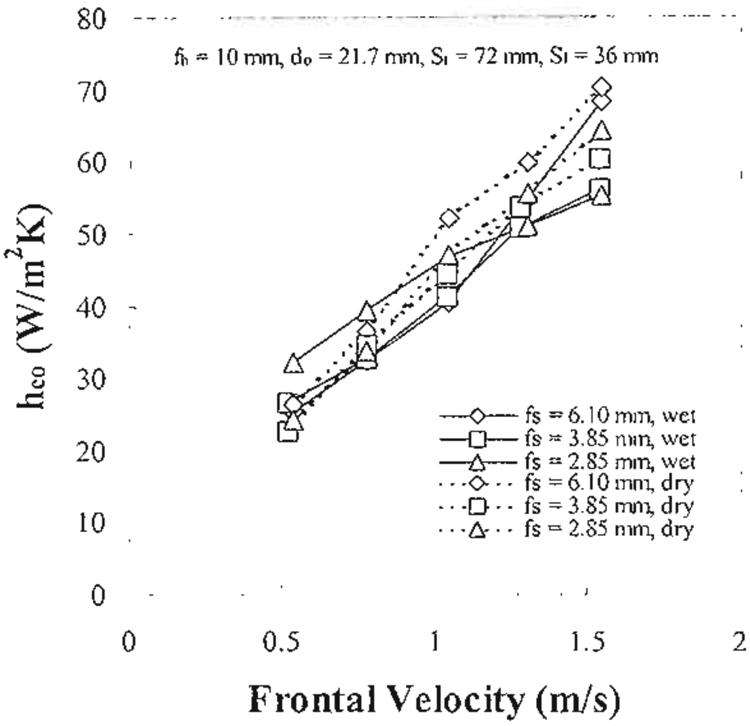

Figure 4.8 Comparisons of the heat transfer coefficient in dry and wet condition in case of different fin spacing at S_t = 72 mm and S_l = 36 mm.

Figure 4.10 shows the effect of tube arrangement on the sensible heat transfer coefficient. It is found that higher transverse tube pitch tends to have lower heat transfer coefficient and again this result is attributed to the airflow bypass effect. In case of S_t = 84 mm and S_l = 24.2 mm, more airflow is prone to flowing across the space between adjacent tube. Therefore, the amount of air stream contributed to the heat transfer is decreased when compared to that of S_t = 72 mm and S_l = 36 mm.

The associated effect of geometric parameters on the heat transfer performance are correlated in terms of the Colburn j factor, and is given as,

$$j = 0.0208\,\mathrm{Re}_D^m \left(\frac{d_o}{S_t}\right)^{-2.5950} \left(\frac{f_t}{f_s}\right)^{0.7905} \left(\frac{S_l}{S_t}\right)^{0.2391} \left(\frac{d_o}{d_f}\right)^{0.2761} \qquad (4.21)$$

where

$$m = -0.2871 + 0.5322\left(\frac{d_o}{S_t}\right) - 1.2856\left(\frac{f_t}{f_s}\right) + 0.1845\left(\frac{S_l}{S_t}\right). \qquad (4.22)$$

In Figure 4.11, one can see the proposed j correlation can predict 95% of the experimental data within ±15% accuracy.

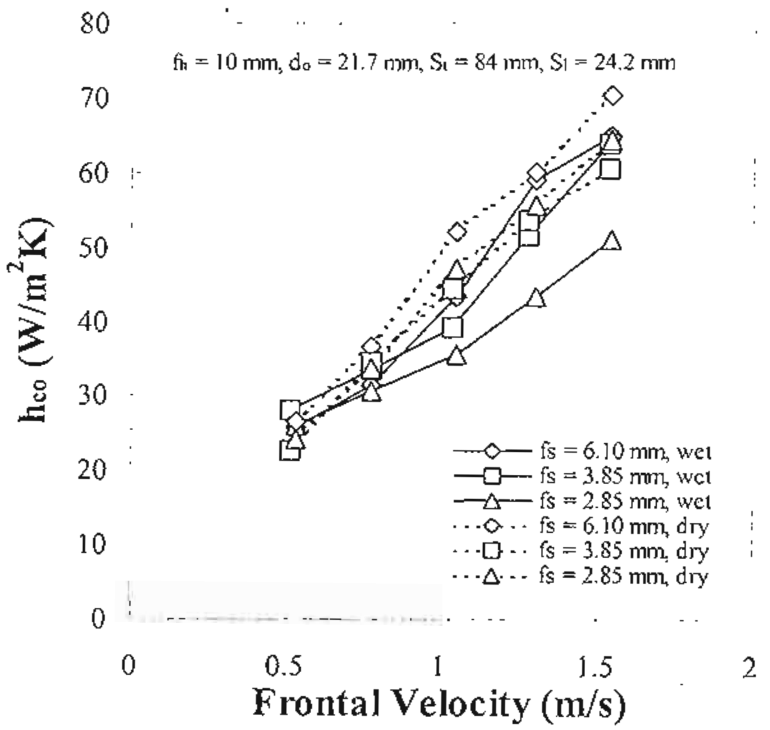

Figure 4.9 Comparisons of the heat transfer coefficient in dry and wet condition in case of different fin spacing at S_t = 84 mm and S_l = 24.2 mm.

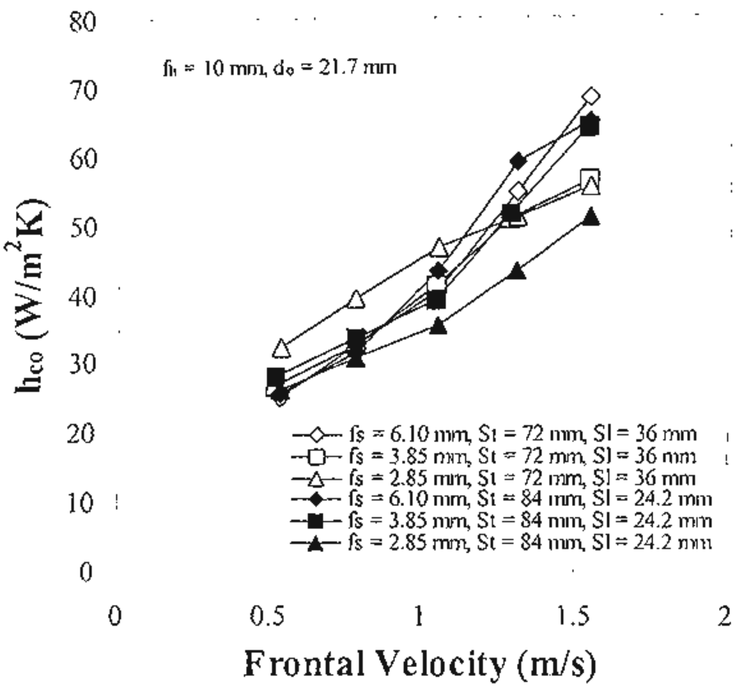

Figure 4.10 Comparisons of the heat transfer coefficient in wet condition in case of different tube arrangement.

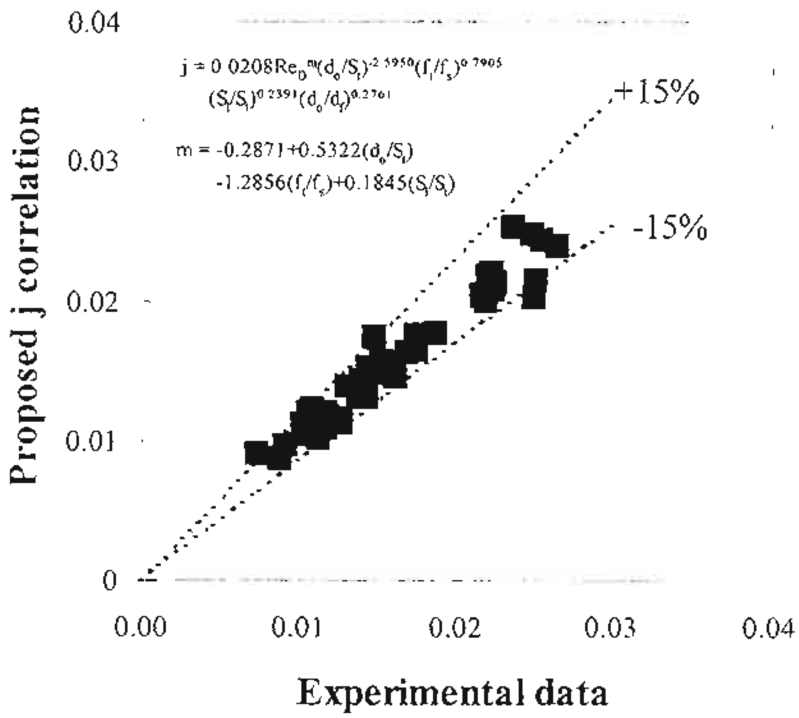

Figure 4.11 Comparison of the heat transfer data with the proposed correlation.

4.3.2 Inline Arrangement

4.3.2.1 Pressure Drop

Figures 4.12-4.15 show the air stream pressure drops in the cross flow heat exchanger. It is found that the air stream pressure drop increases with the frontal velocity of air. Moreover, when compare with the result obtained from previous chapter in the case of dry surface heat exchanger, the pressure drop is slightly higher than that of dry surface. This is because only small amount of water vapor is condensed on the heat exchanger surface.

Figures 4.12-4.14 also show the pressure drop increases with tube diameter (d_o) and fin height (f_h). However, it decreases with the increasing of fin spacing (f_s). These phenomena come from the increasing of surface area resulted in higher the airflow resistance. The effect of tube arrangement is also found in Figure 4.15. Higher transverse pitch of tube bank (S_t) gives lower pressure drop.

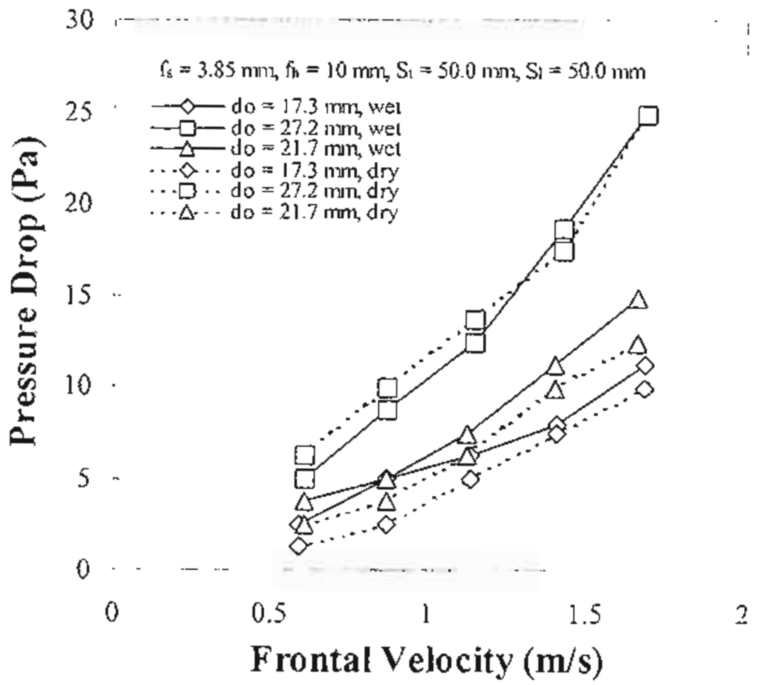

Figure 4.12 Effect of tube diameter on the pressure drop.

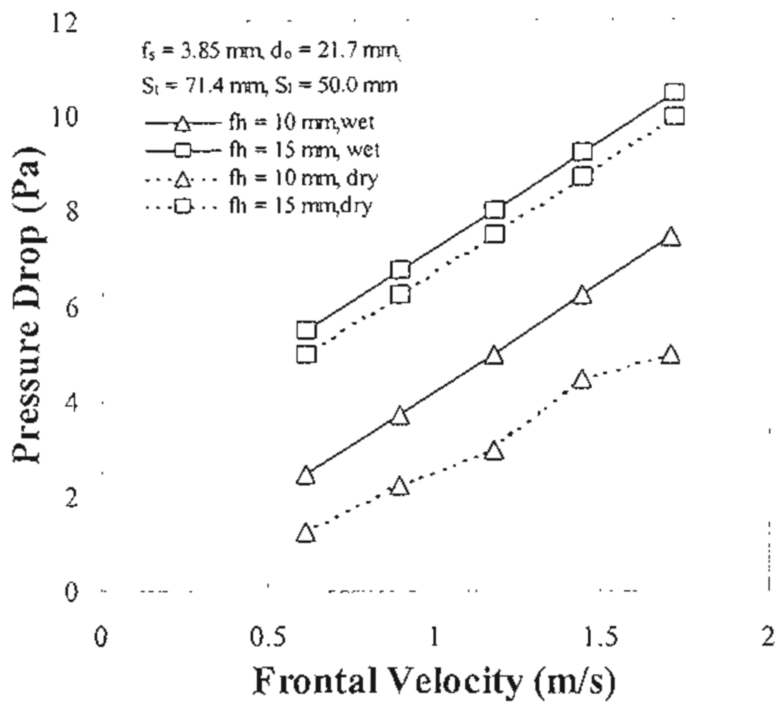

Figure 4.13 Effect of fin height on the pressure drop.

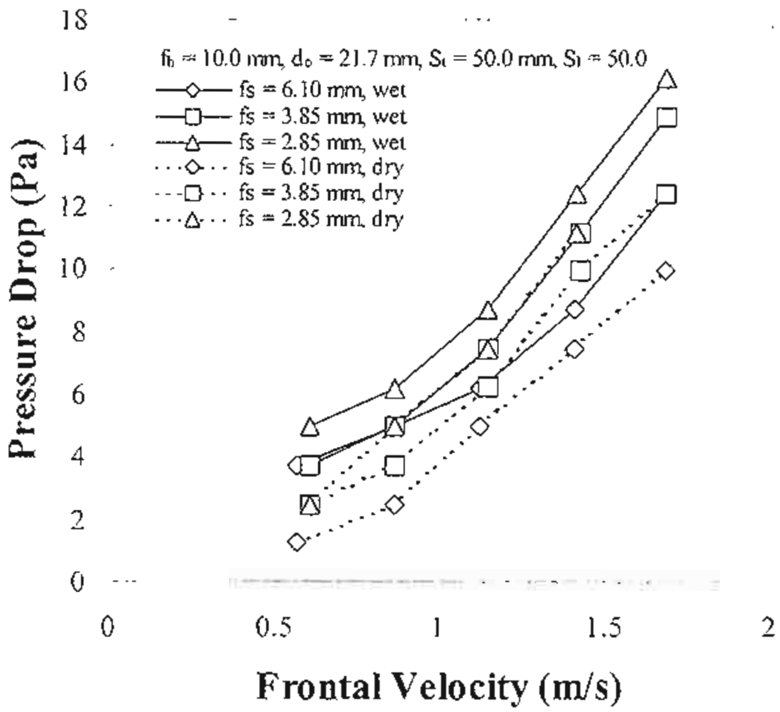

Figure 4.14 Effect of fin spacing on the pressure drop.

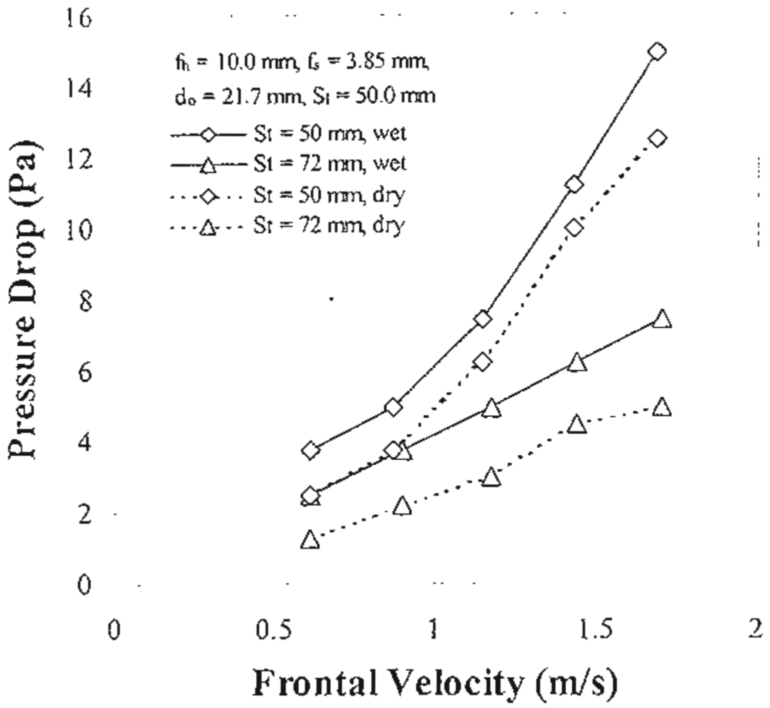

Figure 4.15 Effect of transverse pitch on the pressure drop.

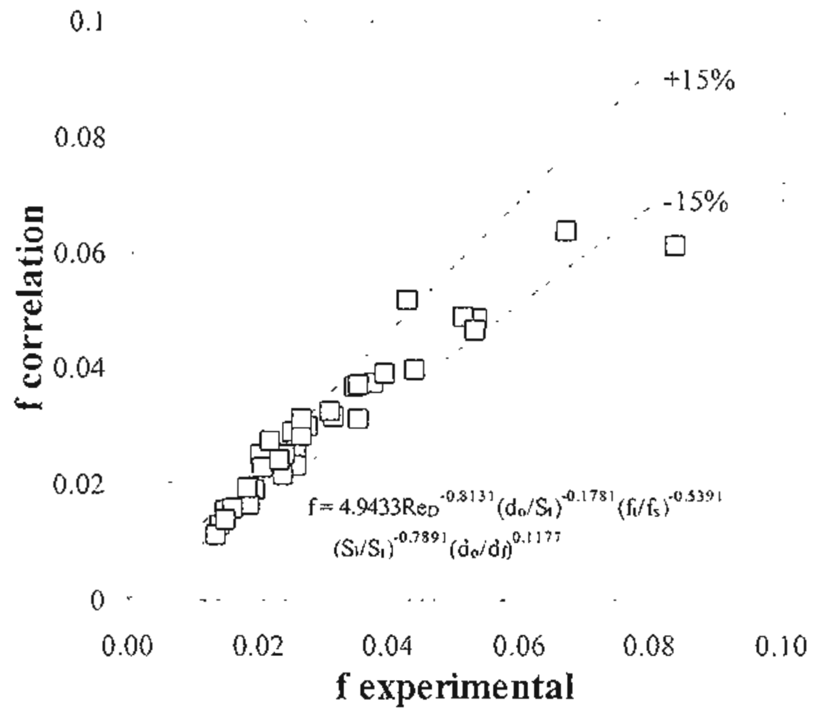

Figure 4.16 The comparison of f factor from experiment and correlation.

In this research, the correlation for predicting the air stream pressure drop including the effect of various quantities is also developed and the model is in a form of

$$f = 4.9433\,\mathrm{Re}_D^{-0.8131}\left(\frac{d_o}{S_t}\right)^{-0.1781}\left(\frac{f_t}{f_s}\right)^{-0.5391}\left(\frac{S_l}{S_t}\right)^{-0.7891}\left(\frac{d_o}{d_f}\right)^{0.1177} \quad (4.23)$$

From Figure 4.16, it is found that the f model can predict about 82.3% of the experimental data within ±15% accuracy.

4.3.2.2 Sensible heat transfer coefficient

Figure 4.17 shows the effect of tube diameter on the sensible heat transfer coefficient at various frontal velocities of air stream. The fin spacing (3.85 mm), fin thickness (0.4 mm), and the fin height (10 mm) are taken for this comparison. The transverse and the longitudinal tube pitches are 50 mm. As expected, the heat transfer coefficient rises with the frontal velocity. However, it is interesting to note that the heat transfer coefficient increases with the reduction of tube diameter. This phenomenon is attributed to the ineffective area behind the tube which increases with the tube diameter especially, the inline arrangement. Wang et al. [15] performed flow visualizations via dye injection technique for fin-and-tube heat exchangers having inline arrangement. Their visual results unveil a very large flow circulation behind the tube row. Consequently this large recirculation does not only contribute to the decrease of heat transfer coefficient but also to the rise of pressure drop. In addition, the large recirculation may also block the subsequent tube row and degrades the heat transfer performance hereafter.

Figure 4.19 shows the effect of fin height on the airside performance for inline arrangement. In this comparison, the associated fin heights are 10 and 15 mm and the fin spacing and the tube diameter are 3.85 mm and 21.7 mm with the transverse and the longitudinal pitches are 71.4 and 50 mm, respectively. As seen in the figure, the influence of fin height shows tremendous influence on the heat transfer performance. The heat transfer coefficients drop drastically with the increase of fin height. This is probably due to the airflow bypass effect. Actually the airflow is prone to flowing the portion where the flow resistance is small. In case of f_h = 15 mm, the airflow resistance around fin tube is larger than that for f_h = 10 mm. Therefore, part of the directed airflow just bypasses the tube row without effective contribution to the heat transfer and lower heat transfer coefficient is obtained.

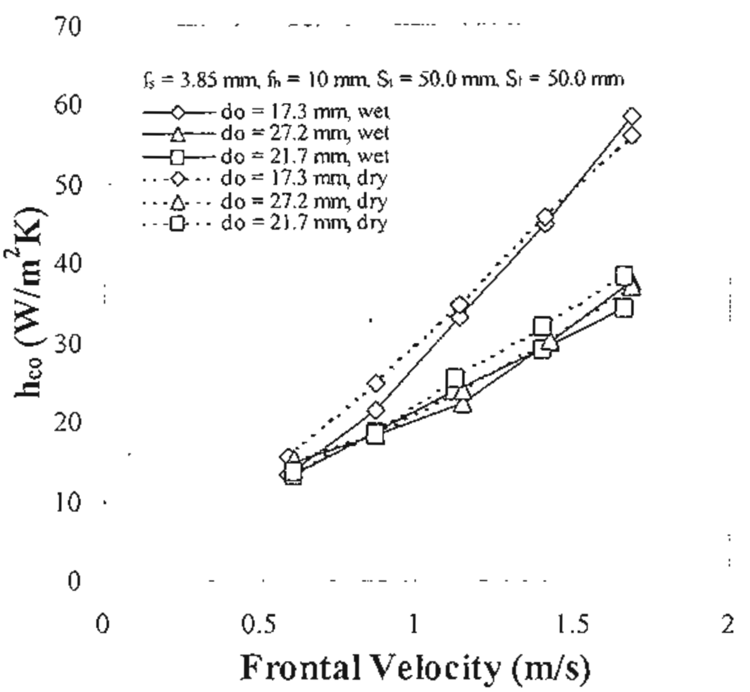

Figure 4.17 Effect of tube diameter on the sensible heat transfer coefficient.

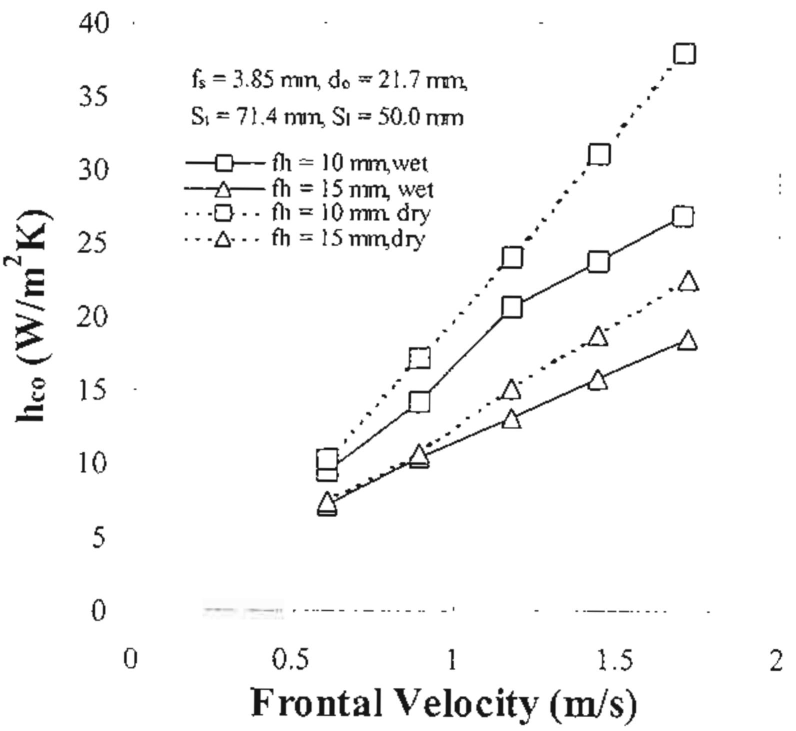

Figure 4.18 Effect of fin height on the sensible heat transfer coefficient.

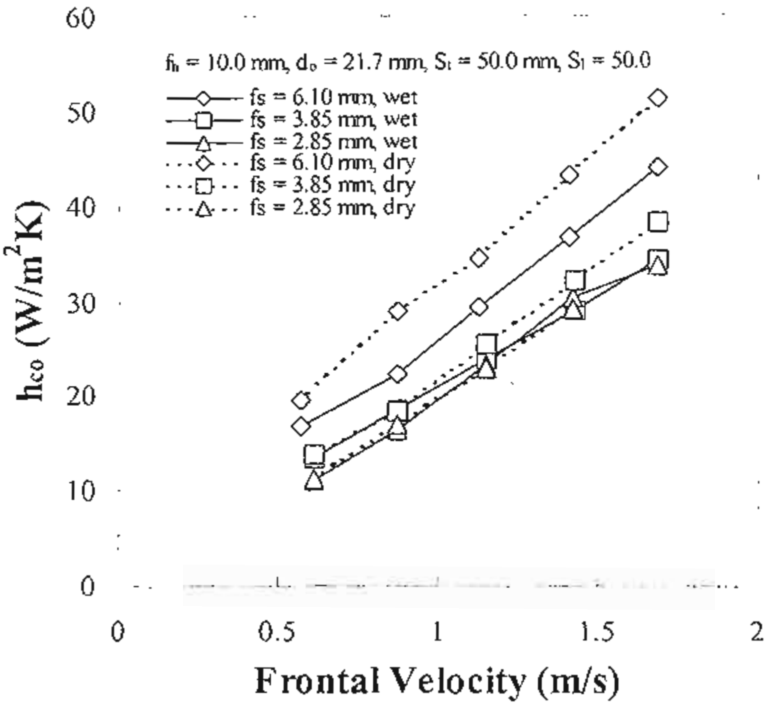

Figure 4.19 Effect of fin spacing on the sensible heat transfer coefficient.

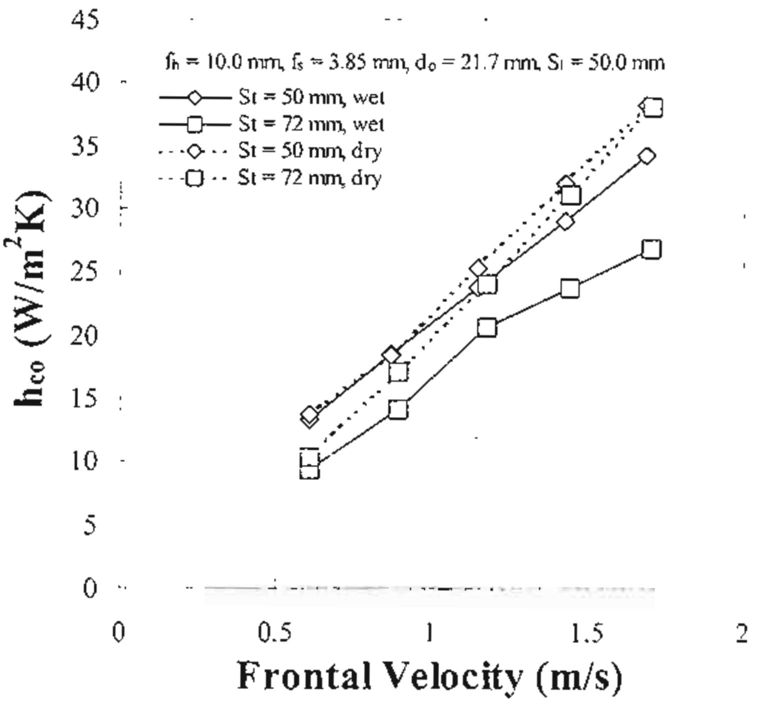

Figure 4.20 Effect of transverse pitch on the sensible heat transfer coefficient.

The effect of the fin spacing on the airside performance is shown in Figure 4.19. It was found that the increase of fin spacing gives a rise to the heat transfer coefficient. An explanation of this phenomenon is the same as that in the previous case which concludes that the result comes from the airflow bypass effect. The result of airflow bypass effect is also shown in Figure 4.20. It can be seen that the high transverse tube pitch (S_t = 71.4 mm) gives lower heat transfer coefficient than that of the low value (S_t = 50 mm).

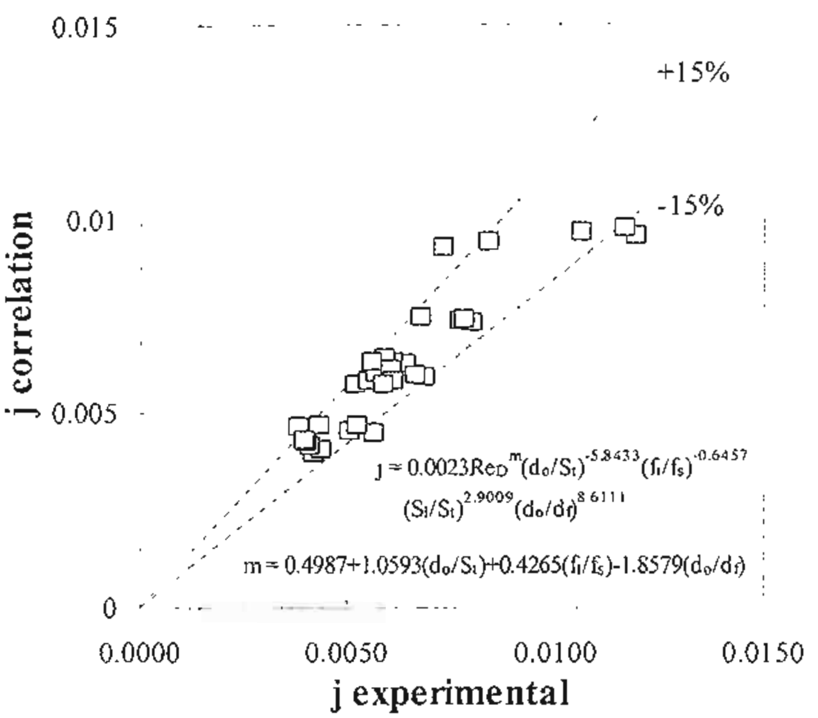

Figure 4.21 The comparison of j factor from experiment and correlation.

Comparison of the heat transfer coefficient under dehumidifying process with that of non-dehumidifying condition is also shown in Figures 4.17-4.20. The heat transfer phenomena of the wet surface heat exchanger are close to those of the dry surface. However, the heat transfer coefficient of the wet surface is lower than that of dry surface. The explanation is the same as the staggered arrangement that the present results are generally in agreement with the trend of Wang et al. [20].

In this research, the correlation for predicting the Colburn j factor including the effect of various quantities is also developed and the model is

$$j = 0.0023\,\mathrm{Re}_D^m\left(\frac{d_o}{S_t}\right)^{-5.8433}\left(\frac{f_l}{f_s}\right)^{-0.6457}\left(\frac{S_l}{S_t}\right)^{2.9009}\left(\frac{d_o}{d_f}\right)^{8.6111}, \qquad (4.24)$$

where

$$m = 0.4987 + 1.0593\left(\frac{d_o}{S_t}\right) + 0.4265\left(\frac{f_t}{f_s}\right) - 1.8579\left(\frac{d_o}{d_f}\right). \quad (4.25)$$

It is found that the j model can predict about 85.7% of the experimental data within ±15% accuracy. The comparison is also shown in Figure 4.21.

4.4 Conclusion

This study experimentally investigated the airside performance of a cross flow heat exchangers having crimped spiral configurations under the dehumidification. The effects of tube diameter, fin spacing, transverse tube pitch are examined. Based on the experimental observations, the following results are concluded:

8. The pressure drop of wet surface heat exchanger increases with the mass flow rate of air and the result is slightly higher or close to that of dry surface because only water condensate can be easily drained in the present comparatively large fin spacing and individual finned configuration.
9. The heat transfer coefficient of wet surface is slightly lower than that of dry surface.
10. The effect of tube diameter on the airside performance is significant. Larger tube diameter not only gives rise to lower heat transfer coefficient but also contribute significantly to the increase of pressure drops. This phenomenon is applicable in both dry and wet condition.
11. For wet surface, the influence of fin height is negligible whereas there is a small effect in dry surface.
12. The effect of fin spacing on the heat transfer performance is rather small. However, the increasing of fin spacing tends to have a lower heat transfer coefficient.
13. The tube arrangement plays an importance role on the heat transfer coefficient, the lower transverse pitch gives the higher heat transfer coefficient.
14. Airside performance in the present study is presented in terms of f and the j factor. The proposed correlations in case of staggered arrangement can predict 75% and 95% of experimental data within ±15%. In case of inline arrangement, the proposed correlations can predict the j and the f factors can estimated about 85.7% and 82.3% of experimental data within ±15% accuracy.

CHAPTER 5
RESEARCH OUTPUT

The output of this research work can be classified into two groups. The first group is the advantage of this work that can help the designer who design the cross flow heat exchanger using crimped spiral finned tube producing from Thai industry.

The second output of this work is the publication. The researchers published the research result as follows:

The international journal

1. Nuntaphan A., Kiatsiriroat T., Wang C.C., Airside Performance at Low Reynolds Number of Cross Flow Heat Exchanger Using Crimped Spiral Fins, Int. Communications in Heat and Mass Transfer, Accepted.
2. Nuntaphan A., Kiatsiriroat T., Wang C.C., Heat Transfer and Friction Characteristics of Crimped Spiral Finned Heat Exchangers With Dehumidification, Applied Thermal Engineering, Submitted.

The national journal

1. Nuntaphan A., Kiatsiriroat T., Thermal Behavior of Crimped Spiral Fin Tube Bank Under Dehumidifying Process: A Case Study of Inline Arrangement, Songklanakarin J. of Sci. and Tech., Accepted

Conference

1. Nuntaphan A., Kiatsiriroat T., Heat Transfer Characteristic of Cross Flow Heat Exchanger Using Crimped Spiral Fins a Case Study of Staggered Arrangement, 17^{th} Conference on Mechanical Engineering Network of Thailand, Prachinburi, 2003
2. Nuntaphan A., Kiatsiriroat T., Air-side Heat Transfer Coefficient of Thermosyphon Heat Pipe with Crimped Spiral Fins: a Case Study of Staggered Arrangement, 2^{nd} Conference on Heat and Mass Transfer in Thermal Equipment, Chiang Mai, 2003

The detail of each paper is shown in the appendix.

REFERENCES

1. Briggs, D.E., and Young, E.M., 1963, Convection Heat Transfer and Pressure Drop of Air Flowing Across Triangular Pitch Banks of Finned Tubes, Chemical Engineering Progress Symposium Series, 59(41), 1-10.
2. Robinson, K.K., and Briggs, D.E., 1966, Pressure Drop of Air Flowing Across Triangular Pitch Banks of Finned Tubes, Chemical Engineering Progress Symposium Series, 62(64), 117-184.
3. Rabas, T.J., Eckels, P.W., and Sabatino, R.A., 1981, The Effect of Fim Density on the Heat Transfer and Pressure Drop Performance of Low Finned Tube Banks, Chemical Engineering Communications, 10(1), 127-147
4. ESDU International plc., 1986, High-fin Staggered tube Banks: Heat Transfer and Pressure Drop for Turbulent Single Phase Gas Flow, ESDU Item 86022.
5. Schmidt, T.E., 1987, Der warmenbergeng an rippensohen and die berechnung von rohrundel war me austauschern Kaltetech, 15(4), 98; 15(2), 370
6. ANSI/ASHRAE 41.1-1986, 1986, Standard Method for Temperature Measurement, American Society of Heating, Refrigerating, and Air-Conditioning Engineers, Inc.
7. ANSI/ASHRAE41.2-1987, 1987, Standard Method for Laboratory Air-flow Measurement, American Society of Heating, Refrigerating, and Air-Conditioning Engineers, Inc.
8. ANSI/ASHRAE 41.3-1989, 1989, Standard Method for Pressure Measurement, American Society of Heating, Refrigerating, and Air-Conditioning Engineers, Inc.
9. ANSI/ARI 410-81, 1981. Standard for Forced Circulation Air-cooling and Air-heating Coils, American National Standard
10. ESDU International plc., 1991, Effectiveness – NTU Relationships for the Design and Performance Evaluation of Two-Stream Heat Exchangers, ESDU Item 86018.
11. Gnielinski V., 1976, New Equation for Heat and Mass Transfer in Turbulent Pipe and Channel Flow, Int. Chem. Engng, 16, 359-368.
12. Schmidt, Th.E., 1949, Heat Transfer Calculation for Extended Surfaces, Refrigeration Engineering, 351-357.
13. Hewitt G.F., Shires G.L. and Bott T.R., 1994, Process Heat Transfer, Boca Raton, CRC Press, USA.

14. Wang, C.C., Lou, J., Lin, Y.T. and Liu, M.S., 2002, Flow Visualization of Wave-type Vortex Generators Having Inline Fin-tube Arrangement, Int. J. of Heat and Mass Transfer, 45, 1933-1944.
15. Wang, C.C., Lou, J., Lin, Y.T. and Wei, C.S., 2002, Flow Visualization of Annular and Delta Winlet Vortex Generators in Fin-and-tube Heat Exchanger Application, Int. J. of Heat and Mass Transfer, 45, 3803-3815.
16. Rich, D.G., 1973, ASHRAE Transactions, 79(2), 137-145.
17. Wang, C.C., Chang, Y.J., Hsieh, Y.J. and Lin, Y.T., 1996, Sensible heat and friction characteristics of plate fin-and-tube heat exchangers having plane fins, Int. J. of Refrigeration, 19, 223-230.
18. Threlkeld J. L., 1970, Thermal Environmental Engineering, Prentice-Hall Inc., New York.
19. Myers R.J., 1967, The Effect of Dehumidification on the Air-side heat Transfer Coefficient for a Finned-tube Coil, M.S. Thesis, University of Minnesota, Minneapolis.
20. Wang C.C, Hsieh Y.C., Lin Y.T., 1997, Performance of Plate Finned Tube Heat Exchanger Under Dehumidifying Conditions, ASME Journal of Heat Transfer 119, 109-119.
21. Wang C.C., Chang Y.P, Chi K.Y., Chang Y.J., 1998, An Experimental Study of Heat Transfer and Friction Characteristics of Typical Louver Fin and Tube Heat Exchangers, Int. J. of Heat and Mass Transfer 41(4-5), 817-822.
22. Elmahdy A.H., 1975, Analytical and Experimental Multi-row, Finned-tube Heat Exchanger Performance during Cooling and Dehumidification Process, Ph.D. thesis, Carleton University, Ottawa, Canada.
23. Eckels P.W., Rabas T.J., 1987, Dehumidification: on the Correlation of Wet and Dry Transport Process in Plate Finned-tube Heat Exchangers, ASME Journal of Heat Transfer 109, 572-582.
24. Mirth D.R.. Ramadhyani S., 1993, Prediction of Cooling-coils Performance Under Condensing Conditions, International Journal of Heat and Fluid Flow, 14(4), 391-400.
25. McQuiston F.C., 1978, Heat mass and Momentum Transfer Data for Five Plate-fin Tube Transfer Surface, ASHRAE Transactions 84(1), 266-293.
26. McQuiston F.C. , 1978, Correlation of Heat mass and Momentum Transport Coefficients for Plate-fin Tube Transfer Surfaces with Staggered Tubes, ASHRAE Transactions 84(1) 294-309.

APPENDIX

PUBLICATIONS

1. Nuntaphan A., Kiatsiriroat T., Wang C.C., Airside Performance at Low Reynolds Number of Cross Flow Heat Exchanger Using Crimped Spiral Fins, Int. Communications in Heat and Mass Transfer, Accepted.
2. Nuntaphan A., Kiatsiriroat T., Wang C.C., Heat Transfer and Friction Characteristics of Crimped Spiral Finned Heat Exchangers With Dehumidification, Applied Thermal Engineering, Submitted.
3. Nuntaphan A., Kiatsiriroat T., Thermal Behavior of Crimped Spiral Fin Tube Bank Under Dehumidifying Process: A Case Study of Inline Arrangement, Songklanakarin J. of Sci. and Tech., Accepted
4. Nuntaphan A., Kiatsiriroat T., Heat Transfer Characteristic of Cross Flow Heat Exchanger Using Crimped Spiral Fins a Case Study of Staggered Arrangement, 17th Conference on Mechanical Engineering Network of Thailand, Prachinburi, 2003
5. Nuntaphan A., Kiatsiriroat T., Air-side Heat Transfer Coefficient of Thermosyphon Heat Pipe with Crimped Spiral Fins: a Case Study of Staggered Arrangement, 2nd Conference on Heat and Mass Transfer in Thermal Equipment, Chiang Mai, 2003

ELSEVIER SCIENCE

INTERNATIONAL JOURNAL OF HEAT AND MASS TRANSFER
INTERNATIONAL COMMUNICATIONS IN HEAT AND MASS TRANSFER

Professor J.P. Hartnett, *Editor*
University of Illinois at Chicago
Energy Resources Center (M/C 156)
851 South Morgan Street, 1227 SEO
Chicago, Illinois 60607-7054

Professor W.J. Minkowycz, *Editor*
University of Illinois at Chicago
Mechanical Engineering (M/C 251)
842 West Taylor Street, 2049 ERF
Chicago, Illinois 60607-7022
Tel: (312) 996-3467
Fax: (312) 413-0447
E-mail: wjm@uic.edu

January 15, 2004

Dr. Atipoang Nuntaphan
Mae Moh Training Center
Electricity Generating Authority of Thailand
Mae-Moh, Lampang 52220
Thailand

Subj: Ms. #CJ03/2732 — "Air-Side Performance at Low Reynolds Number of Cross Flow Heat Exchanger Using Crimped Spiral Fins" by A. Nuntaphan, T. Kiatsiriroat, and C.C. Wang

Dear Dr. Nuntaphan:

Thank you for the above-referenced manuscript which you have submitted for possible publication in the **International Communications in Heat and Mass Transfer**. I am pleased to advise you that the reviews are favorable and therefore I intend to accept your work for the journal. However, before I can schedule it for a particular issue, the enclosed Transfer of Copyright Agreement must be filled out, signed and returned to this office.

Thank you for your cooperation and interest in the **Communications** journal.

Sincerely yours,

W.J. Minkowycz
Coordinating Editor and
Professor of Mechanical Engineering

WJM:rms
enclosure

AIR-SIDE PERFORMANCE AT LOW REYNOLDS NUMBER OF CROSS FLOW HEAT EXCHANGER USING CRIMPED SPIRAL FINS

A. Nuntaphan
South East Asia Center for Training in Energy for Development
Electricity Generating Authority of Thailand
Mae Moh Lampang 52220 Thailand

T. Kiatsiriroat
Department of Mechanical Engineering, Chiang Mai University
Chiang Mai 50202 Thailand

C.C. Wang
Energy & Resources Laboratories, Industrial Technology Research Institute
Hsinchu, Taiwan 310, R.O.C.

ABSTRACT

A total of 23 cross flow heat exchangers having crimped spiral configurations is studied. The effect of tube diameter, fin spacing, transverse tube pitch, and tube arrangements are examined. For the inline arrangement, the pressure drop increases with the rise of tube diameter but the associated heat transfer coefficient decreases with it. The increase of fin height also gives rise to considerable increase of pressure drop and decrease of heat transfer coefficients for the inline arrangement. However, for the staggered arrangement, the effect of the fin height on the pressure drop is much smaller than that of the inline arrangement due to the major contribution to the total pressure drops from the blockage of the airflow from staggered arrangement. Effect of the fin spacing on the airside performance is strongly related to the transverse tube pitch for both inline and staggered arrangements. Correlations of the present crimped spiral fins in both staggered and inline arrangements are developed. The proposed correlations give fairly good predictive ability against the present test data.

Introduction

There are many types of heat exchanger applicable to the recovery of waste heat such as shell-and-tube, plate, and cross-flow heat exchangers. Among them, the cross flow type is especially suitable for recovering heat from high the temperature air. Normally, the liquid always flows inside the tube whereas the gas flows across the tube bank. Because the dominant resistance occurs on the airside, it is a common practice to employ fins (such as circular fins) on the tube bundle to increase the gas side performance. For circular fin geometries, there are many empirical correlations available in the literature such as the correlations of Briggs and Young [1], Robinson and Briggs [2], Rabas et al. [3] and ESDU [4] for evaluating the air side heat transfer coefficient and pressure drop of the staggered tube bank.

In case of inline arrangement, despite of its comparatively low heat transfer performance, its lower pressure drop and high reliability (easy to maintain and clean) are very attractive in very severe environment. For the heat transfer performance, Schmidt [5] recommended a correlation for predicting the heat transfer coefficient of the inline arrangement.

However, circular fin implemented in typically industrial application is usually in the form of crimped spiral fin as shown in Fig. 1. Unfortunately, there is no airside data reported in the literature. In this regard, it is the objective of this study to present relevant airside data of the crimped spiral fins. Especially in case of low Reynolds number of air stream which is the condition of the cross flow heat exchanger recovering heat from the flue gas of small package boiler which is many in Thailand. The relevant important geometric parameters such as tube diameter, fin spacing, fin height, and tube spacing influencing the airside performance are also investigated. Moreover the empirical correlations capable of evaluating the airside performance are also developed.

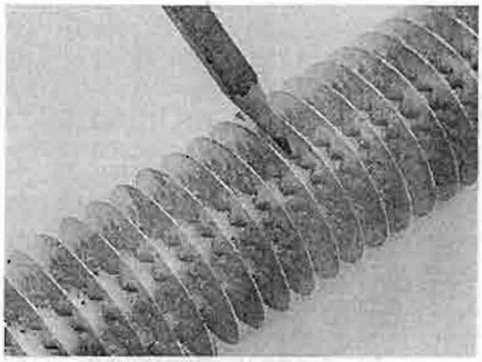

FIG. 1

Schematic of the crimped spiral fin geometry

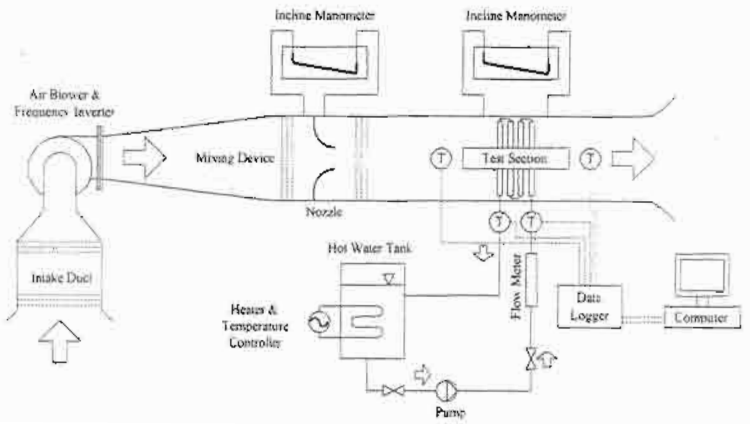

FIG. 2

Schematic diagram of the experimental setup

Experimental Set-up

Fig. 2 presents the schematic of the experimental setup. The air stream at room temperature flows through the tube bank with hot water circulated inside the tubes. In this experiment, the water flow rate is kept at a constant flowrate of 8 L/min. An accurate flowmeter is used for the measurement with a precision of ±0.1 L/min. The inlet temperature of water is maintained at 65°C. Both of the inlet and outlet temperatures of water are measured by a set of calibrated T-type thermocouples and the signals are recorded by a temperature data logger.

Table 1
Geometric dimensions of cross flow heat exchanger

No	d_o (mm)	d_i (mm)	f_s (mm)	f_h (mm)	f_t (mm)	S_t (mm)	S_l (mm)	n_r	n_t	arrangement
1	17.3	13.3	6.10	10.0	0.4	50.0	50.0	4	10	inline
2	21.7	16.5	6.10	10.0	0.4	71.4	50.0	4	7	inline
3	21.7	16.5	6.10	10.0	0.4	50.0	50.0	4	10	inline
4	21.7	16.5	3.85	10.0	0.4	71.4	50.0	4	7	inline
5	21.7	16.5	3.85	10.0	0.4	50.0	50.0	4	10	inline
6	21.7	16.5	2.85	10.0	0.4	71.4	50.0	4	7	inline
7	21.7	16.5	2.85	10.0	0.4	50.0	50.0	4	10	inline
8	21.7	16.5	3.85	15.0	0.4	71.4	50.0	4	7	inline
9	27.2	21.6	3.85	10.0	0.4	50.0	50.0	4	10	inline
10	21.7	16.5	6.10	10.0	0.4	72.0	36.0	4	6	staggered
11	21.7	16.5	3.85	10.0	0.4	72.0	36.0	4	6	staggered
12	21.7	16.5	2.85	10.0	0.4	72.0	36.0	4	6	staggered
13	21.7	16.5	6.10	10.0	0.4	84.0	24.2	4	5	staggered
14	21.7	16.5	3.85	10.0	0.4	84.0	24.2	4	5	staggered
15	21.7	16.5	2.85	10.0	0.4	84.0	24.2	4	5	staggered
16	21.7	16.5	6.10	10.0	0.4	50.0	43.3	4	9	staggered
17	21.7	16.5	3.85	10.0	0.4	50.0	43.3	4	9	staggered
18	21.7	16.5	2.85	10.0	0.4	50.0	43.3	4	9	staggered
19	21.7	16.5	6.10	10.0	0.4	55.6	48.2	4	8	staggered
20	21.7	16.5	3.85	10.0	0.4	55.6	48.2	4	8	staggered
21	21.7	16.5	2.85	10.0	0.4	55.6	48.2	4	8	staggered
22	21.7	16.5	3.85	15.0	0.4	55.6	48.2	4	8	staggered
23	27.2	21.6	3.85	10.0	0.4	50.0	43.3	4	9	staggered

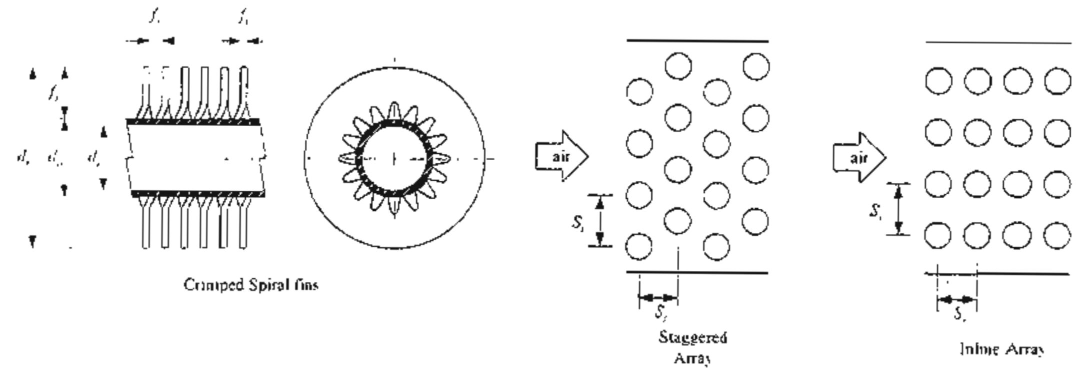

FIG. 3

Details of crimped spiral fins geometry and tube arrangements

The airflow across the heat exchanger is generated by a 1.5 kW centrifugal air blower with the controllable range of 0.1-0.5 kg/s by using a frequency inverter. The mass flow rate of air stream is measured by a standard nozzle and an inclined manometer with ±0.5 Pa accuracy. The inlet and the outlet temperatures of air stream are also measured by another set of T-type thermocouple mesh. The inlet and outlet temperature measuring meshes consist of 16 and 41 thermocouples, respectively. Note that all of thermocouples have been calibrated to ±0.1 °C accuracy. The pressure drop across the heat exchanger is also measured by the inclined manometer with ±0.5 Pa accuracy.

A total of 23 crimped spiral fin heat exchangers having various geometric parameters are tested in this study. Table 1 lists the details of the tested samples. Relevant definitions of the geometrical parameters can be also shown in Fig. 3. Notice that both inline and staggered arrangements are tested in this study. The effects of tube diameter, fin height, fin spacing, fin thickness, and tube arrangements on the airside performance are examined accordingly.

Data Reduction

During the experiment, hot water flowing inside the tube bank transfers heat to the outside air. The airside and the tube side heat transfer rates can be calculated as

$$Q_a = \dot{m}_a Cp_a (T_{ao} - T_{ai}), \tag{1}$$

$$Q_w = \dot{m}_w Cp_w (T_{wi} - T_{wo}), \tag{2}$$

Where Q_a and Q_w are the heat transfer rate of air and water respectively. In this experiment, the heat transfer rate used in the calculation is the mathematical average of the air side and the tube side heat transfer rates as

$$Q_{ave} = 0.5(Q_a + Q_w). \tag{3}$$

The performance of the heat exchangers is analyzed by conventional ε-NTU technique, the effectiveness is defined as

$$\varepsilon = \frac{Q_{ave}}{(\dot{m}Cp)_{\min} \Delta T_{\max}}. \tag{4}$$

The relationship of the effectiveness and the number of transfer unit (NTU) for the present 4 tube rows configuration is as follow (ESDU [6]);

$$\varepsilon = \frac{1}{C^*}\left\{1 - e^{-4KC^*}\left[1 + C^* K^2(6 - 4K + K^2) + 4(C^*)^2 K^4 (2-K) + \frac{8(C^*)^3 K^6}{3}\right]\right\}, \tag{5}$$

$$K = 1 - e^{-NTU/4}, \tag{6}$$

$$NTU = \frac{UA}{(\dot{m}Cp)_{\min}}, \tag{7}$$

$$C^* = \frac{(\dot{m}Cp)_{\min}}{(\dot{m}Cp)_{\max}}, \tag{8}$$

Once the overall resistance is obtained from eqs. (1-8), the heat transfer coefficients can be obtained from the following overall resistance equation:

$$\frac{1}{UA} = \frac{1}{\eta_o h_o A_o} + \frac{\ln(d_o / d_i)}{2\pi k L} + \frac{1}{h_i A_i}. \tag{9}$$

Where h is the heat transfer coefficient, A is the surface area, d is tube diameter, L is total tube length, k is thermal conductivity of tube material. η_o is surface efficiency and the subscripts o, i denote the air side and the tube side, respectively. The tube side heat transfer coefficient can be calculated from Gnielinski correlation [7] as

$$h_i = \left(\frac{k}{d}\right)_i \frac{(\mathrm{Re}_{Di} - 1000)\mathrm{Pr}(f_i/2)}{1 + 12.7\sqrt{f_i/2}(\mathrm{Pr}^{2/3} - 1)}, \tag{10}$$

$$f_i = [1.58\ln(\mathrm{Re}_{Di}) - 3.28]^{-2}, \tag{11}$$

Where Re_{Di} is the tube-side Reynolds number. The relation of the surface efficiency in eq. (9) and the fin efficiency η is

$$\eta_o = 1 - \frac{A_f}{A_o}(1 - \eta), \tag{12}$$

$$A_o = A_f + A_b, \tag{13}$$

Where A_o is the total surface area of finned tube, A_f is surface area of fin, A_b is the surface area of the bare tube. The fin efficiency η can be approximated from the Schmidt approximation [8]:

$$\eta = \frac{\tanh(mr\phi)}{mr\phi}, \tag{14}$$

where

$$m = \sqrt{\frac{2h_o}{k_f f_t}}, \tag{15}$$

$$\phi = \left(\frac{R_{eq}}{r} - 1\right)\left[1 + 0.35\ln\left(\frac{R_{eq}}{r}\right)\right], \tag{16}$$

$$\frac{R_{eq}}{r} = 1.27\frac{X_M}{r}\left(\frac{X_L}{X_M} - 0.3\right)^{1/2}, \tag{17}$$

$$X_L = \frac{\sqrt{(S_t/2)^2 + S_L}}{2}, \tag{18}$$

$$X_M = 0.5S_t, \tag{19}$$

where k_f is thermal conductivity of the fin, S_t and S_L are transverse and longitudinal pitches of the tube bank and f is fin thickness.

The total surface area of finned tube and the total surface area of the fin can be estimated by assuming equal to that of the circular fin as [9]:

$$A_o = \frac{nL\pi}{f_s + f_t}\left(0.5(d_f^2 - d_o^2) + d_f f_t + d_o f_s\right), \tag{20}$$

$$A_f = \frac{nL\pi}{f_s + f_t}\left(0.5(d_f^2 - d_o^2) + d_f f_t\right), \tag{21}$$

where n is the total number of tube, d_f is outer diameter of finned tube, f_s is spacing between adjacent fin and f_t is fin thickness.

In this study, the air side heat transfer coefficient and the pressure drop across tube bank are in the form of the Colburn j factor and the fanning friction factor (f) respectively and these factor are defined as

$$j = \frac{h_o \Pr^{2/3}}{\rho_a C_{pa} V_{max}}, \tag{22}$$

$$f = \frac{A_c \rho_i}{A_o \rho_m}\left[\frac{2\rho_i \Delta P}{G_c^2} - \left(1+\sigma^2\right)\left(\frac{\rho_i}{\rho_o} - 1\right)\right]. \tag{23}$$

where V_{max} is the maximum air velocity of tube bank base on the minimum flow area, A_c is the minimum flow area, σ is the contraction ratio, G_c is the mass flux of air flow based on the minimum flow area and the subscripts i, o, m represent the inlet, outlet, and mean value, respectively.

Results and Discussion

Inline Arrangement

In the case of inline arrangement, there are nine samples of inline arrangement as shown in Table 1. Fig. 4 shows the effect of tube diameter on the airside performance. Results are termed as heat transfer coefficient and the pressure drop vs. frontal velocity. In this comparison, the fin spacing (3.85 mm), fin thickness (0.4 mm), and the fin height (10 mm) are all the same. The transverse and the longitudinal tube pitches are 50 mm. As expected, the pressure drop rises with the tube diameter. However, it is interesting to note that the heat transfer coefficient increases with the reduction of tube diameter. It is likely that this phenomenon is attributed to the ineffective area behind the tube increases with the tube diameter. The ineffective are is especially pronounced for an inline arrangement. Wang et al. [11] performed flow visualizations via dye injection technique for fin-and-tube heat exchangers having inline arrangement. Their visual results unveil a very huge flow circulation behind the tube row. Consequently this huge recirculation not only contributes to the decrease of heat transfer coefficient but also to the rise of pressure drop. In addition, the huge recirculation may also block the subsequent tube row and degrade the heat transfer performance hereafter.

Fig. 5 shows the effect of fin height on the airside performance for inline arrangement. In this comparison, the associated fin heights are 10 and 15 mm and the fin spacing and the tube diameter are 3.85 mm and 21.7 mm with the transverse and the longitudinal pitches are 71.4 and 50 mm, respectively. As seen in the figure, the influence of fin height shows tremendous influence on the heat transfer performance and the pressure drop. Although the increase of fin height is only 50%, the corresponding increase of fin surface area is roughly 53% that eventually leads to a dramatic increase of pressure drop (roughly 100%). Unlike those of pressure drops, the heat transfer coefficients are dropped drastically with the increase of fin height. This is probably due to the airflow bypass effect. Actually the airflow is prone to flowing the portion where the flow resistance is small. In case of f_h = 15 mm, the airflow resistance around fin tube is larger than f_h = 10 mm. Therefore, part of the directed airflow just bypass the tube row without effective contribution to the heat transfer and lower heat transfer coefficient is obtained.

The effects of the fin spacing on the airside performance at different transverse tube pitch (50 and 71.4 mm) are shown in Fig. 6. At a larger transverse tube pitch of 71.4 mm, one can see the effect of fin spacing on pressure drops is rather small. Surprisingly, the reduction of the fin spacing does not give rise to the pressure drops. This may be related to the presence of the bypass airflow between the tubes. Since the bypass airflow does not increase the pressure drops, therefore no detectable change of pressure drops is seen at a very large transverse tube pitch of 71.4 mm. On the contrary, the reduction of fin spacing give rise to pressure drops at a smaller transverse tube pitch of S_t = 50 mm. This is due to the significant decrease of bypass airflow and the reduction of the associated hydraulic diameter. From Fig. 6, it is also found that the increase of fin spacing give rise to heat transfer coefficient. An explanation of this phenomenon is the same as the effect of fin height that the result comes from airflow bypass effect. As is known, the corresponding pressure drop rises with the decrease fin spacing. Therefore, lower fin spacing gets higher bypass airflow and the heat transfer coefficient is decreased at smaller fin spacing.

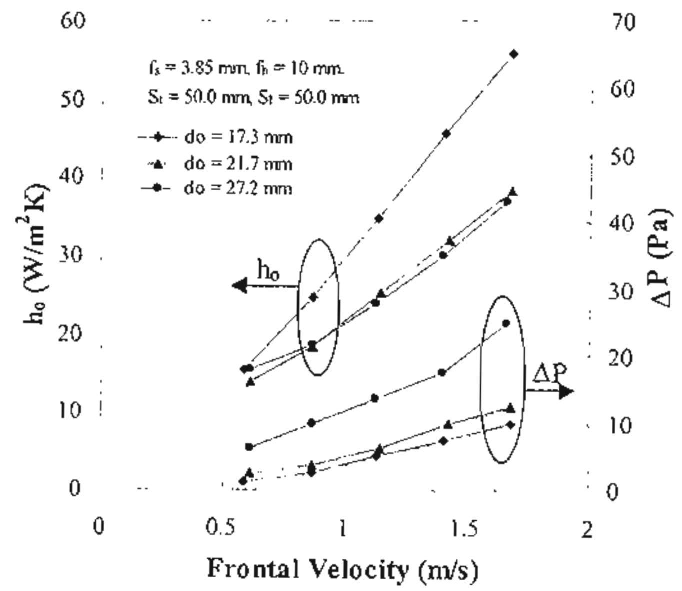

FIG.4

Effect of tube diameter on the airside performance for the inline arrangement

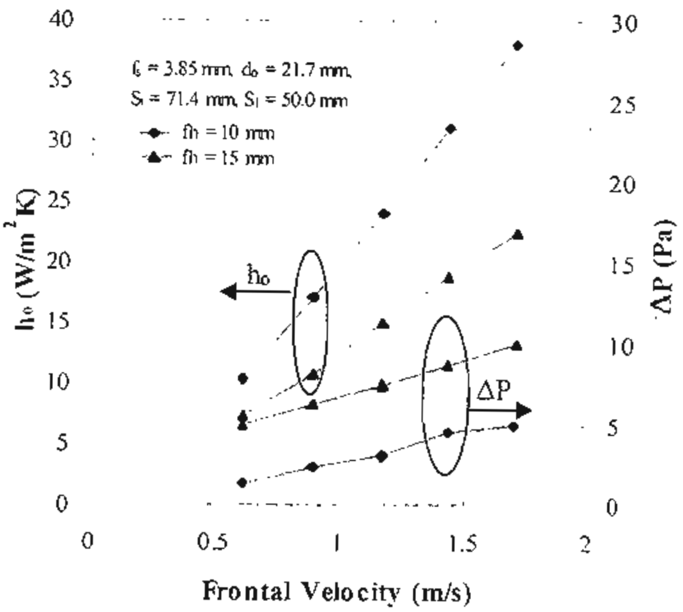

FIG. 5

Effect of fin height on the airside performance for the inline arrangement

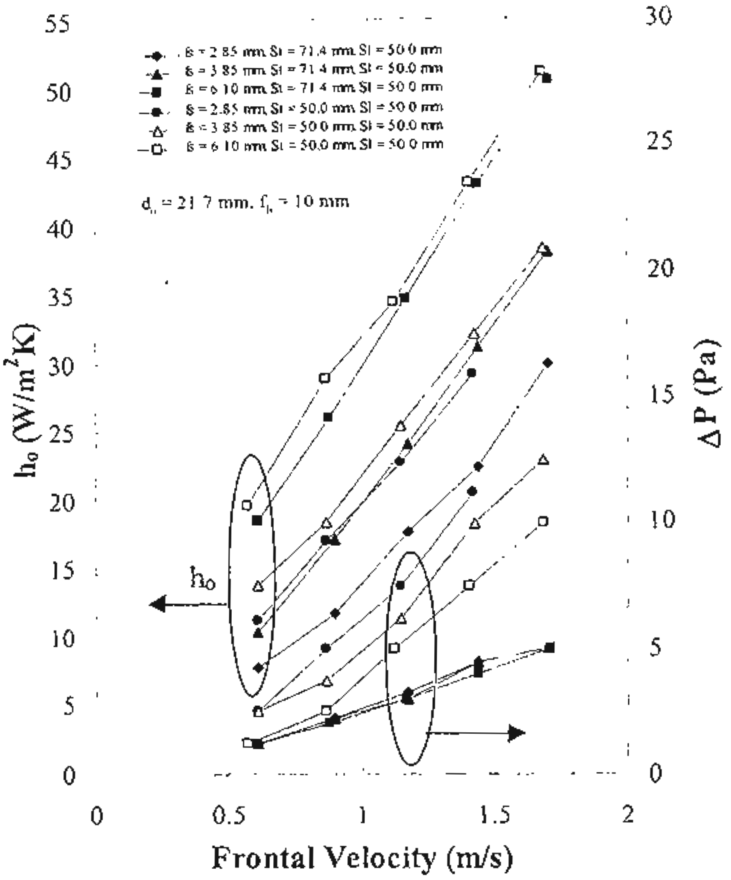

FIG. 6

Effect of fin spacing and tube arrangement on the airside performance for the inline arrangement

<u>Staggered Arrangement</u>

For staggered arrangement, Fig. 7 shows effect of tube diameter on the air side performance. The geometrical parameters of fin spacing, fin height, transverse pitch and longitudinal pitch are 3.85 mm, 10 mm, 50 mm and 4.33 mm, respectively. Analogous to that of inline arrangement but the influence is comparatively less to some extent, the heat transfer coefficient and the pressure drop decrease with the tube diameter. Explanation of this phenomenon is the same as that of inline arrangement. However, the recirculation region for staggered arrangement behind the tube is much smaller than that of the inline arrangement due to the airflow across the adjacent tubes is directed by the subsequent tube row. The directed oblique airflow will reduce the recirculation area behind the tube. This phenomenon can be also made clear from the flow visualization experiment by Wang et al. [12] in staggered arrangement. Their visualization indicated a much smaller recirculation area of the staggered arrangement than that of inline arrangement.

The effect of fin height on the airside performance is shown in Fig. 8. It is found that the heat transfer coefficients of f_h = 10 mm are slightly higher than those of f_h = 15 mm and the explanation is similar to that of inline arrangement. However, the pressure drops for both fin height are about the same irrespective of the fin area of f_h = 15 mm are approximately 53% higher than that of f_h = 10 mm. The results are quite different from those of inline arrangement in which one can see an approximately two times increase of pressure drops for f_h = 15 mm relative to that of f_h = 10 mm. Explanation of this phenomenon can be made clear as follows. For the same fin height of f_h = 10 mm. one can see a dramatic increase of pressure drops of six times for staggered arrangement relative to that of inline arrangement. This implies the major contribution to the total pressure drops comes from the type of arrangement. For staggered arrangement, the airflow is directed by the subsequent tube row in which most of the pressure loss is generated. On the contrary, since the air flow across the inline arrangement is not directed by the subsequent tube row. The pressure drop is mainly affected by the friction caused by the fins and the recirculation area behind the tube. Thus one can see a very small increase of the pressure drop with the rise of fin height for staggered arrangement.

Fig. 9 shows the effect of fin spacing, and S_t on the airside heat transfer coefficients and pressure drops. The tube diameter is 21.7 mm and the fin height is 10 mm. From Fig. 8, it can be concluded that higher fin spacing gives lower pressure drops. For a smaller transverse tube pitch (S_t = 50 mm), one can see the effect of fin spacing on the heat transfer coefficients is negligible. This result is analogous to that of continuous fin geometry as reported by Rich [13] and Wang et al. [14]. However, for a larger transverse pitch of 84 mm, the heat transfer coefficients decrease with the decrease of fin spacing. Again explanation of this phenomenon may arise from the influence of airflow bypass effect. As is known, the corresponding pressure drop rises with the decrease fin spacing. As a consequence, although the airflow is directed by the tube row, the airflow is prone to flowing the portion where the flow resistance is smaller. For a very large of transverse tube pitch of 84 mm, part of the directed airflow just bypass the tube row and fin without effective contribution to the heat transfer, thereby causing a drop of heat transfer coefficients at smaller fin spacing. This flow bypass phenomenon becomes much where the transverse tube pitch is reduced. Therefore, one can see no appreciable change of heat transfer coefficients for S_t = 50 mm.

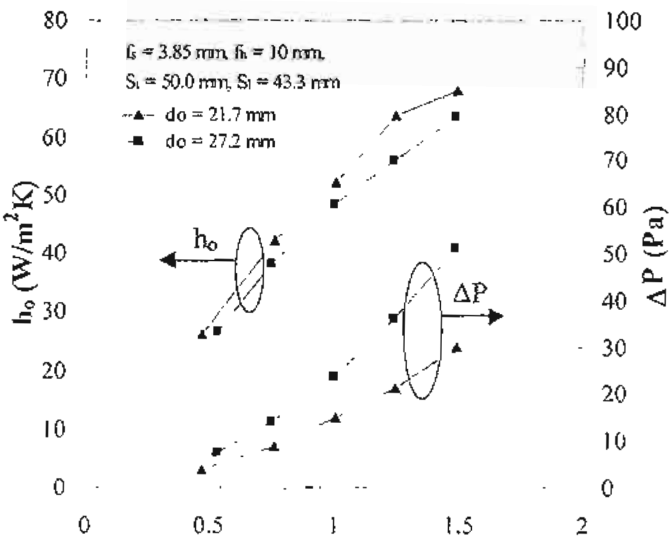

FIG. 7

Effect of tube diameter on the airside performance for the staggered arrangement

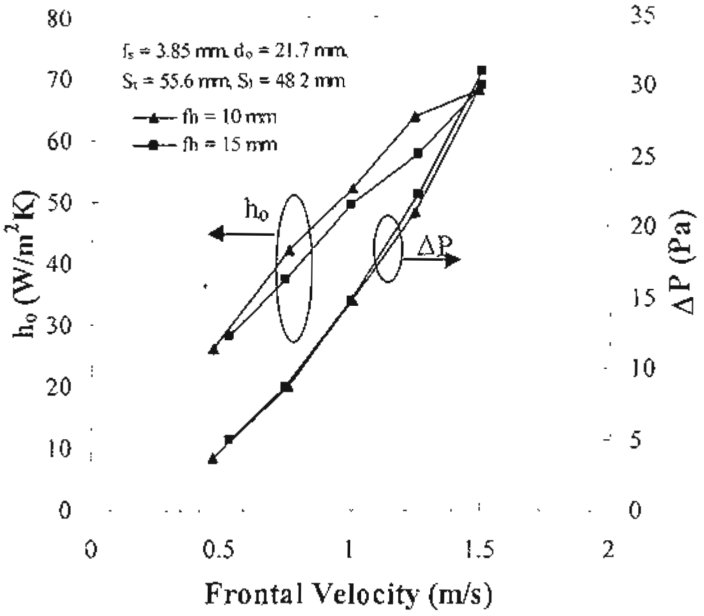

FIG. 8

Effect of fin height on the airside performance for the staggered arrangement

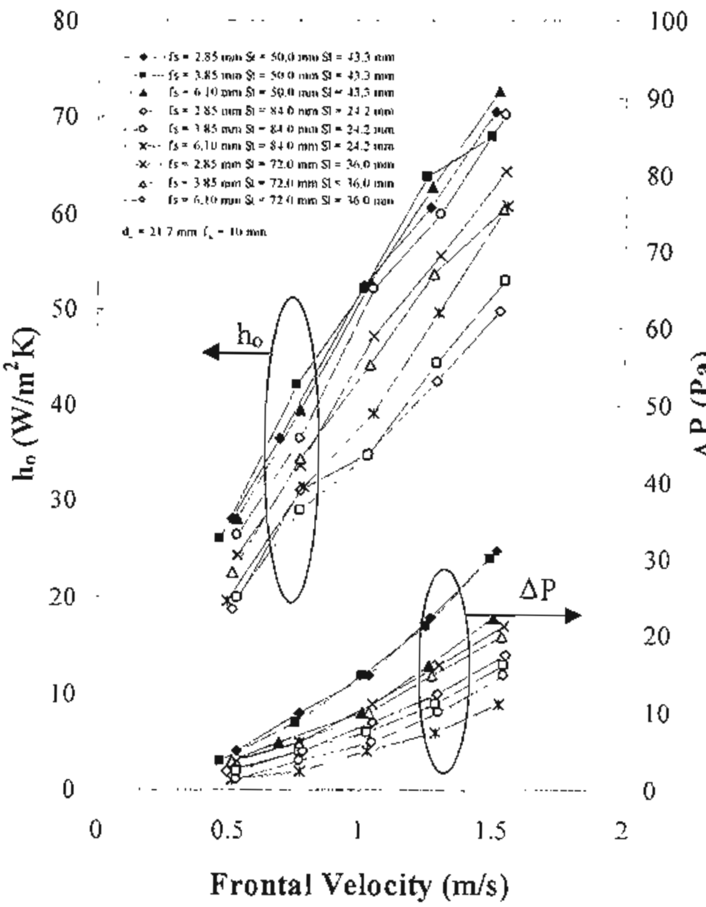

FIG. 9

Effect of fin spacing and tube arrangement on the airside performance for staggered arrangement

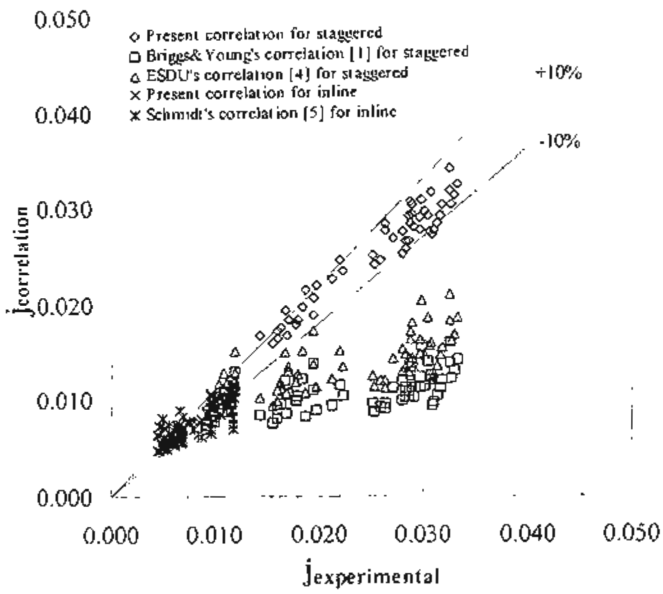

FIG. 10

Comparison of the heat transfer correlations with experimental data

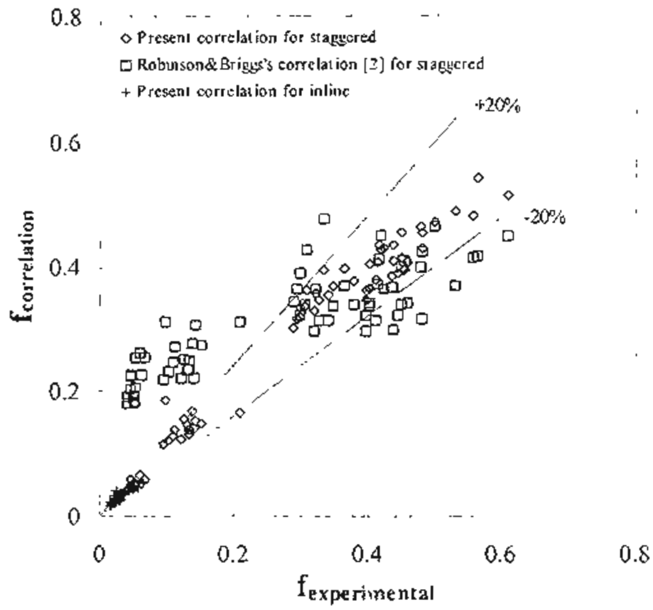

FIG. 12

Comparison of the frictional correlations with experimental data

Empirical Correlations

Based on the previous discussions, it is obvious from the test data that no single curve can be expected to describe the complex behaviors about the heat transfer and frictional characteristics in both inline and staggered arrangements. For easier engineering calculations, we had performed multiple linear regression technique to obtain the relevant correlations. The corresponding correlations are given as follows:

Correlation of the heat transfer performance of the inline arrangement:

$$j = 3.9048\times10^{-4}\,\mathrm{Re}_D^{\,0.0637}\left(\frac{f_t}{f_s}\right)^{-0.8363}\left(\frac{S_l}{S_t}\right)^{1.9926}\left(\frac{S_t}{d_o}\right)^{2.2810}\left(\frac{d_f}{d_o}\right)^{-2.1720} \tag{24}$$

Correlation of the heat transfer performance of the staggered arrangement:

$$j = 0.1970\,\mathrm{Re}_D^{\,-0.1295}\left(\frac{f_t}{f_s}\right)^{-0.1452}\left(\frac{S_l}{S_t}\right)^{1.1874}\left(\frac{S_t}{d_o}\right)^{0.8238}\left(\frac{d_f}{d_o}\right)^{0.0010} \tag{25}$$

Correlation of the frictional performance of the inline arrangement:

$$f = 0.1635\,\mathrm{Re}_D^{\,-0.4172}\left(\frac{f_t}{f_s}\right)^{-0.5215}\left(\frac{S_l}{S_t}\right)^{-1.2235}\left(\frac{S_t}{d_o}\right)^{-0.6334}\left(\frac{d_f}{d_o}\right)^{1.2000} \tag{26}$$

Correlation of the frictional performance of staggered arrangement:

$$f = 2.1768\,\mathrm{Re}_D^{\,-0.2679}\left(\frac{f_t}{f_s}\right)^{-0.2468}\left(\frac{S_l}{S_t}\right)^{1.8680}\left(\frac{S_t}{d_o}\right)^{0.3011}\left(\frac{d_f}{d_c}\right)^{-0.4470} \tag{27}$$

Figs. 10-11 show the comparison of j and f of the experimental results with the proposed correlations. For the heat transfer correlations, eqs. (24)-(25) can predict 89.7% and 88.4% of the experimental data with ±10% and the friction factor correlations, eqs. (26)-(27) give a predictive ability of 79.6% and 91.3% of the experimental data within ±20%. The standard deviation of the correlations eqs. (24)-(27) are 7.90%, 7.15%, 16.70%, and 13.7%, respectively.

The comparison of the proposed correlations and the previous correlations are also investigated. In case of the inline arrangement, it is found that Schmidt's correlation [5] can predicts 71.8% of the experimental data with ±30%. Actually, Schmidt's correlation did not include the effect of the geometrical of finned tube. Therefore, lower accuracy is obtained.

In case of the staggered arrangement, the correlations of Briggs and Young [1] and ESDU [4] give approximately 30% lower than the present correlation and the friction factor correlation of Robinson and Briggs [2] gives over predicting of the experimental value at low friction factor. These results come from the effect of crimped spiral finned tube which differs from that of the circular finned tube.

Conclusion

The present experimental study reports the airside performance of the crimped spiral fin heat exchanger. The effects of tube diameter, fin spacing, transverse tube pitch, and tube arrangements are examined. On the basis of previous discussions, the following conclusions are made:

1. For an inline arrangement, the pressure drops increase with the rise of tube diameter but the associated heat transfer coefficients decrease with it. The increase of fin height also gives rise to considerable increase of pressure drop but decrease of heat transfer coefficient.
2. For the inline arrangement, the effect of fin spacing on the airside performance varies with the transverse tube pitch. For a larger transverse tube pitch of 71.4 mm, there is an effect on heat transfer coefficient but no detectable influence of the fin spacing on frictional characteristics. It is likely that this phenomenon is related to

the considerable airflow bypass between tube rows. On the contrary, at a smaller transverse tube pitch of 50 mm. one can see smaller fin spacing results in higher pressure drops and lower heat transfer coefficients.

3. For the staggered arrangement, the effect of tube diameter on the airside performance is analogous to that of inline arrangement but to a comparatively small extent. This is because the recirculation zone behind the tube row is much smaller in a staggered arrangement. The effect of the fin height on the pressure drops is much smaller than that of inline arrangement due to the major contribution to the pressure drops is from the blockage of the subsequent tube row in a staggered arrangement.
4. The effect of fin spacing on the airside performance for staggered arrangement also varies with the transverse tube pitch. For a smaller transverse tube pitch of 50 mm, there is no appreciable influence of the fin spacing on heat transfer. On the contrary, at a larger transverse tube pitch of 84 mm, one can see smaller fin spacing leads to lower heat transfer coefficients. This is also attributed to the presence of airflow pass effect.
5. Correlations of the present crimped spiral fins in both staggered and inline arrangement are developed. The proposed correlations give fairly good predictive ability against the present test data.

Acknowledgement

The authors gratefully acknowledge the support provided by the Thailand Research Fund for carrying out this study. Part of the finacial support provided by the Energy R&D foundation funding from the Energy Commission of the Ministry of Economic Affairs, Taiwan is also appreciated.

Nomenclature

A	Area (m^2)
A_c	Minimum flow area (m^2)
Cp	Specific heat (J/kgK)
d_f	Outside diameter of finned tube (mm)
d_i	Inside diameter of bare tube (mm)
d_o	Outside diameter of bare tube (mm)
f	Friction factor
f_h	Fin height (mm)
f_s	Fin Spacing (mm)
f_t	Fin thickness (mm)
G_c	Mass flux of air base on minimum low area (kg/sm^2)
h	Heat transfer coefficient (W/m^{2}K)
k	Thermal conductivity (W/mK)
L	Length (m)
m	Mass flow rate (kg/s)
n_r	Number of tube rows
n_t	Number of tubes in row
NTU	Number of transfer unit
Nu	Nusselt Number
P	Pressure (Pa)
Pr	Prandtl number
Q	Heat transfer rate (W)
Re_D	Reynolds number
S_t	Transverse pitch (mm)
S_l	Longitudinal pitch (mm)
T	Temperature (°C)
U	Overall heat transfer coefficient (W/m^{2}K)
V_{max}	Maximum velocity (m/s)
Greek symbols	
ε	Effectiveness
η	Efficiency
μ	Dynamic viscosity (Pas)
ρ	Density (kg/m^3)
σ	Contraction ratio of cross sectional area
Subscripts	
a	Air
ave	Average
b	Bare tube
f	Fin
i	Inlet, tube side
o	Outlet, air side
w	Water

References

1. Briggs, D.E. and Young, E.H., Chemical Engineering Progress Symposium Series 59, 41, 1 (1963).
2. Robinson, K.K. and Briggs, D.E., Chemical Engineering Progress Symposium Series 62, 64, 177 (1966).
3. Rabas. T.J., Eckels. P.W. and Sabatino, R.A., Chemical Engineering Communications 10, 2, 127 (1981).
4. ESDU International plc., High-fin Staggered Tube Bank: Heat Transfer and Pressure drop for turbulent single phase gas flow, ESDU Item 86022 (1986).
5. Schmidt, Th.E., Der Warmeubergeng an Rippenrohen und die Berechnung von Rohrundel Warme Austauschern, Kalttech. 15(4), 98; 15(12), 370 (1963).
6. ESDU International plc., Effectiveness – NTU Relationships for the Design and Performance Evaluation of Two-Stream Heat Exchangers, ESDU Item 86018 (1991).
7. Gnielinski, V., Int. Chem. Engng 16, 359 (1976).
8. Schmidt, Th.E. , Refrigeration Engineering, 351 (1949).
9. Hewitt, G.F., Shires, G.L. and Bott, T.R., Process Heat Transfer, Boca Raton, CRC Press, p. 1042 (1994).
10. Kays, W.M. and London, A.L., Compact Heat Exchangers, 3rd edition, McGraw-Hill, New York (1984).
11. Wang, C.C., Lou, J., Lin, Y.T. and Liu, M.S., Int. J. of Heat and Mass Transfer 45, 1933 (2002).
12. Wang, C.C., Lou, J., Lin, Y.T. and Wei, C.S., Int. J. of Heat and Mass Transfer 45, 3803 (2002).
13. Rich, D.G. (1973), ASHRAE Transactions, 79, 2, 137 (1973).
14. Wang, C.C., Chang, Y.J., Hsieh, Y.J. and Lin, Y.T., Int. J. of Refrigeration, 19, 223 (1996).

Heat Transfer and Friction Characteristics of Crimped Spiral Finned Heat Exchangers With Dehumidification

A. NUNTAPHAN
Mae Moh Training Center
Electricity Generating Authority of Thailand
Mae Moh, Lampang 52220 Thailand

T. KIATSIRIROAT
Department of Mechanical Engineering, Chiang Mai University
Chiang Mai 50202 Thailand

C.C. WANG
Energy & Resources Laboratories, Industrial Technology Research Institute
Hsinchu, Taiwan 310, R.O.C.

ABSTRACT

This study experimentally examined the airside performance of a total of 10 cross flow heat exchangers having crimped spiral configurations under the dehumidification. The effect of tube diameter, fin spacing, fin height, transverse tube pitch, and tube arrangements are examined. The results indicate that the heat transfer coefficient of wet surface is slightly lower than that of dry surface. The effect of tube diameter on the airside performance is significant. Larger tube diameter not only gives rise to lower heat transfer coefficient but also contribute significantly to the increase of pressure drops. This phenomenon is applicable in both dry and wet condition. For wet surface, the influence of fin height is negligible and the effect of fin spacing on the heat transfer performance is rather small. However, the increasing of fin spacing tends to have a lower heat transfer coefficient. The tube arrangement plays an importance role on the heat transfer coefficient, the lower transverse pitch gives the higher heat transfer coefficient. The proposed correlations can predict 75% and 95% of experimental data within 15%.

Keywords: Air-side performance, dehumidification, crimped spiral fins

Submitted to *Applied Thermal Engineering*

Address of Correspondence and proof:
Dr. Atipoang Nuntaphan
Mae Moh Training Center
Electricity Generating Authority of Thailand
Mae Moh Lampang 52220 Thailand
Tel. 6654-256938, Fax. 6654-256907, email: atipoang.n@egat.co.th

1. INTRODUCTION

The cross flow heat exchanger plays an important role in waste heat recovery process, especially, in economizer where flue gas is changing heat with water. Normally, the water is always flowing inside the tube while the hot gas is flowing outside. Because the heat transfer resistance at gas-side dominates the heat transfer of heat exchanger, many attempts have been carried out to improve the gas-side heat transfer. Circular fins or Spiral fins are commonly exploited for recovering heat from flue gas due to its durability and reliability. A schematic of the crimped spiral fin is shown in Figure 1. It should be noticed that the inner crimped edge gives a good attachment between the fins and the tube.

When using a set of crimped spiral finned tube in the cross flow heat exchanger, the designer should concern about the heat transfer coefficient and the gas or air stream pressure drop of the tube bank. Many research works were pertained to the airside performance, such as Briggs and Young [1], Robinson and Briggs [2] and Rabas et al. [3]. These works are in association with the circular finned tube bank. For the case of crimped spiral fins, Nuntaphan et al. [4] had reported the relevant airside performance. However, the aforementioned studies were performed in fully dry conditions. For practical waste heat recovery system, the heat exchanger may accompany with condensation of moisture air on the heat exchanger surface. Although the designers try to avoid this situation due to considerablly corrosive problem associated with it, condensation may still take place from time to time. This is commonly encountered if the load is not constant such as small boilers where the steam consumption varies with time and the the flue gas temperature fluctuates in wide range. In that regard, the airside performance in the presence of dehumidification is rather important. Unfortunately, there are simply no data reported for the crimped spiral finned heat exchangers. Hence, it is the objective of this work is to report the heat transfer and friction characteristic of cross flow heat exchanger using crimped spiral fin in the presence of dehumidification. Moreover, the heat transfer and friction correlations are also developed in this work.

2. EXPERIMENTAL SET-UP

Figure 2 presents the schematic of the experimental set-up. The hot air stream flows through the tube bank and the water at room temperature circulates inside the tubes. In this experiment, the water flow rate is kept constant at 8 L/min. An accurate water flow meter is used for the measurement with a precision of ±0.1 L/min. The inlet temperature of water is approximately 30°C. Both the inlet and outlet temperatures of water are measured by a set of calibrated K-type thermocouples and a temperature data logger records these signals.

A 1.5 kW centrifugal air blower accompanied with a frequency inverter having a controllable range of 0.1-0.5 kg/s air is used to conduct flowing air across the heat exchanger. A standard nozzle and an inclined manometer are adopted to measure the mass flow rate of air stream. The uncertainty of the inclined manometer is ±0.5 Pa accuracy. The inlet temperature of air stream is kept constant at 65 °C by the set of heaters and the temperature controller. The inlet and the outlet dry bulb temperatures of air stream are also measured by another set of two meshes of K-type thermocouples. The inlet and the outlet wet bulb temperatures of air stream are also measured. Note that all of thermocouples have been calibrated to ±0.1 °C accuracy. The pressure drop across the heat exchanger is measured by another set of inclined manometer with calibrated uncertainty of ± 0.5 Pa accuracy.

A total of 10 crimped spiral fin heat exchangers having various geometric parameters are tested in this study. Table 1 lists the details of the tested samples. Relevant definitions of the geometrical parameters can be also shown in Figure 3. Notice that the samples are all of staggered arrangement. The effects of tube diameter, fin height, fin spacing, fin thickness, and tube arrangements on the airside performance are examined accordingly.

3. DATA REDUCTION

The heat transfer rate of cross flow heat exchanger under dehumidifying condition can be calculated as follows:

$$Q_a = \dot{m}_a (i_{a,in} - i_{a,out}), \tag{1}$$

$$Q_w = \dot{m}_w C_{pw} (T_{w,out} - T_{w,in}). \tag{2}$$

Note that Equation (1) and Equation (2) denote heat transfer rate in the air-side and the tube-side, respectively. In this study, the mathematical average of the heat rate is used, i.e.,

$$Q_{avg} = 0.5(Q_a + Q_w). \tag{3}$$

The average heat transfer rate is related to the rate equation given in the following (enthalpy based potential),

$$Q_{avg} = U_{o,w} A_o F \Delta i_m . \tag{4}$$

Where F is the correction factor of unmixed/unmixed configuration.

The log-mean enthalpy potential Δi_m is (Threlkeld [5])

$$\Delta i_m = \frac{(i_{a,in} - i_{r,out}) - (i_{a,out} - i_{r,in})}{\ln\left(\frac{i_{a,in} - i_{r,out}}{i_{a,out} - i_{r,in}}\right)}. \tag{5}$$

Myers [6] derived the enthalpy-based overall heat transfer coefficient ($U_{o,w}$) to individual resistance as

$$\frac{1}{U_{o,w}} = \frac{b'_r A_o}{h_i A_{p,i}} + \frac{b'_p x_p A_o}{k_p A_{p,m}} + \frac{1}{h_{o,w}\left(\frac{A_{p,o}}{b'_{w,p} A_o} + \frac{A_f \eta_{f,wet}}{b'_{w,m} A_o}\right)}, \tag{6}$$

where

$$h_{o,w} = \frac{1}{\frac{C_{p,o}}{b'_{w,m} h_{c,o}} + \frac{y_w}{k_w}}. \quad (7)$$

Note that the ratio of water film thickness and thermal conductivity of water (y_w / k_w) is very small compared to other terms [7] and it is neglected in this study.

The tube side heat transfer coefficient can be calculated from Gnielinski correlation [8] as

$$h_i = \frac{(f_i/2)(\mathrm{Re}_{Di} - 1000)\mathrm{Pr}}{1.07 + 12.7\sqrt{f_i/2}\left(\mathrm{Pr}^{2/3} - 1\right)}\left(\frac{k_i}{d_i}\right), \quad (8)$$

where

$$f_i = \frac{1}{(1.58 \ln \mathrm{Re}_{Di} - 3.28)^2}. \quad (9)$$

The four quantities in Equation 7 can be estimated follow the method of Wang et al. [7] base on the enthalpy-temperature ratios. b'_r and b'_p, they can be calculated as

$$b'_r = \frac{i_{s,p,i,m} - i_{r,m}}{T_{p,i,m} - T_{r,m}}, \quad (10)$$

$$b'_p = \frac{i_{s,p,o,m} - i_{s,p,i,m}}{T_{p,o,m} - T_{p,i,m}}. \quad (11)$$

The quantity $b'_{w,p}$ is the slope of saturated enthalpy curve evaluated at the outer mean water film temperature at the base surface and can be approximated at the slope of saturated enthalpy curve evaluated at the base surface temperature of tube [7]. However, the quantity $b'_{w,m}$. which defines as the slope of saturated enthalpy curve evaluated at the outer mean water film temperature at the fin surface, can not be calculated directly. Consequently, a trial and error procedure of iteration is needed (Wang et al. [7]) Detailed procedures are in the following:

1. Assume a value of $T_{w,m}$ and calculate the quantity $b'_{w,m}$

2. Calculate $h_{o,w}$ from Equation 6

3. Calculate the quantity $i_{s,w,m}$ by this following relation

$$i_{s,w,m} = i - \frac{C_{p,a} h_{o,w} \eta_{f,wet}}{b'_{w,m} h_{c,o}} \times \left(1 - U_{o,w} A_o \left[\frac{b'_r}{h_i A_{p,i}} + \frac{x_p b'_p}{k_p A_{p,m}}\right]\right)(i - i_{r,m}). \quad (15)$$

4. Determine the new $T_{w,m}$ at $i_{s,w,m}$ and repeat the procedure again until the torlance is met.

The wet fin efficiency is calculated as (Wang et al [7]):

$$\eta_{f,wet} = \frac{2r_i}{M_T(r_o^2 - r_i^2)} \times \left[\frac{K_1(M_T r_i) I_1(M_T r_o) - K_1(M_T r_o) I_1(M_T r_i)}{K_1(M_T r_o) I_o(M_T r_i) + K_o(M_T r_i) I_1(M_T r_o)}\right], \quad (16)$$

where

$$M_T = \sqrt{\frac{2h_{o,w}}{k_f f_t}} = \sqrt{\frac{2h_{c,o}}{k_f f_t}} \sqrt{\frac{b'_w}{C_{p,a}}}. \quad (17)$$

In this research work, the sensible heat transfer coefficient ($h_{c,o}$) and the pressure drop of air stream across tube bank are presented in terms of the Colburn factor (j) and the friction factor (f) factors,

$$j = \frac{h_{c,o}}{G_{max} C_{p,a}} \mathrm{Pr}^{2/3}, \quad (18)$$

$$f = \frac{A_{min}}{A_o} \frac{\rho_i}{\rho_m} \left[\frac{2\rho_i \Delta P}{G_c^2} - (1 + \sigma^2)\left(\frac{\rho_i}{\rho_o} - 1\right)\right]. \quad (19)$$

4. RESULTS AND DISCUSSION

4.1 Pressure drop

The associated pressure drops for all the test samples are shown in Figures 4-7. In Figure 4, the influence of tube diameter is examined. As seen in the figure, the pressure drops for wet condition is only slightly higher than that of dry condition. This is because the fin spacing in this figure is comparatively large (3.85 mm). In that respect, the condensate can easily drain without adhering to the interspacing of fins, thereby giving only a slight increase of pressure drops of the wet surface relative to dry conditions. However, one can find a considerable influence of tube size on the total pressure drop. For the same frontal velocity of 1.5 m/s, the associated pressure drop for d_o = 27.2 mm is roughly 2.5 times higher that of d_o = 17. 3 mm.

The effect of fin height on the total pressure drops is shown in Figure 5. The pressure drops increase with fin height because of more fin surface is provided. The effective surface area of f_h = 0.015 m is roughly 30% higher than that of f_h = 0.01 m and the corresponding increase of pressure drop is also around 30~40% which indicate a linear relationship of the fin height and total pressure drop. Conversely, one can go back to Figure 4 where the effective surface area increase caused by the tube size is less than 10% because the surface area is dominated by secondary surface (fins). However, the pressure drops is greatly increased with the tube size. The excess pressure drop are attributed to (1) large form drag of the large tube; and (2) ineffective flow separation zone behind the tube which may increase its influence to further downstream and results in more pressure drops associated with it. This phenomenon is analogous to the continuous fin pattern reported by Wang et al. [9].

The effect of fin spacing on the pressure drops is shown in Figure 7. Notice that there is very small difference between dry and wet conditions since the tube diameter and fin height is relatively small which in term helps to drain the water condensate. Again smaller fin spacing increases the effective surface area and correspondingly higher pressure drops. In essence, the pressure drop increases with tube diameter (d_o), fin height (f_h) and decrease with it for a smaller fin spacing (f_s). Among them, the influence of tube diameter is most pronounced. The effect of tube arrangement is also found in Figure 6-7. Higher transverse pitch of tube bank (S_t) gives rise to lower pressure drop. Again this is also attributed to the increase of surface area. The relevant influences of geometric parameters on the friction characteristics are correlated in terms of friction factor, and is given as,

$$f = 17.02\,\mathrm{Re}_D^{-0.5636}\left(\frac{d_o}{S_t}\right)^{0.3956}\left(\frac{f_t}{f_s}\right)^{-0.3728}\left(\frac{S_l}{S_t}\right)^{1.2804}\left(\frac{d_o}{d_f}\right)^{-0.1738} \quad (20)$$

From Figure 8, one can see the proposed friction factor correlation can predict 75% of the experimental data within ±15% accuracy.

4.2 Sensible heat transfer coefficient

The related heat transfer coefficients vs. frontal velocity for all the test samples are shown in Figures 9-13. For comparison purpose, the relevant heat transfer coefficient in dry condition is also shown in the figure. It is found that the heat transfer coefficient of wet surface is slightly lower than that of dry surface. Actually, there are many studies showing the comparison of the heat transfer coefficients between wet and dry surface heat exchanger. Some studies indicated that the heat transfer coefficient is augmented in wet surface conditions. such as Myers [6], Elmahdy [10] and Eckels and Rabas [10] who reported results for the continuous plate finned tube. These investigators argued that the presence of water condensate may roughen the heat transfer surface, leading to higher heat transfer coefficient. However, some of the studies showed a drop of heat transfer coefficient of wet surface, such as the wavy finned tube heat exchanger by Mirth and Ramadhyani [12] who reported about 17-50% decreasing of heat transfer coefficient of wet surface. One possible cause of the degradation is due to water film resistance and condensate blocking. Moreover Wang et al. [7] shows the decreasing of the Colburn j factor of plate finned tube heat exchangers when the Reynolds number lower than 2,000. However, at the higher Reynolds number, the j factor of wet surface is slightly higher than that of dry surface. The present results are generally in agreement with the trend of Wang et al. [7].

The effect of tube diameter on the heat transfer performance is shows in Figure 9, it is found that the larger tube diameter (d_o = 27.2 mm) has a lower heat transfer coefficient than that of the small one (d_o = 17.3 mm). This phenomenon is attributed to the ineffective area behind the tube increases with the tube diameter. Wang et al. [13] performed flow visualizations via dye injection technique for fin-and-tube heat exchangers having inline arrangement. Their visual results unveil a very huge flow circulation behind the tube row. Consequently this huge recirculation not only contributes to the decrease of heat transfer coefficient but also to the rise of pressure drop as shown in the preceding discussions. In addition, the huge recirculation may also block the subsequent tube row and degrade the heat transfer performance hereafter.

Figure 10 shows the effect of fin height on the heat transfer coefficient. As seen in the figure, the influence of the fin height is negligible in wet condition. For the fully dry case, Nuntaphan et al [4] reported the 15 mm fin height gives lower heat transfer coefficient than that of 10 mm. This result comes from the airflow by pass effect. Actually the airflow is prone to flowing the portion where the flow resistance is small. In case of f_h = 15 mm, the airflow resistance across the finned tube portion is larger than that of f_h = 10 mm. Therefore, part of the directed airflow just bypass the tube row without effective contribution to the heat transfer, hence showing a lower heat transfer coefficient. However, in case of wet surface, the condensate of water vapor covering the surface of heat exchanger become dominant and it increases the airflow resistance around tube. Therefore the effect of fin height is comparatively reduced.

The effect of fin spacing shown in Figures 11 and 12. As seen in the figure, the effect of fin spacing is small. However, small fin spacing tends to have lower heat transfer coefficient, and this is particularly pronounced in Figure 12 where S_t = 84 mm and S_l = 24.2 mm. This result may be related to the water condensate effect. The presence of water condensate increases the air flow resistances into the heat exchanger, thereby causing more airflow to bypass. This phenomenon becomes more significant with S_t = 84 mm because more bypass airflow. In that regard, one can see a moderately decrease of heat transfer coefficient at smaller fin spacing. The reports of McQuiston [14,15] also show the decreasing of sensible heat transfer coefficient when the fin density is higher than 10 fins per inch.

Figure 13 shows the effect of tube arrangement on the sensible heat transfer coefficient. It is found that higher transverse tube pitch tends to have lower heat transfer coefficient and again this result is attributed to the airflow bypass effect. In case of S_t = 84 mm and S_l = 24.2 mm, more airflow is prone to flowing across the space between adjacent tube. Therefore, the amount of air stream contributed to the heat transfer is decreased when compared to that of S_t = 72 mm and S_l = 36 mm.

The associated effect of geometric parameters on the heat transfer performance are correlated in terms of the Colburn j factor, and is given as,

$$j = 0.0208\,\mathrm{Re}_D^{m}\left(\frac{d_o}{S_t}\right)^{-2.5950}\left(\frac{f_t}{f_s}\right)^{0.7905}\left(\frac{S_l}{S_t}\right)^{0.2391}\left(\frac{d_o}{d_f}\right)^{0.2761} \tag{21}$$

where

$$m = -0.2871 + 0.5322\left(\frac{d_o}{S_t}\right) - 1.2856\left(\frac{f_t}{f_s}\right) + 0.1845\left(\frac{S_l}{S_t}\right). \tag{22}$$

In Figure 14, one can see the proposed j correlation can predict 95% of the experimental data within ±15% accuracy.

5. CONCLUSION

This study experimentally investigated the airside performance of a total of 10 cross flow heat exchangers having crimped spiral configurations under the dehumidification. The effects of tube diameter, fin spacing, transverse tube pitch are examined. Based on the experimental observations, the following results are concluded:

1. The pressure drop of wet surface heat exchanger increases with the mass flow rate of air and the result is slightly higher or close to that of dry surface because only water condensate can be easily drained in the present comparatively large fin spacing and individual finned configuration.
2. The heat transfer coefficient of wet surface is slightly lower than that of dry surface.
3. The effect of tube diameter on the airside performance is significant. Larger tube diameter not only gives rise to lower heat transfer coefficient but also contribute significantly to the increase of pressure drops. This phenomenon is applicable in both dry and wet condition.
4. For wet surface, the influence of fin height is negligible whereas there is a small effect in dry surface.
5. The effect of fin spacing on the heat transfer performance is rather small. However, the increasing of fin spacing tends to have a lower heat transfer coefficient.
6. The tube arrangement plays an importance role on the heat transfer coefficient, the lower transverse pitch gives the higher heat transfer coefficient.
7. Airside performance in the present study is presented in terms of f and the j factor. The proposed correlations can predict 75% and 95% of experimental data within ±15%.

6. ACKNOWLEDGEMENT

The authors gratefully acknowledge the support provided by the Thailand Research Fund for carrying out this study. Part of the financial support provided by the Energy R&D foundation funding from the Energy Commission of the Ministry of Economic Affairs, Taiwan is also appreciated.

REFERENCES

1. D.E. Briggs, E.H. Young, 1963, Convective Heat Transfer and Pressure Drop of Air Flowing Across Triangular Pitch Banks of Finned Tubes, Chemical Engineering Progress Symposium Series 59 (41) (1963) 1-10.
2. K.K. Robinson, D.E. Briggs, Pressure Drop of Air Flowing Across Triangular Pitch Banks of Finned Tubes, Chemical Engineering Progress Symposium Series 62 (64) (1966) 177-184.
3. T.J. Rabas, P.W. Eckels, R.A. Sabatino, The Effect of Fin Density on the Heat Transfer and Pressure Drop Performance of Low Finned Tube Banks, Chemical Engineering Comunications 10 (2) (1981) 127-147.
4. A. Nuntaphan, T. Kiatsiriroat, Heat Transfer Characteristic of Cross Flow Heat Exchanger Using Crimped Spiral Fins a Case Study of Staggered arrangement, The 17th Conference of Mechanical Engineering Network of Thailand, Thailand 2003.
5. J.L. Threlkeld, Thermal Environmental Engineering, Prentice-Hall Inc., New York, 1970.
6. R.J. Myers, The Effect of Dehumidification on the Air-side heat Transfer Coefficient for a Finned-tube Coil, M.S. Thesis, University of Minnesota, Minneapolis, 1967.
7. C.C. Wang, Y.C. Hsieh, Y.T. Lin, Performance of Plate Finned Tube Heat Exchanger Under Dehumidifying Conditions, ASME Journal of Heat Transfer 119 (1997) 109-119.
8. V. Gnielinski, New Equation for Heat and Mass Transfer in Turbulent Pipe and Channel Flow, Int. Chem. Engng 16 (1976) 359-368.
9. C.C. Wang, Y.P Chang, K.Y. Chi, Y.J. Chang, An Experimental Study of Heat Transfer and Friction Characteristics of Typical Louver Fin and Tube Heat Exchangers, Int. J. of Heat and Mass Transfer 41 (4-5) (1998) 817-822.

10. A.H. Elmahdy, Analytical and Experimental Multi-row, Finned-tube Heat Exchagner Performance during Cooling and Dehumidification Process, Ph.D. thesis, Carleton University, Ottawa, Canada, 1975.

11. P.W. Eckels, T.J. Rabas, Dehumidification: on the Correlation of Wet and Dry Transport Process in Plate Finned-tube Heat Exchangers, ASME Journal of Heat Transfer 109, (1987) 572-582.

12. D.R. Mirth, S. Ramadhyani, Prediction of Cooling-coils Performance Under Condensing Conditions, International Journal of Heat and Fluid Flow, 14 (4) (1993) 391-400.

13. C.C. Wang, J. Lou, Y.T. Lin, C.S. Wei, Flow Visualization of Annular and Delta Winlet Vortex Generators in Fin-and-tube Heat Exchanger Application, Int. J. of Heat and Mass Transfer 45 (2002) 3803-3815.

14. F.C. McQuiston, Heat mass and Momentum Transfer Data for Five Plate-fin Tube Transfer Surface, ASHRAE Transactions 84 (1) (1978) 266-293.

15. F.C. McQuiston , Correlation of Heat mass and Momentum Transport Coefficients for Plate-fin Tube Transfer Surfaces with Staggered Tubes, ASHRAE Transactions 84 (1) (1978) 294-309.

Nomenclature

A_{min} minimum free flow area

A_o total surface area

$A_{p,i}$ inside surface area of tube

$A_{p,m}$ mean surface area of tube

$A_{p,o}$ outside surface area of tube

b'_p slope of straight line between the outside and inside tube wall temperature

b'_r slope of the air saturation curved at the mean coolant temperature

$b'_{w,m}$ slope of the air saturation curved at the mean water film temperature of the external surface

$b'_{w,p}$ slope of the air saturation curve at the mean water film temperature of the primary surface

$C_{p,a}$ moist air specific heat at constant pressure

$C_{p,w}$ water specific heat at coolant pressure

d_f outside diameter of finned tube

d_i tube inside diameter

d_o tube outside diameter

f friction factor

f_h fin height

f_i in-tube friction factor of water

f_s fin spacing

f_t fin thickness

F correction factor

G_{max} maximum mass velocity based on minimum flow area

$h_{c,o}$ sensible heat transfer coefficient for wet coil

h_i inside heat transfer coefficient

$h_{o,w}$ total heat transfer coefficient for wet external fin

I_0 modified Bessel function solution of the first kind, order 0

I_1 modified Bessel function solution of the first kind, order 1

i air enthalpy

$i_{a,in}$ inlet air enthalpy

$i_{a,out}$ outlet air enthalpy

$i_{r,m}$ saturated air enthalpy at the mean refrigerant temperature

$i_{r,in}$ saturated air enthalpy at the inlet of refrigerant temperature

$i_{r,out}$ saturated air enthalpy at the outlet of refrigerant temperature

$i_{s,p,i,m}$ saturated air enthalpy at the mean inside tube wall temperature

$i_{s,p,o,m}$ saturated air enthalpy at the mean outside tube wall temperature

$i_{s,w,m}$ saturated air enthalpy at the mean water film temperature of the external surface

Δi_m mean enthalpy difference

j the Colburn factor

K_0 modified Bessel function solution of the second kind, order 0

K_1 modified Bessel function solution of the second kind, order 1

k_f thermal conductivity of fin

k_i thermal conductivity of tube side fluid

k_p thermal conductivity of tube

k_w thermal conductivity of water

m parameter

$\dot{m}_a$ air mass flow rate

$\dot{m}_w$ water mass flow rate

n_r number of tube row

n_t number of tube in each row

ΔP pressure drop

Pr Prandtl number

Q_{avg} mathematical average heat transfer rate

Q_a air-side heat transfer rate

Q_w water side heat transfer rate

r_i distance from the center of the tube to the fin base

r_o distance from the center of the tube to the fin tip

Re_{Di} Reynolds number base on inside diameter of bare tube

Re_D Reynolds number base on outside diameter of bare tube

S_l longitudinal tube pitch

S_t transverse tube pitch

$T_{w,m}$ mean temperature of water film

$T_{w,in}$ water temperature of at the tube inlet

$T_{w,out}$ water temperature of at the tube outlet

$T_{p,i,m}$ mean temperature of the inner tube wall

$T_{p,o,m}$ mean temperature of the outer tube wall

$T_{r,m}$ mean temperature of refrigerant coolant

$U_{o,w}$ overall heat transfer coefficient

x_p thickness of tube wall

y_w thickness of condensate water film

$\eta_{f,wet}$ wet fin efficiency

ρ_i mass density of inlet air

ρ_o mass density of outlet air

ρ_m mean mass density of air

σ contraction ratio

Caption of table and figures

Table 1 Geometric dimensions of cross flow heat exchanger

Figure 1 Details of crimped spiral fin.

Figure 2 Schematic diagram of the experimental set-up.

Figure 3 Relevant definitions of the geometrical parameters of crimped spiral fins.

Figure 4 Comparisons of the pressure drop comparison in dry and wet condition for samples 1 and 10.

Figure 5 Comparisons of the pressure drop comparison in dry and wet condition for samples 8 and 9.

Figure 6 Comparisons of the pressure drop comparison in dry and wet condition for samples 2, 3, and 4.

Figure 7 Comparisons of the pressure drop comparison in dry and wet condition for samples 5, 6, and 7.

Figure 8 Comparison of the frictional data with the proposed correlation.

Figure 9 Comparisons of the heat transfer coefficient in dry and wet condition for samples 1 and 10.

Figure 10 Comparisons of the heat transfer coefficient in dry and wet condition for samples 8 and 9.

Figure 11 Comparisons of the heat transfer coefficient in dry and wet condition for samples 2, 3, and 4.

Figure 12 Comparisons of the heat transfer coefficient in dry and wet condition for samples 5, 6, and 7.

Figure 13 Comparisons of the heat transfer coefficient in dry and wet condition for samples 2, 3, 4, 5, 6, and 7.
Figure 14 Comparison of the heat transfer data with the proposed correlation.

Table 1 Geometric dimensions of cross flow heat exchanger

No	d_o (mm)	d_i (mm)	f_s (mm)	f_h (mm)	f_t (mm)	S_t (mm)	S_l (mm)	n_r	n_t	arrangement
1	17.3	13.3	3.85	10.0	0.4	50.0	43.3	4	9	staggered
2	21.7	16.5	6.10	10.0	0.4	72.0	36.0	4	6	staggered
3	21.7	16.5	3.85	10.0	0.4	72.0	36.0	4	6	staggered
4	21.7	16.5	2.85	10.0	0.4	72.0	36.0	4	6	staggered
5	21.7	16.5	6.10	10.0	0.4	84.0	24.2	4	5	staggered
6	21.7	16.5	3.85	10.0	0.4	84.0	24.2	4	5	staggered
7	21.7	16.5	2.85	10.0	0.4	84.0	24.2	4	5	staggered
8	21.7	16.5	3.85	10.0	0.4	55.6	48.2	4	8	staggered
9	21.7	16.5	3.85	15.0	0.4	55.6	48.2	4	8	staggered
10	27.2	21.6	3.85	10.0	0.4	50.0	43.3	4	9	staggered

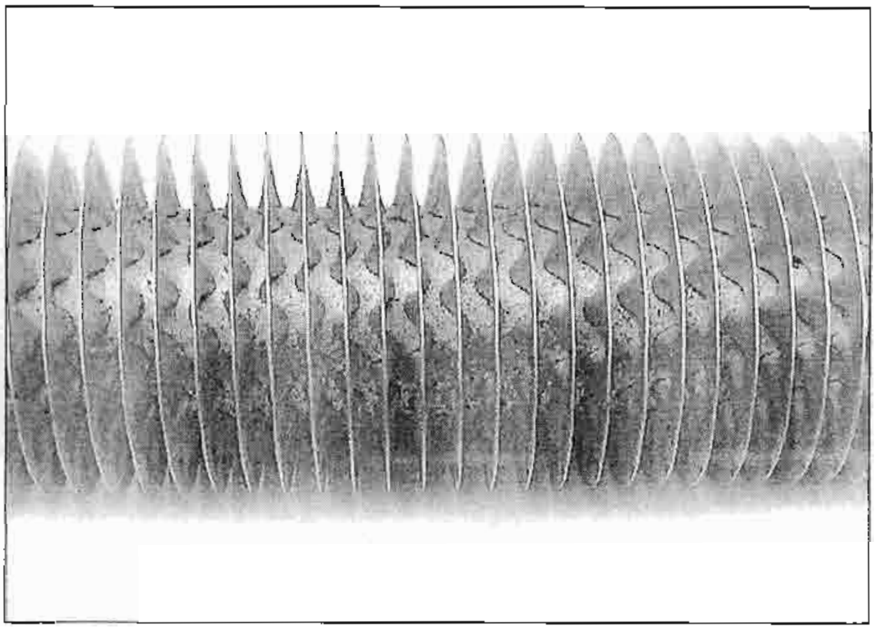

Figure 1 Details of crimped spiral fin.

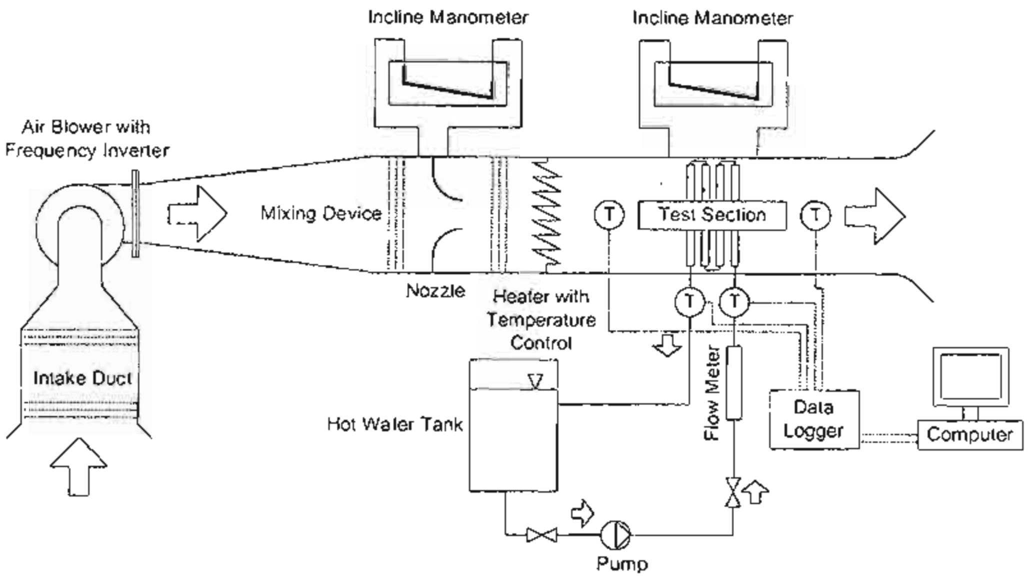

Figure 2 Schematic diagram of the experimental set-up.

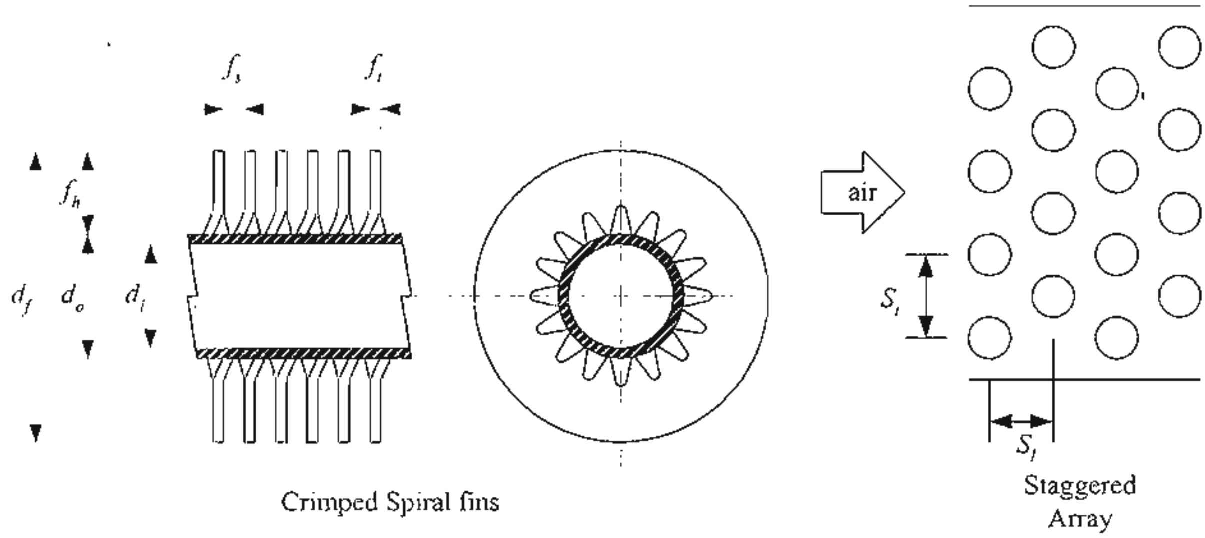

Crimped Spiral fins

Figure 3 Relevant definitions of the geometrical parameters of crimped spiral fins.

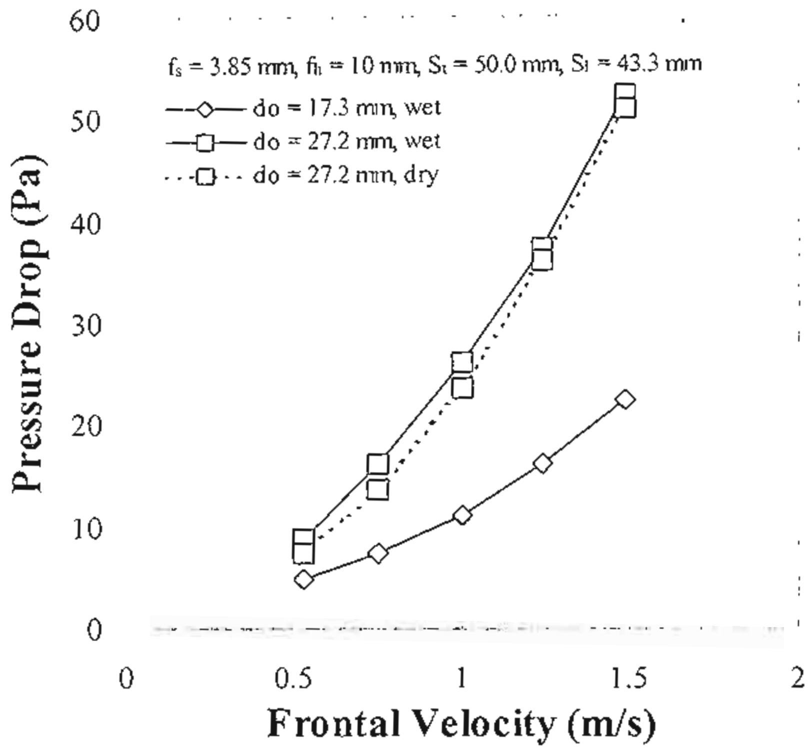

Figure 4 Comparisons of the pressure drop comparison in dry and wet condition

for samples 1 and 10.

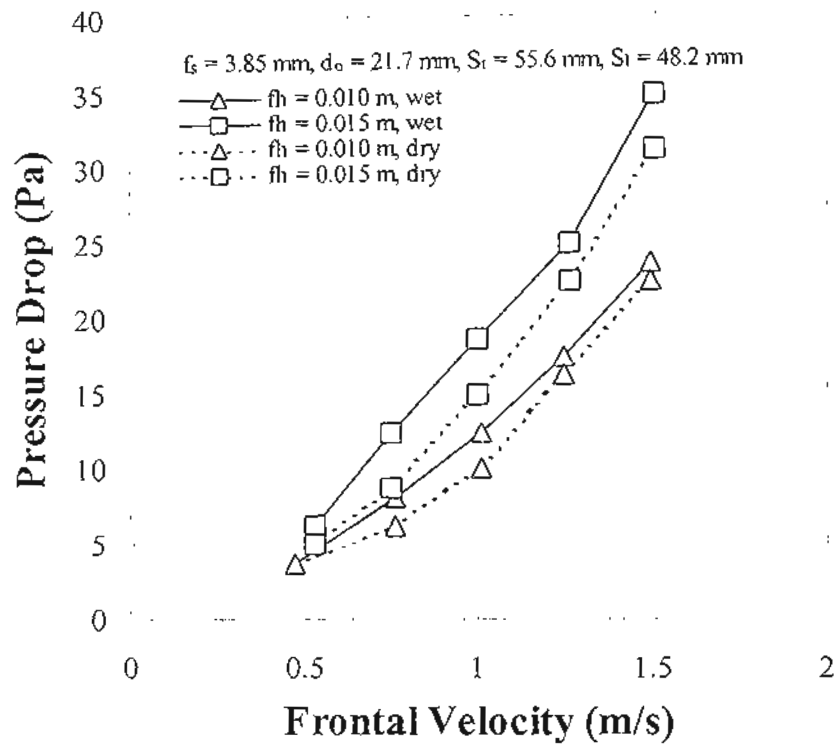

Figure 5 Comparisons of the pressure drop comparison in dry and wet condition for samples 8 and 9.

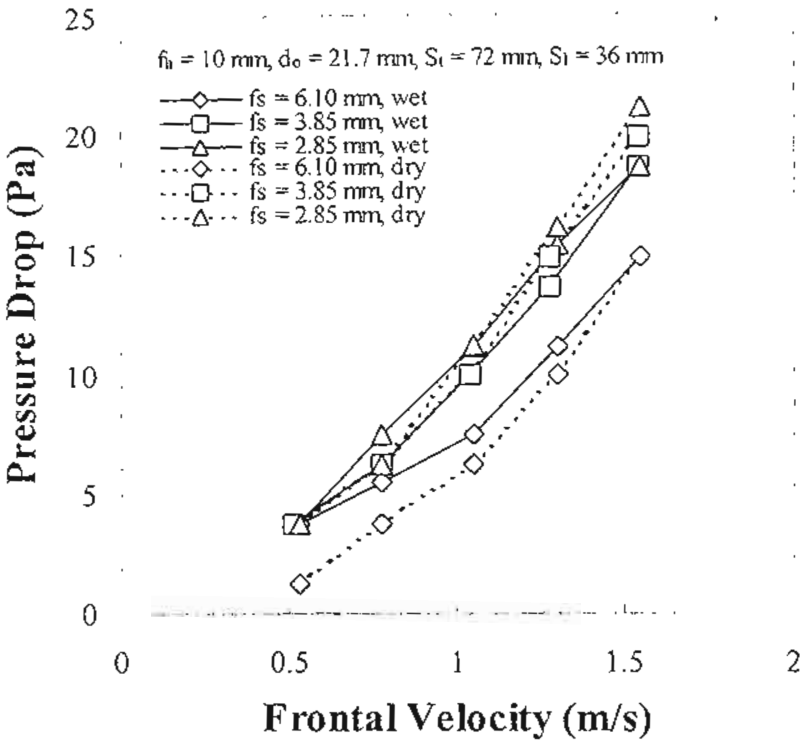

Figure 6 Comparisons of the pressure drop comparison in dry and wet condition for samples 2, 3, and 4.

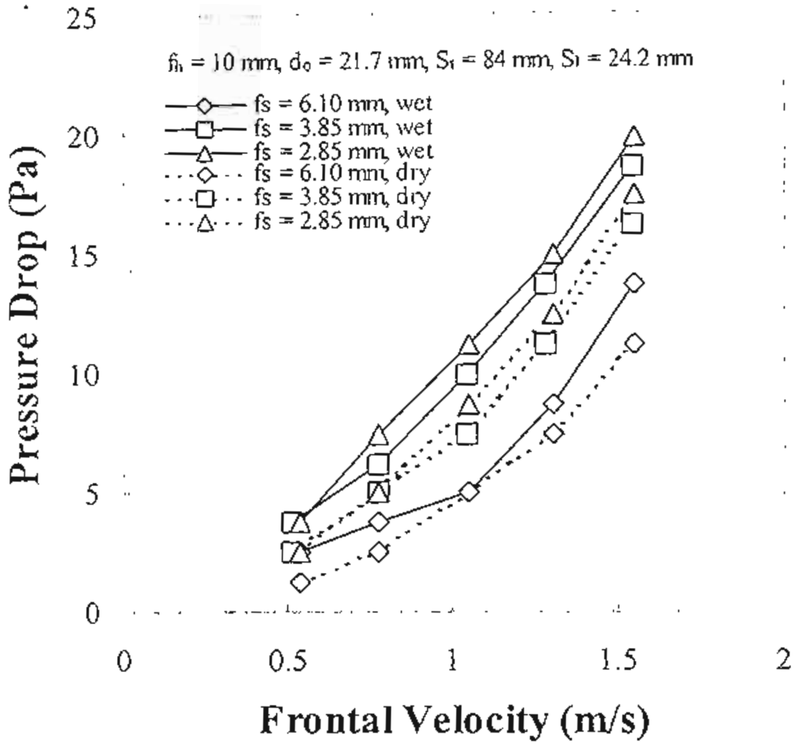

Figure 7 Comparisons of the pressure drop comparison in dry and wet condition

for samples 5, 6, and 7.

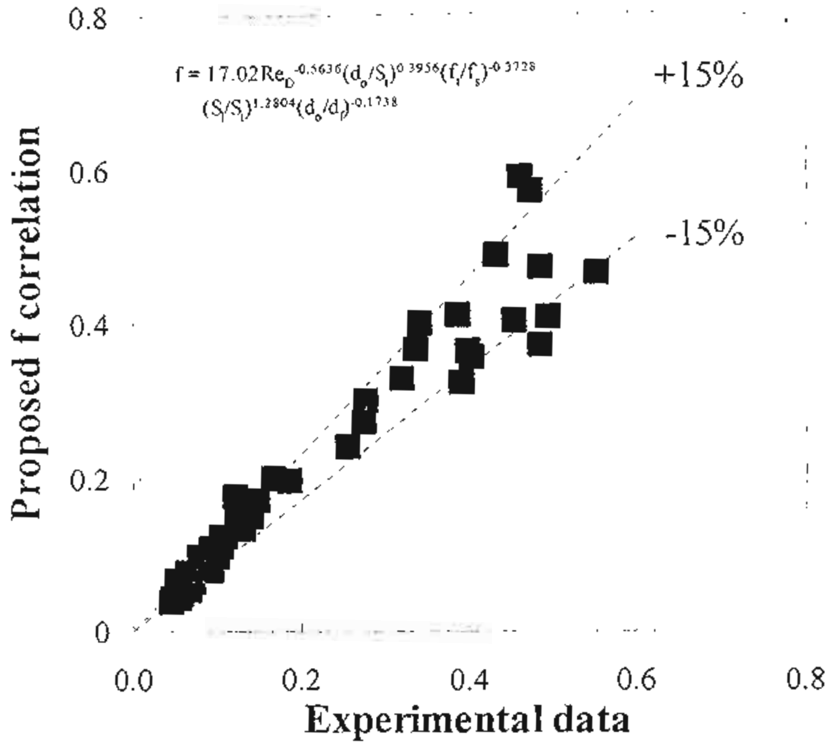

Figure 8 Comparison of the frictional data with the proposed correlation.

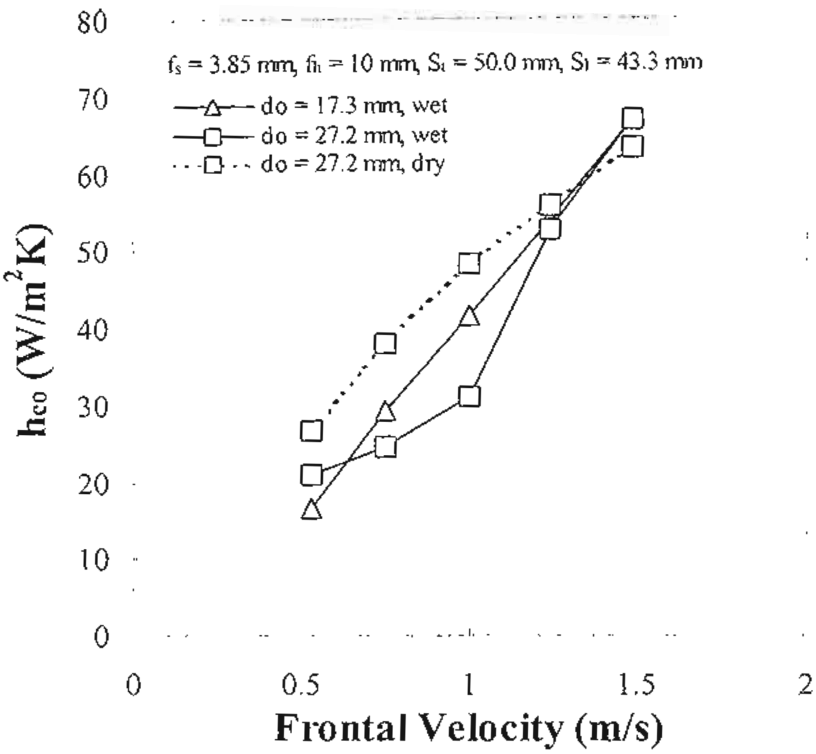

Figure 9 Comparisons of the heat transfer coefficient in dry and wet condition for samples 1 and 10.

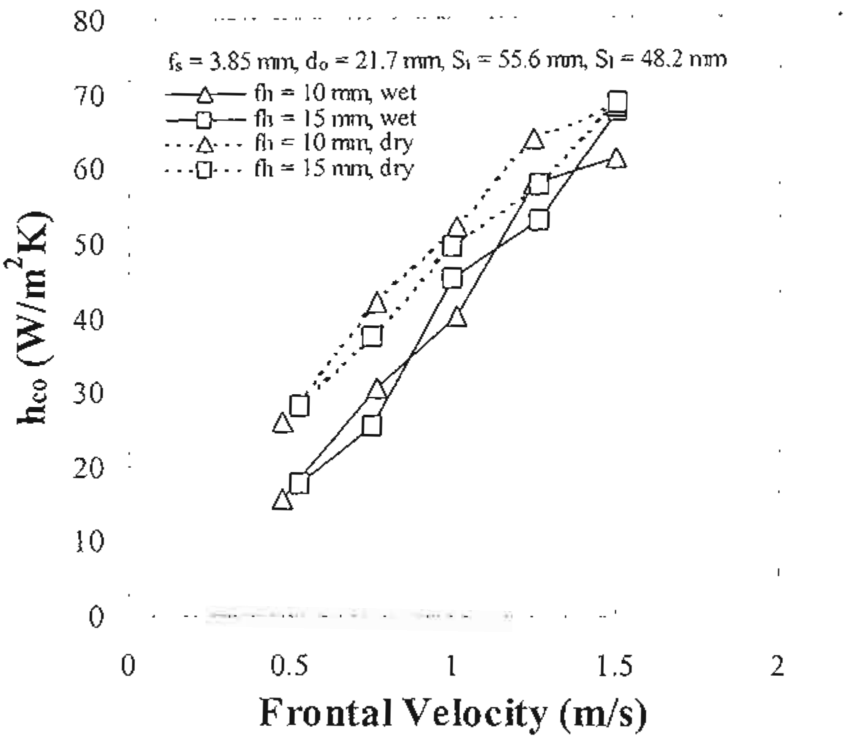

Figure 10 Comparisons of the heat transfer coefficient in dry and wet condition for samples 8 and 9.

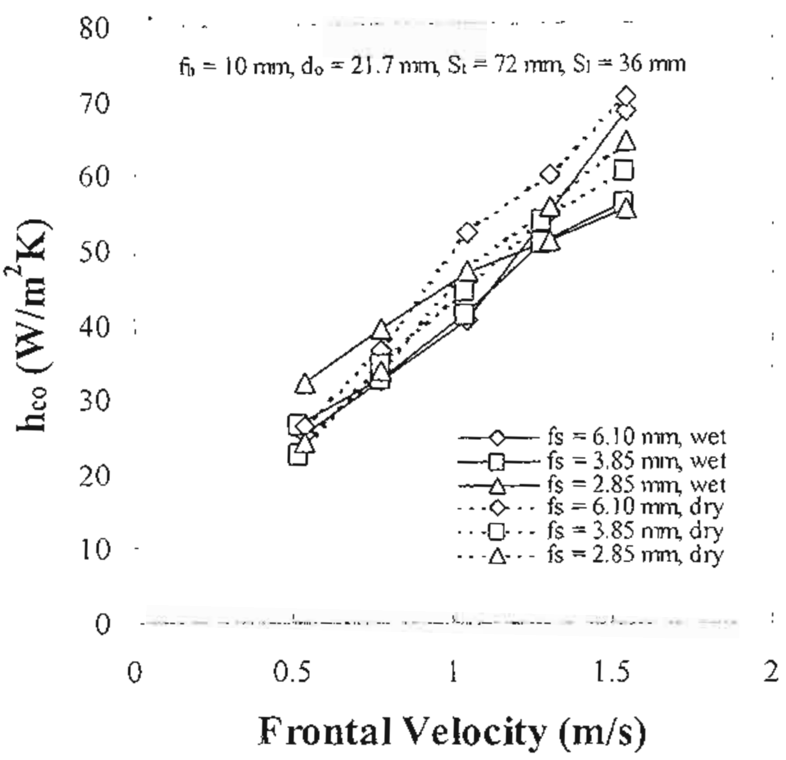

Figure 11 Comparisons of the heat transfer coefficient in dry and wet condition

for samples 2, 3, and 4.

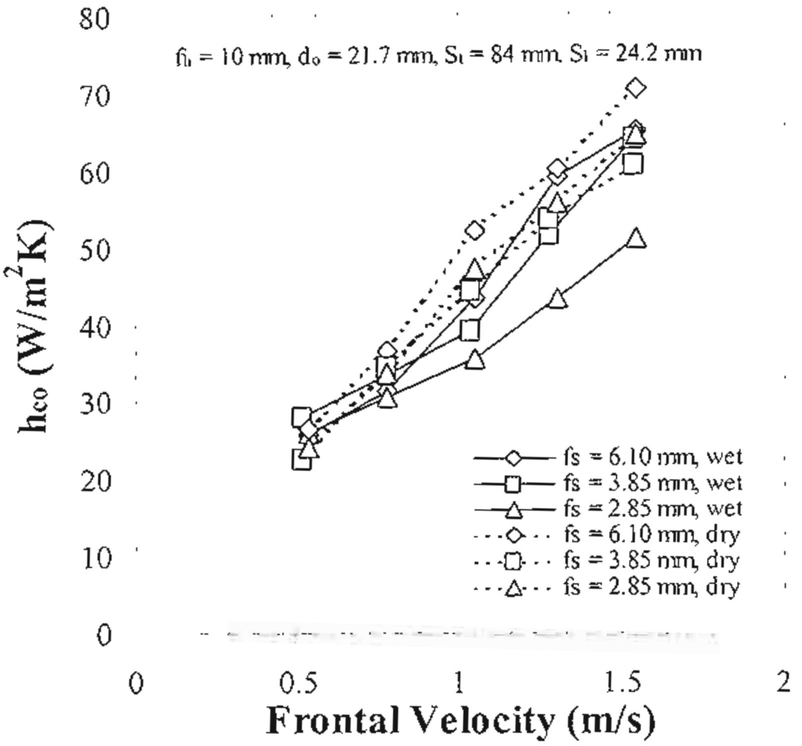

Figure 12 Comparisons of the heat transfer coefficient in dry and wet condition for samples 5, 6, and 7.

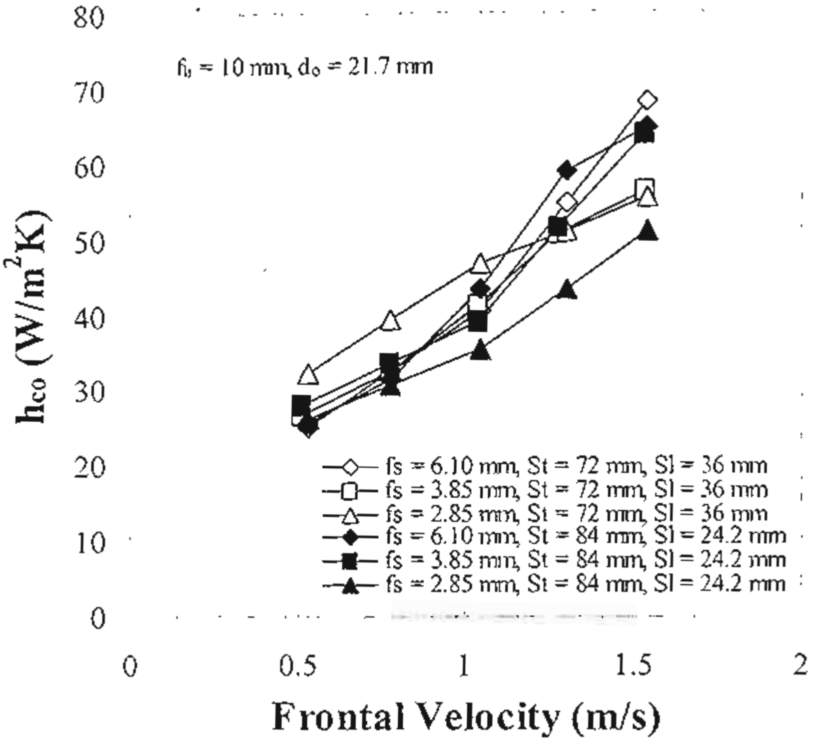

Figure 13 Comparisons of the heat transfer coefficient in wet condition

for samples 2, 3, 4, 5, 6, and 7.

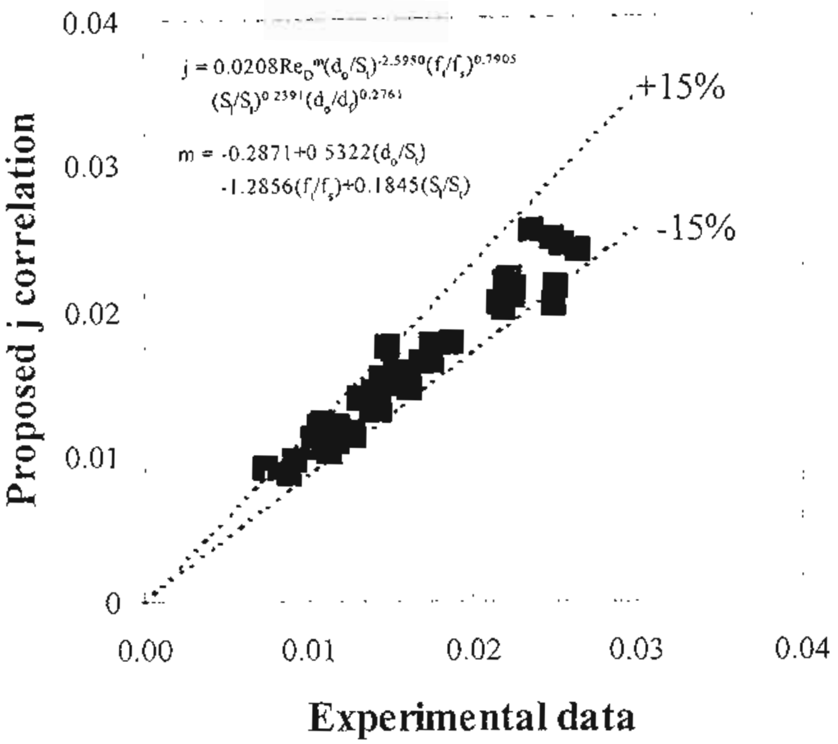

Figure 14 Comparison of the heat transfer data with the proposed correlation.

Thermal Behavior of Crimped Spiral Fin Tube Bank Under Dehumidifying Process: A Case Study of Inline Arrangement

Atipoang Nuntaphan[1] and Tanongkiat Kiatsiriroat[2]

Abstract

Nuntaphan, A. and Kiatsiriroat, T.
Thermal Behavior of Crimped Spiral Fin Tube Bank Under Dehumidifying Process: A Case Study of Inline Arrangement
Songklanakarin J. Sci. Technol.

A cross flow heat exchangers having crimped spiral fin and inline arrangement configurations under dehumidification is studied. The effect of tube diameter, fin spacing, fin height, transverse tube pitch are examined. From the experiment, it is found that the heat transfer and the frictional characteristics of the heat exchanger under dehumidification is close to that of the non-dehumidifying process. However, the air stream pressure drop and the heat transfer coefficient of the wet surface heat exchanger are higher and lower than those of the dry surface respectively. Moreover, equations are developed for predicting the f and the j factors of a tested heat exchanger. Results from the developed equations agree well with the experimental data.

Keywords: Air-side performance, dehumidification, crimped spiral fins

[1]Ph.D. (Thermal Technology), Engineer Level 6, Mae Moh Training Center, Electricity Generating Authority of Thailand, Mae Moh, Lampang 52220, [2]D.Eng. (Energy Technology), Professor, Department of Mechanical Engineering, Chiang Mai University, Chiang Mai 50202, Thailand.
Corredponding e-mail : atipoang.n@egat.co.th

บทคัดย่อ

อดิพงศ์ นันทพันธุ์[1] และ ทนงเกียรติ เกียรติศิริโรจน์[2]

พฤติกรรมทางความร้อนของกลุ่มท่อติดครีบแบบเกลียวชนิดขอบหยักภายใต้สภาวะการควบแน่นของไอน้ำ : กรณีศึกษาการจัดเรียงท่อในแนวเดียวกัน

งานวิจัยนี้ได้ศึกษาสมรรถนะเครื่องแลกเปลี่ยนความร้อนแบบไหลตามขวางที่ใช้ครีบเกลียวชนิดขอบหยักและจัดเรียงกลุ่มท่อในแนวเดียวกันภายใต้สภาวะของการเกิดการควบแน่นของไอน้ำในอากาศบนพื้นผิวเครื่องแลกเปลี่ยนความร้อน โดยงานวิจัยนี้ได้ศึกษาอิทธิพลของขนาดของท่อ ระยะห่างระหว่างครีบ ความสูงของครีบ และรูปแบบการจัดเรียงท่อที่มีต่อสมรรถนะของระบบ จากการทดลองพบว่าคุณลักษณะการถ่ายเทความร้อนและความดันอากาศตกคร่อมเครื่องแลกเปลี่ยนความร้อนภายใต้สภาวะที่มีการควบแน่นของไอน้ำในอากาศจะใกล้เคียงกับสภาวะที่ไม่มีการควบแน่นของไอน้ำ แต่อย่างไรก็ตามพบว่าค่าสัมประสิทธิ์การถ่ายเทความร้อนและค่าความดันอากาศตกคร่อมเครื่องแลกเปลี่ยนความร้อนของกรณีศึกษานี้ต่ำกว่าและสูงกว่ากรณีที่ไม่มีการควบแน่นของไอน้ำตามลำดับ นอกจากนี้ยังได้ทำการพัฒนาสมการสหสัมพันธ์เพื่อใช้คำนวณค่าความดันอากาศตกคร่อม และค่าสัมประสิทธิ์การถ่ายเทความร้อนเครื่องแลกเปลี่ยนความร้อน ซึ่งสมการที่พัฒนาขึ้นสามารถใช้ทำนายผลการทดลองได้เป็นอย่างดี

---

[1]วิศวกรระดับ 6 กองศูนย์ฝึกอบรมแม่เมาะ การไฟฟ้าฝ่ายผลิตแห่งประเทศไทย อำเภอแม่เมาะ จังหวัดลำปาง 52220 [2]ภาควิชาวิศวกรรมเครื่องกล คณะวิศวกรรมศาสตร์ มหาวิทยาลัยเชียงใหม่ อำเภอเมือง จังหวัดเชียงใหม่ 50200

The cross flow heat exchanger plays an important role in waste heat recovery process, especially. in economizer where flue gas exchanges heat with water. Normally, water flows inside the tube while hot gas flows outside. Because the heat transfer resistance at gas-side dominates the heat transfer of heat exchanger, many attempts have been carried out to improve the gas-side heat transfer. Circular fins or spiral fins are normally used for recovering heat from flue gas. In this study, the crimped spiral fin was taken and the detail of crimped spiral finned tube was shown in Figure 1. It should be noticed that the inner crimped edge gives a good attachment between the fins and the tube.

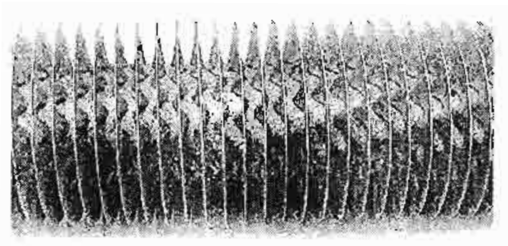

Figure 1 The crimped spiral fin.

When using a set of crimped spiral finned tubes in a cross flow heat exchanger, the designer should concern about the heat transfer coefficient and the gas or air stream pressure drop of the tube bank. Many research works have been performed to find out these values, such as Briggs and Young [1963], Robinson and Briggs [1966], Rabas et al [1981] and Schmidt [1963] in case of circular finned tube bank and Nuntaphan and Kiatsirirat [2003] in case of crimped spiral fins. However, these studies were deal with the dry coil conditions. Actually, in the case of waste heat recovery system, the heat exchanger faces with condensation of moisture in the hot gas or air stream at the heat exchanger surface. Although the designer tries to avoid this condition because the finned tube might be corroded, but in case of small boiler, condensation of moisture always occurs. There are very few reports about the performance of the tube bank particularly the cross flow heat exchanger using crimped spiral finned especially in case of inline arrangement. Despite of its comparatively low heat transfer performance, its lower pressure drop and high reliability (easy to maintain and clean) are very attractive in very severe environment. Therefore, the aim of this work is to study the heat transfer and friction characteristic of cross flow heat exchanger using crimped spiral fin in case of inline arrangement. This heat exchanger faces with vapor condensation. Moreover, the heat transfer and friction correlations are also developed in this work.

EXPERIMENTAL SET-UP

Figure 2 presents the schematic of the experimental set-up. The hot air stream flows through the tube bank and the water at room temperature circulates inside the tubes. In this experiment, the water flow rate is kept constant at 8 L/min. An accurate water flow meter is used for the measurement with a precision of ±0.1 L/min. The inlet temperature of water is approximately 30°C. Both of the inlet and outlet temperatures of water are measured by a set of calibrated K-type thermocouples and a temperature data logger records these signals.

A 1.5 kW centrifugal air blower with a frequency inverter with a controllable range of 0.1-0.5 kg/s air flowing across the heat exchanger. A standard nozzle and an inclined manometer measure the mass flow rate of air stream with ±0.5 Pa accuracy. The inlet temperature of air stream is kept constant at 65 °C by a set of heaters and a temperature controller. The inlet and the outlet dry bulb and wet bulb temperatures of the air stream are also measured by a number of K-type thermocouples which are positioned at various locations along the flow cross-sections. Note that all of thermocouples have been calibrated to ±0.1 °C accuracy. The inclined manometer also measures the pressure drop across the heat exchanger with ±0.5 Pa accuracy.

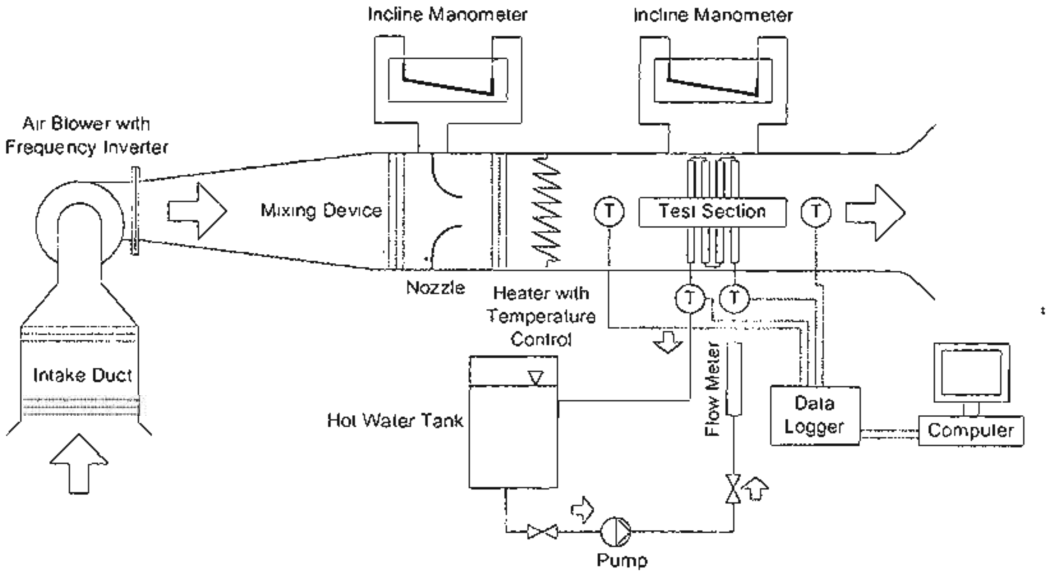

Figure 2 Schematic diagram of the experimental set-up.

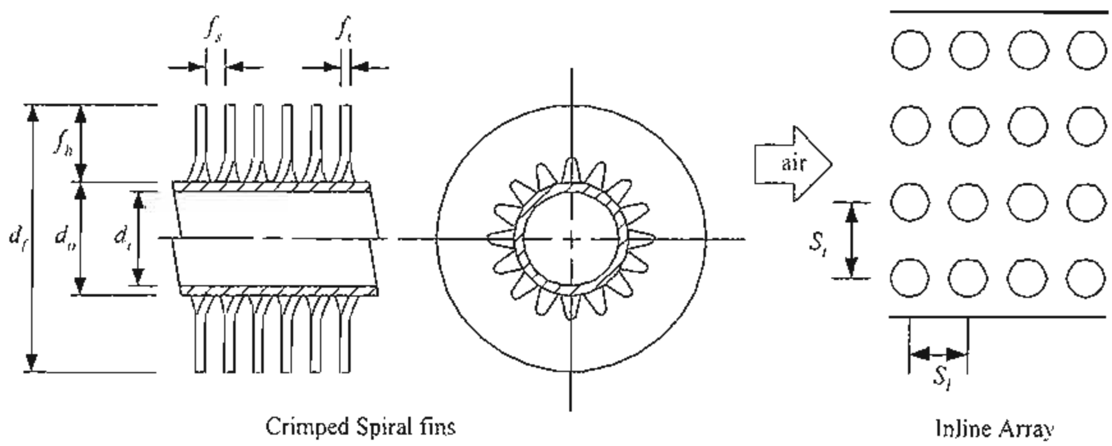

Figure 3 Relevant definitions of the geometrical parameters of crimped spiral fins.

A total of 10 crimped spiral fin heat exchangers having various geometric parameters are tested in this study. Table 1 lists the details of the tested samples. Relevant definitions of the geometrical parameters can be also shown in Figure 3. The effects of tube diameter, fin height, fin spacing, fin thickness, and tube arrangements on the airside performance are examined accordingly.

Table 1 Geometric dimensions of cross flow heat exchanger

No	d_o (mm)	d_i (mm)	f_s (mm)	f_h (mm)	f_t (mm)	S_t (mm)	S_l (mm)	n_r	n_t	arrangement
1	17.3	13.3	3.85	10.0	0.4	50.0	50.0	4	10	inline
2	27.2	21.6	3.85	10.0	0.4	50.0	50.0	4	10	inline
3	21.7	16.5	6.10	10.0	0.4	50.0	50.0	4	10	inline
4	21.7	16.5	3.85	10.0	0.4	50.0	50.0	4	10	inline
5	21.7	16.5	2.85	10.0	0.4	50.0	50.0	4	10	inline
6	21.7	16.5	3.85	10.0	0.4	71.4	50.0	4	7	inline
7	21.7	16.5	3.85	15.0	0.4	71.4	50.0	4	7	inline

DATA REDUCTION

The heat transfer rate of cross flow heat exchanger under dehumidifying condition can be calculated as follows:

$$Q_a = \dot{m}_a \left(i_{a,in} - i_{a,out}\right), \tag{1}$$

$$Q_w = \dot{m}_w C_{pw} \left(T_{w,out} - T_{w,in}\right). \tag{2}$$

Note that the heat transfer rates in Equation (1) and Equation (2) are the air-side and the tube-side, respectively. In this study, the average heat transfers rate can be evaluated as

$$Q_{avg} = 0.5\left(Q_a + Q_w\right). \tag{3}$$

The average heat transfer rate can be defined as a function of the overall heat transfer coefficient based on the mean enthalpy difference as

$$Q_{avg} = U_{o,w} A_o F \Delta i_m . \tag{4}$$

F is the correction factor in the case of cross flow unmixed/unmixed configuration. Threlkeld [1970] defines the mean enthalpy difference for counter flow tube bank as

$$\Delta i_m = \frac{\left(i_{a,in} - i_{r,out}\right) - \left(i_{a,out} - i_{r,in}\right)}{\ln\left(\dfrac{i_{a,in} - i_{r,out}}{i_{a,out} - i_{r,in}}\right)}. \tag{5}$$

Mayer [1967] showed the relation of the overall heat transfer coefficient ($U_{o,w}$) and other heat transfer resistance as

$$\frac{1}{U_{o,w}}=\frac{b_r' A_o}{h_i A_{p,i}}+\frac{b_p' x_p A_o}{k_p A_{p,m}}+\frac{1}{h_{o,w}\left(\frac{A_{p,o}}{b_{w,p}' A_o}+\frac{A_f \eta_{f,wet}}{b_{w,m}' A_o}\right)}, \tag{6}$$

where

$$h_{o,w}=\frac{1}{\frac{C_{p,a}}{b_{w,m}' h_{c,o}}+\frac{y_w}{k_w}}. \tag{7}$$

Note that the ratio of water film thickness and thermal conductivity of water (y_w / k_w) is very small compared to other terms [1997] and they are neglected in this study.

The tube side heat transfer coefficient can be calculated from Gnielinski correlation [1976] as

$$h_i=\frac{(f_i/2)(\mathrm{Re}_{Di}-1000)\mathrm{Pr}}{1.07+12.7\sqrt{f_i/2}\left(\mathrm{Pr}^{2/3}-1\right)}\left(\frac{k_i}{d_i}\right), \tag{8}$$

where

$$f_i=\frac{1}{(1.58\ln \mathrm{Re}_{Di}-3.28)^2}. \tag{9}$$

The four quantities in Equation 7 can be estimated following the method of Wang et al. [1997] based on the enthalpy-temperature ratios. In case of b_r' and b_p', they can be calculated as

$$b_r'=\frac{i_{s,p,i,m}-i_{r,m}}{T_{p,i,m}-T_{r,m}}, \tag{10}$$

$$b_p'=\frac{i_{s,p,o,m}-i_{s,p,i,m}}{T_{p,o,m}-T_{p,i,m}}. \tag{11}$$

The quantity $b_{w,p}'$ is the slope of saturated enthalpy curve evaluated at the outer mean water film temperature at the base surface and in case of no loss, it can be approximated from the slope of the saturated enthalpy curve evaluated at the base surface temperature of the tube. However, the quantity $b'_{w,m}$, which defined as the slope of saturated enthalpy curve evaluated at the outer mean water film temperature at the fin surface, can not be calculated directly. Consequently, the trial and error procedure is selected to find out this value. Wang et al. [1997] also gave the steps of this method as follows:

1. Assume a value of $T_{w,m}$ and calculate the quantity $b'_{w,m}$
2. Calculate $h_{o,w}$ from Equation 6
3. Calculate the quantity $i_{s,w,m}$ by this following relation

$$i_{s,w,m} = i - \frac{C_{p,a} h_{o,w} \eta_{f,wet}}{b'_{w,m} h_{c,o}} \times \left(1 - U_{o,w} A_o \left[\frac{b'_r}{h_i A_{p,i}} + \frac{x_p b'_p}{k_p A_{p,m}}\right]\right)(i - i_{r,m}). \quad (12)$$

4. Determine the new $T_{w,m}$ at $i_{s,w,m}$ and repeat the procedure again until the error is in limit.

The wet fin efficiency can be evaluated by the method of Wang et al [1997] as:

$$\eta_{f,wet} = \frac{2r_i}{M_T\left(r_o^2 - r_i^2\right)} \times \left[\frac{K_1(M_T r_i) I_1(M_T r_o) - K_1(M_T r_o) I_1(M_T r_i)}{K_1(M_T r_o) I_o(M_T r_i) + K_o(M_T r_i) I_1(M_T r_o)}\right], \quad (13)$$

where

$$M_T = \sqrt{\frac{2h_{o,w}}{k_f f_t}} = \sqrt{\frac{2h_{c,o}}{k_f f_t}} \sqrt{\frac{b'_w}{C_{p,a}}}. \quad (14)$$

In this work, the sensible heat transfer coefficient ($h_{c,o}$) and pressure drop of air stream across tube bank are presented in term of the Colburn factor (j) and the friction factor (f) factors as

$$j = \frac{h_{c,o}}{G_{max} C_{p,a}} \mathrm{Pr}^{2/3}, \quad (15)$$

$$f = \frac{A_{min}}{A_o} \frac{\rho_i}{\rho_m} \left[\frac{2\rho_i \Delta P}{G_c^2} - \left(1 + \sigma^2\right)\left(\frac{\rho_i}{\rho_o} - 1\right)\right]. \quad (16)$$

RESULTS AND DISCUSSION

Sensible Heat Transfer Coefficient

Figure 4 shows the effect of tube diameter on the sensible heat transfer coefficient at various frontal velocities of air stream. The fin spacing (3.85 mm), fin thickness (0.4 mm), and the fin height (10 mm) are taken for this comparison. The transverse and the longitudinal tube pitches are 50 mm. As expected, the heat transfer coefficient rises with the frontal velocity. However, it is interesting to note that the heat transfer coefficient increases with the reduction of tube diameter. This phenomenon is attributed to the ineffective area behind the tube which increases with the tube diameter especially, the inline arrangement. Wang et al. [2002] performed flow visualizations via dye injection technique for fin-and-tube heat exchangers having inline arrangement. Their visual results unveil a very large flow circulation behind the tube row. Consequently this large recirculation does not only contribute to the decrease of heat transfer coefficient but also to the rise of pressure drop. In addition, the large recirculation may also block the subsequent tube row and degrades the heat transfer performance hereafter.

Figure 5 shows the effect of fin height on the airside performance for inline arrangement. In this comparison, the associated fin heights are 10 and 15 mm and the fin spacing and the tube diameter are 3.85 mm and 21.7 mm with the transverse and the longitudinal pitches are 71.4 and 50 mm, respectively. As seen in the figure, the influence of fin height shows tremendous influence on the heat transfer performance. The heat transfer coefficients drop drastically with the increase of fin height. This is probably due to the airflow bypass effect. Actually the airflow is prone to flowing the portion where the flow resistance is small. In case of f_h = 15 mm, the airflow resistance around fin tube is larger than that for f_h = 10 mm. Therefore, part of the directed airflow just bypasses the tube row without effective contribution to the heat transfer and lower heat transfer coefficient is obtained.

The effect of the fin spacing on the airside performance is shown in Figure 6. It was found that the increase of fin spacing gives a rise to the heat transfer coefficient. An explanation of this phenomenon is the same as that in the previous case which concludes that the result comes from the airflow bypass effect. The result of airflow bypass effect is also shown in Figure 7. It can be seen that the high transverse tube pitch (S_t = 71.4 mm) gives lower heat transfer coefficient than that of the low value (S_t = 50 mm).

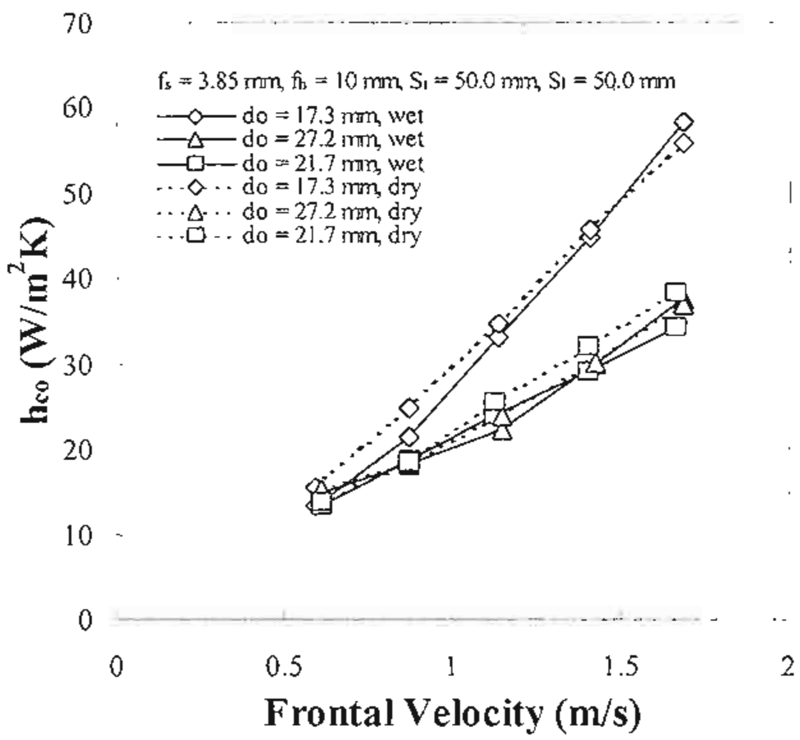

Figure 4 Effect of tube diameter on the sensible heat transfer coefficient.

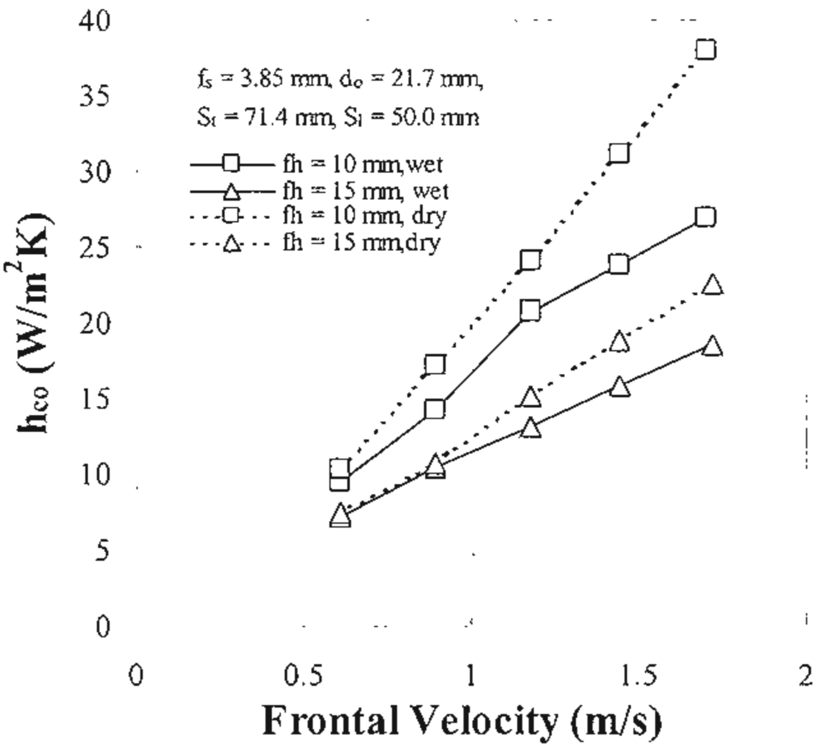

Figure 5 Effect of fin height on the sensible heat transfer coefficient.

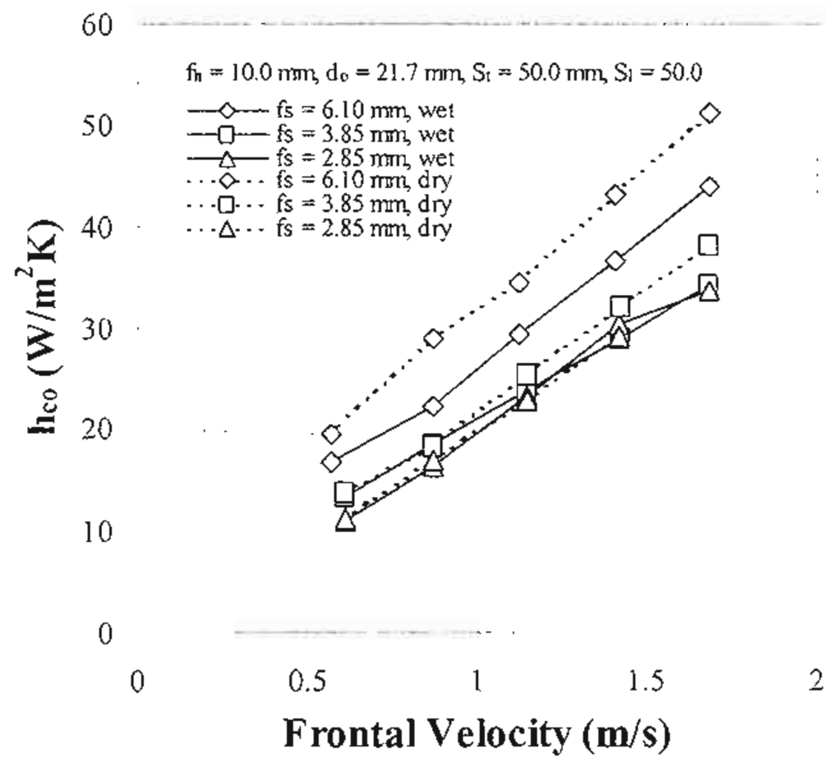

Figure 6 Effect of fin spacing on the sensible heat transfer coefficient.

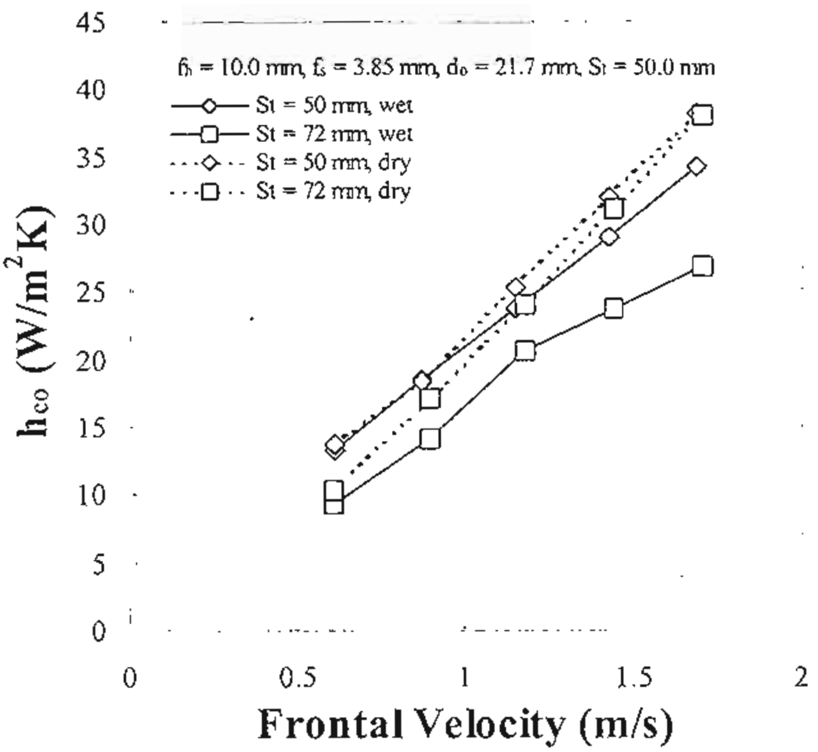

Figure 7 Effect of transverse pitch on the sensible heat transfer coefficient.

Comparison of the heat transfer coefficient under dehumidifying process with that of non-dehumidifying condition from the report of Nuntaphan and Kiatsiriroat [2003] is also shown in Figures 4-7. The heat transfer phenomena of the wet surface heat exchanger are close to those of the dry surface. However, the heat transfer coefficient of the wet surface is lower than that of dry surface. Actually, there are many reports showing the comparison of the heat transfer coefficient between wet and dry surface heat exchanger. Some experiment shows the heat transfer augmentation of wet surface, such as Meyers [1967], Elmahdy [1975] and Eckels and Rabas [1987] for the continuous plate finned tube. However, some reports show the decreasing in the heat transfer coefficient of wet surface, such as for the wavy finned tube. Mirth and Ramadhyani [1993] showed 17-50% decreasing of heat transfer coefficient of wet surface. Moreover Wang et al [1997] showed the decreasing of the Colburn j factor of plate finned tube when the Reynolds number lower than 2,000. However, at the higher Reynolds number, the j factor of wet surface is slightly higher than that of dry surface. The present results are generally in agreement with the trend of Wang et al. [1997].

In this research, the correlation for predicting the Colburn j factor including the effect of various quantities is also developed and the model is

$$j = 0.0023\,\mathrm{Re}_D^m \left(\frac{d_o}{S_t}\right)^{-5.8433} \left(\frac{f_l}{f_s}\right)^{-0.6457} \left(\frac{S_l}{S_t}\right)^{2.9009} \left(\frac{d_o}{d_f}\right)^{8.6111}, \quad (17)$$

where

$$m = 0.4987 + 1.0593\left(\frac{d_o}{S_t}\right) + 0.4265\left(\frac{f_l}{f_s}\right) - 1.8579\left(\frac{d_o}{d_f}\right). \quad (18)$$

It is found that the j model can predict about 85.7% of the experimental data within ± 15% accuracy. The comparison is also shown in Figure 8.

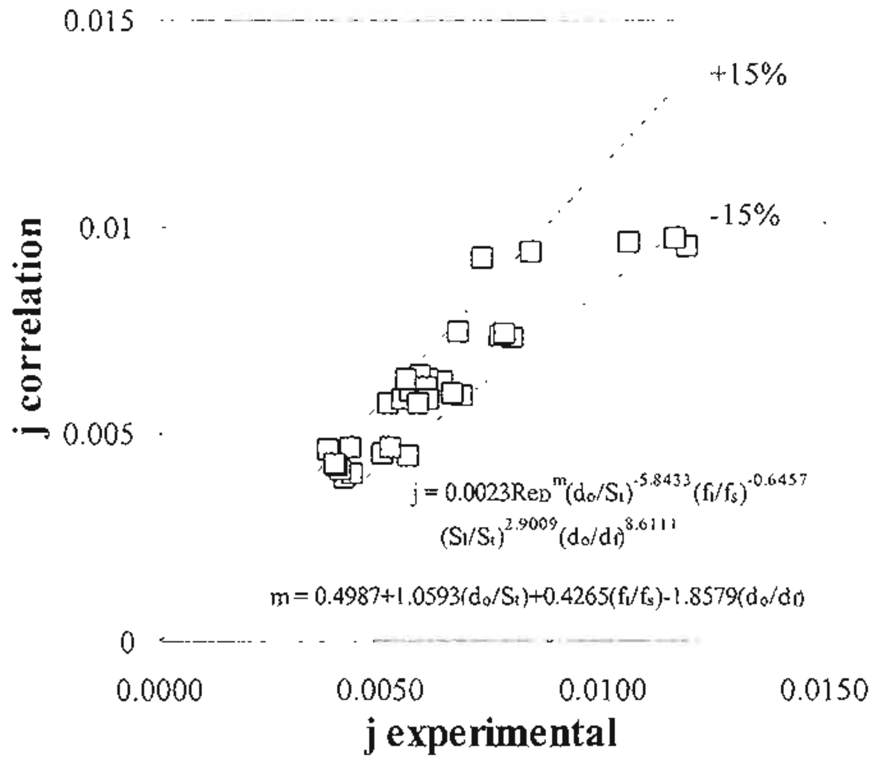

Figure 8 The comparison of j factor from experiment and correlation.

Pressure Drop

Figures 9-12 show the air stream pressure drops in the cross flow heat exchanger. It is found that the air stream pressure drop increases with the frontal velocity of air. Moreover, when compare with the result obtained from Nuntaphan and Kiatsiriraot [2003] in the case of dry surface heat exchanger, the pressure drop is slightly higher than that of dry surface. This is because only small amount of water vapor is condensed on the heat exchanger surface.

Figures 9-11 also show the pressure drop increases with tube diameter $(d_o)$and fin height (f_h). However, it decreases with the increasing of fin spacing (f_s). These phenomena come from the increasing of surface area resulted in higher the airflow resistance. The effect of tube arrangement is also found in Figure 12. Higher transverse pitch of tube bank (S_t) gives lower pressure drop.

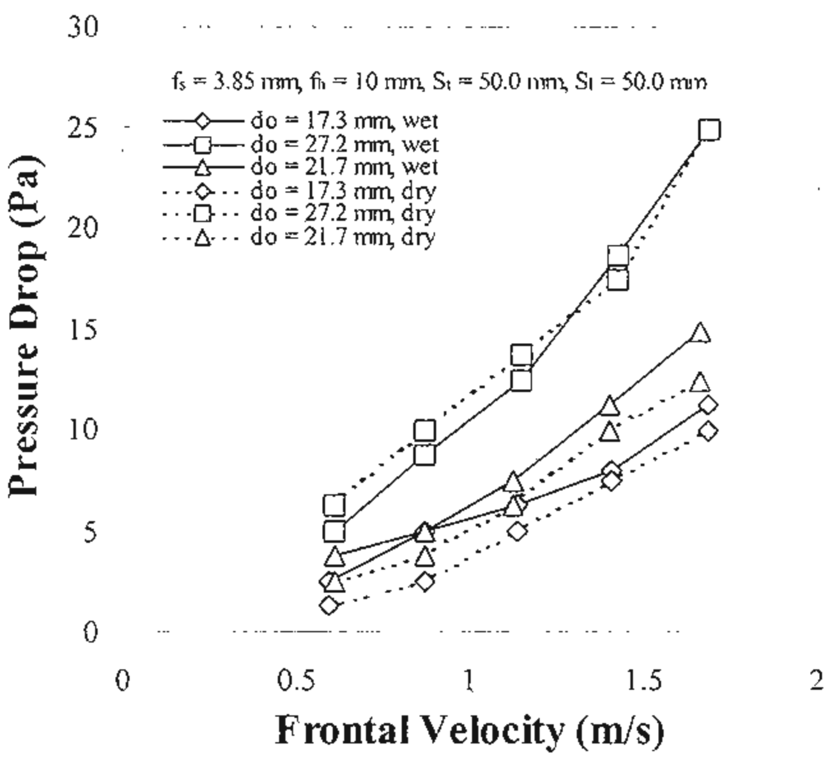

Figure 9 Effect of tube diameter on the pressure drop.

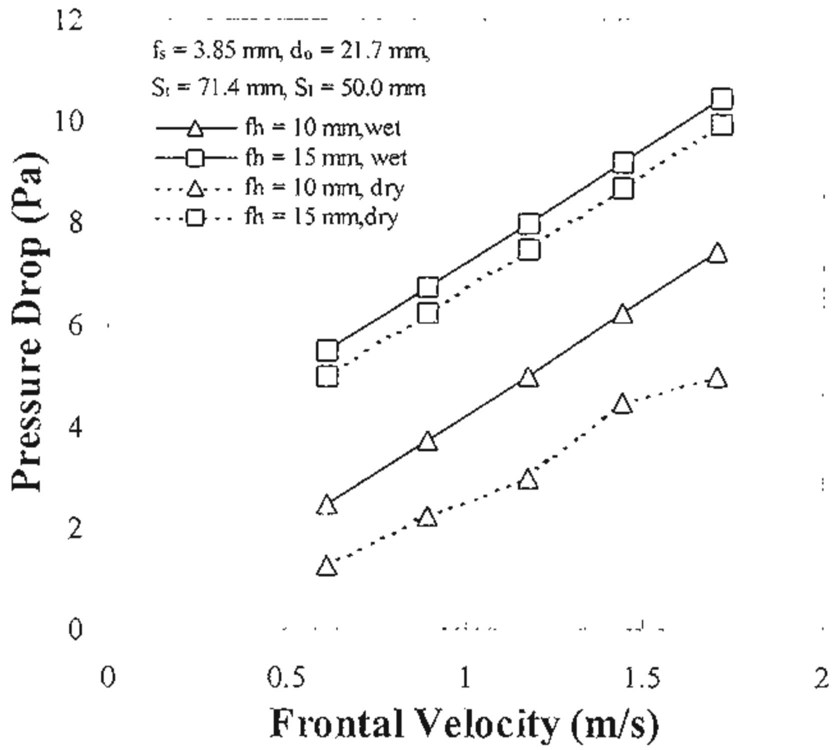

Figure 10 Effect of fin height on the pressure drop.

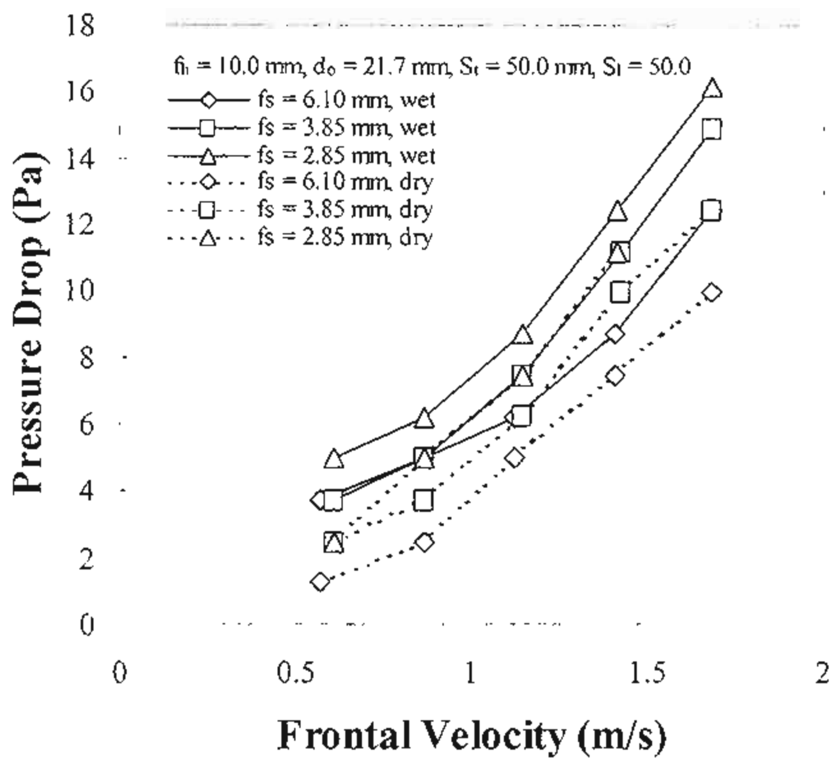

Figure 11 Effect of fin spacing on the pressure drop.

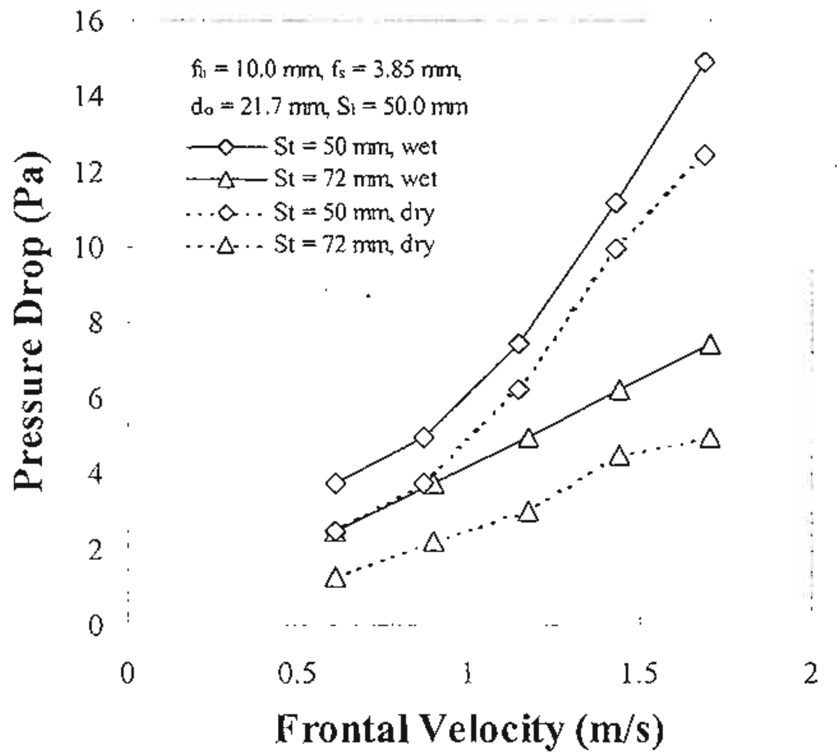

Figure 12 Effect of transverse pitch on the pressure drop.

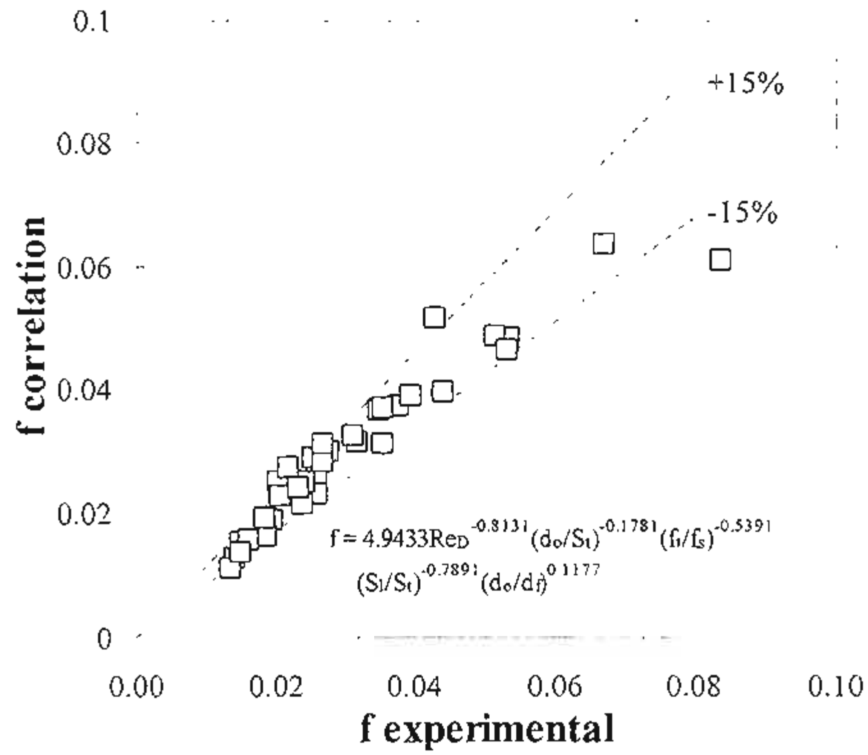

Figure 13 The comparison of *f* factor from experiment and correlation.

In this research. the correlation for predicting the air stream pressure drop including the effect of various quantities is also developed and the model is in a form of

$$f = 4.9433\mathrm{Re}_D^{-0.8131}\left(\frac{d_o}{S_t}\right)^{-0.1781}\left(\frac{f_t}{f_s}\right)^{-0.5391}\left(\frac{S_l}{S_t}\right)^{-0.7891}\left(\frac{d_o}{d_f}\right)^{0.1177} . \qquad (20)$$

From Figure 13, it is found that the f model can predict about 82.3% of the experimental data within ±15% accuracy.

CONCLUSION

From the experiment, it can be concluded as follows:

1. The heat transfer coefficient of wet surface is lower than that of dry surface.
2. The tube diameter, the fin height, the fin spacing and the transverse tube pitch of the cross flow heat exchanger under dehumidifying condition affect the heat transfer coefficient and the result is close to that of dry surface heat exchanger.
3. The air stream pressure drop of wet surface heat exchanger increases with the mass flow rate of air. The result is close to that of dry surface because only small amount of vapor is condensed.
4. The developed models for predicting the j and the f factors can estimated about 85.7% and 82.3% of experimental data within ±15% accuracy.

ACKNOWLEDGEMENT

The authors gratefully acknowledge the support provided by the Thailand Research Fund for carrying out this study.

REFERENCES

1. Briggs D.E. and Young E.H., 1963, Convective Heat Transfer and Pressure Drop of Air Flowing Across Triangular Pitch Banks of Finned Tube, Chem. Engng. Prog. Sym. Series. Vol.59, No. 41, pp.1-10.
2. Eckels P. W. and Rabas T. J., 1987, Dehumidification: on the Correlation of Wet and Dry Transport Process in Plate Finned-tube Heat Exchangers, ASME J. of Heat Transfer, Vol. 109, pp. 572-582.
3. Elmahdy A. H., 1975, Analytical and Experimental Multi-row, Finned-tube Heat Exchagner Performance during Cooling and Dehumidification Process, Ph.D. thesis, Carleton University, Ottawa, Canada.
4. Gnielinski V., 1976, New Equation for Heat and Mass Transfer in Turbulent Pipe and Channel Flow, Int. Chem. Engng, Vol.16, pp. 359-368.
5. McQuiston F. C., 1978, Heat mass and Momentum Transfer Data for Five Plate-fin Tube Transfer Surface, ASHRAE Trans., Part 1, Vol. 84, pp. 266-293.
6. McQuiston F. C., 1978, Correlation of Heat mass and Momentum Transport Coefficients for Plate-fin Tube Transfer Surfaces with Staggered Tubes, ASHRAE Trans., Part 1, Vol. 84, pp. 294-309.
7. Mirth D. R. and Ramadhyani S., 1993, Prediction of Cooling-coils Performance Under Condensing Conditions, Int. J. of Heat and Fluid Flow, Vol. 14, No. 4, pp.391-400.
8. Myers R. J., 1967, The Effect of Dehumidification on the Air-side heat Transfer Coefficient for a Finned-tube Coil, M.S. Thesis, University of Minnesota, Minneapolis.
9. Nuntaphan A. and Kiatsiriroat T., 2003, Heat Transfer Characteristic of Cross Flow Heat Exchanger Using Crimped Spiral Fins a Case Study of Staggered arrangement, The 17th Conference of Mechanical Engineering Network of Thailand, Prachinburi, Thailand.

10. Rabas T.J., Eckels P.W. and Sabatino R.A., 1981, The Effect of Fin Density on the Heat Transfer and Pressure Drop Performance of Low Finned Tube Banks, Chem. Engng. Coms., Vol.10, No.2, pp.127-147.

11. Robinson K.K. and Briggs D.E., 1966, Pressure Drop of Air Flowing Across Triangular Pitch Banks of Finned Tubes, Chem. Engng. Prog. Sym. Series, Vol.62, No.64, pp.177-184.

12. Schmidt, Th.E. (1963), Der Warmeubergeng an Rippenrohen und die Berechnung von Rohrundel Warme Austauschern, Kalttech, 15(4), 98; 15(12), 370.

13. Threlkeld J.L., 1970, Thermal Environmental Engineering, Prentice-Hall Inc., New York, USA.

14. Wang C. C., Hsieh Y.C. and Lin Y. T., 1997, Performance of Plate Finned Tube Heat Exchanger Under Dehumidifying Conditions, ASME J. of Heat Transfer, Vol.119, pp.109-119.

15. Wang, C.C., Lou, J., Lin, Y.T. and Wei, C.S., 2002, Flow Visualization of Annular and Delta Winlet Vortex Generators in Fin-and-tube Heat Exchanger Application, Int. J. of Heat and Mass Transfer, Vol.45, pp. 3803-3815.

Nomenclature

A_{min}	minimum free flow area
A_o	total surface area
$A_{p,i}$	inside surface area of tube
$A_{p,m}$	mean surface area of tube
$A_{p,o}$	outside surface area of tube
b'_p	slope of straight line between the outside and inside tube wall temperature
b'_r	slope of the air saturation curved at the mean coolant temperature
$b'_{w,m}$	slope of the air saturation curved at the mean water film temperature of the external surface
$b'_{w,p}$	slope of the air saturation curve at the mean water film temperature of the primary surface

$C_{p,a}$ moist air specific heat at constant pressure

$C_{p,w}$ water specific heat at coolant pressure

d_f outside diameter of finned tube

d_i tube inside diameter

d_o tube outside diameter

f friction factor

f_h fin height

f_i in-tube friction factor of water

f_s fin spacing

f_t fin thickness

F correction factor

G_{max} maximum mass velocity based on minimum flow area

$h_{c,o}$ sensible heat transfer coefficient for wet coil

h_i inside heat transfer coefficient

$h_{o,w}$ total heat transfer coefficient for wet external fin

I_o modified Bessel function solution of the first kind, order 0

I_1 modified Bessel function solution of the first kind, order 1

i air enthalpy

$i_{a,in}$ inlet air enthalpy

$i_{a,out}$ outlet air enthalpy

$i_{r,m}$ saturated air enthalpy at the mean refrigerant temperature

$i_{r,in}$ saturated air enthalpy at the inlet of refrigerant temperature

$i_{r,out}$ saturated air enthalpy at the outlet of refrigerant temperature

$i_{s,p,i,m}$ saturated air enthalpy at the mean inside tube wall temperature

$i_{s,p,o,m}$ saturated air enthalpy at the mean outside tube wall temperature

$i_{s,w,m}$ saturated air enthalpy at the mean water film temperature of the external surface

Δi_m mean enthalpy difference

j the Colburn factor

K_0 modified Bessel function solution of the second kind, order 0

K_1 modified Bessel function solution of the second kind, order 1

k_f thermal conductivity of fin

k_i thermal conductivity of tube side fluid

k_p thermal conductivity of tube

k_w thermal conductivity of water

m parameter

$\dot{m}_a$ air mass flow rate

$\dot{m}_w$ water mass flow rate

n_r number of tube row

n_t number of tube in each row
ΔP pressure drop
Pr Prandtl number
Q_{avg} mathematical average heat transfer rate
Q_a air-side heat transfer rate
Q_w water side heat transfer rate
r_i distance from the center of the tube to the fin base
r_o distance from the center of the tube to the fin tip
Re_{Di} Reynolds number based on inside diameter of bare tube
Re_D Reynolds number based on outside diameter of bare tube
S_l longitudinal tube pitch
S_t transverse tube pitch
$T_{w,m}$ mean temperature of water film
$T_{w,in}$ water temperature of at the tube inlet
$T_{w,out}$ water temperature of at the tube outlet
$T_{p,i,m}$ mean temperature of the inner tube wall
$T_{p,o,m}$ mean temperature of the outer tube wall
$T_{r,m}$ mean temperature of refrigerant coolant
$U_{o,w}$ overall heat transfer coefficient
x_p thickness of tube wall
y_w thickness of condensate water film
$\eta_{f,wet}$ wet fin efficiency
ρ_i mass density of inlet air
ρ_o mass density of outlet air
ρ_m mean mass density of air
σ contraction ratio

การประชุมวิชาการเครือข่ายวิศวกรรมเครื่องกลแห่งประเทศไทยครั้งที่ 17
15-17 ตุลาคม 2546 จังหวัดปราจีนบุรี

คุณลักษณะการถ่ายเทความร้อนของเครื่องแลกเปลี่ยนความร้อนแบบไหลตามขวางที่ใช้ครีบเกลียวชนิดขอบหยัก กรณีศึกษาการจัดเรียงท่อแบบเหลื่อมกัน

HEAT TRANSFER CHARACTERISTIC OF CROSS FLOW HEAT EXCHANGER USING CRIMPED SPIRAL FINS A CASE STUDY OF STAGGERED ARRANGEMENT

อติพงศ์ นันทพันธุ์*
โครงการศูนย์ฝึกอบรมเพื่อการพัฒนาพลังงานแห่งเอเชียตะวันออกเฉียงใต้ การไฟฟ้าฝ่ายผลิตแห่งประเทศไทย
ที่ทำการ กองศูนย์ฝึกอบรมแม่เมาะ อ. แม่เมาะ จ. ลำปาง 52220 โทร. 0-5425-6932 โทรสาร 0-5425-6907 email mmmatp@egat.or.th

ทนงเกียรติ เกียรติศิริโรจน์
ภาควิชาวิศวกรรมเครื่องกล คณะวิศวกรรมศาสตร์ มหาวิทยาลัยเชียงใหม่ อ. เมือง จ. เชียงใหม่ 50200
โทร. 0-5394-4146 ext. 943 โทรสาร 0-5394-4145 email tanong@dome.eng.cmu.ac.th

Atipoang Nuntaphan*
South East Asia Center for Training in Energy for Development, Electricity Generating Authority of Thailand,
Mae Moh Training Center, Mae Moh, Lampang 52220 Tel. 0-5425-6932 Fax. 0-5425-6907 email mmmatp@egat.or.th

Tanongkiat Kiatsiriroat
Department of Mechanical Engineering, Faculty of Engineering, Chiang Mai University, Muang, Chiang Mai 50200
Tel. 0-5394-4146 ext. 943 Fax. 0-5394-4145 email tanong@dome.eng.cmu.ac.th

บทคัดย่อ

งานวิจัยนี้ศึกษาคุณลักษณะการถ่ายเทความร้อนของเครื่องแลกเปลี่ยนความร้อนแบบไหลตามขวางที่ใช้ครีบเกลียวชนิดขอบหยัก (Crimped Spiral Fins) ในกรณีของการจัดเรียงท่อแบบเหลื่อมกัน โดยทำการแลกเปลี่ยนความร้อนระหว่างอากาศที่อุณหภูมิห้อง กับน้ำอุณหภูมิประมาณ 65°C โดยอัตราการไหลของอากาศอยู่ระหว่าง 0.2-0.5 kg/s และอัตราการไหลของน้ำคงที่เท่ากับ 8 l/min

งานวิจัยนี้ได้ทำการศึกษาผลของพารามิเตอร์ที่มีผลต่อสมรรถนะในการถ่ายเทความร้อนได้แก่ ขนาดของท่อ ระยะห่างระหว่างครีบ ความสูงของครีบ และระยะห่างระหว่างท่อ และนอกจากนี้ได้ทำการสร้างสมการสหสัมพันธ์เพื่อใช้ในการคำนวณค่าสัมประสิทธิ์การถ่ายเทความร้อน และค่าความดันตกคร่อมของระบบศึกษา ซึ่งสมการที่สร้างขึ้น สามารถใช้ทำนายผลการทดลองได้ 98.6% และ 91.3% ในช่วง ±15% และ ±20% ตามลำดับ

Abstract

Heat transfer characteristic of cross flow heat exchanger using crimped spiral fins with staggered arrangement has been studied in this research work. This apparatus exchanges heat between ambient air and 65°C hot water. The mass flow rate of air is risen from 0.2-0.5 kg/s while the water is kept constant at 8 l/min.

The parameters affecting the performance of heat exchanger such as tube diameter, fin spacing, fin height and tube spacing have been investigated. Moreover the empirical correlation for evaluating the heat transfer coefficient and pressure drop are also developed in this work and they can predict 98.6% and 91.3% of the experimental data within the ranges of ±15% and ±20% respectively.

---

* Corresponding author

1. บทนำ

อุปกรณ์ที่สำคัญอย่างหนึ่งในการดึงความร้อนกลับมาใช้ประโยชน์คือ เครื่องแลกเปลี่ยนความร้อน ได้แก่ เครื่องแลกเปลี่ยนความร้อนแบบไหลตามขวาง (Cross Flow Heat Exchanger) และเครื่องแลกเปลี่ยนความร้อนแบบเทอร์โมไซฟอน (Thermosyphon Heat Exchanger) เครื่องแลกเปลี่ยนความร้อนทั้งสองแบบที่กล่าวมาข้างต้นมีส่วนประกอบหลักคือ ท่อซึ่งติดครีบ (Finned Tube) เพื่อเพิ่มสมรรถนะในการถ่ายเทความร้อนโดยทั่วไปจะมีลักษณะเป็นแบบครีบวงกลม (Circular Finned) แสดงดังรูปที่ 1 และในอดีตที่ผ่านมาได้มีนักวิจัยหลายท่านได้เสนอสมการสหสัมพันธ์ (Correlation) เพื่อใช้ในการคำนวณค่าสัมประสิทธิ์การถ่ายเทความร้อนของท่อครีบแบบวงกลม (Circular Finned Tube) ในกรณีของการจัดเรียงท่อแบบเหลื่อมกัน (Staggered) [1-3] และ ในกรณีของการจัดเรียงท่อในแนวเดียวกัน (Inline) [4-5]

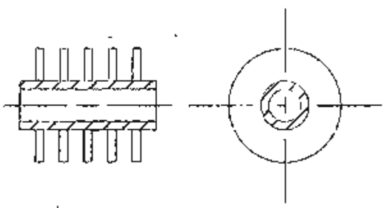

รูปที่ 1 ลักษณะของท่อครีบแบบวงกลม

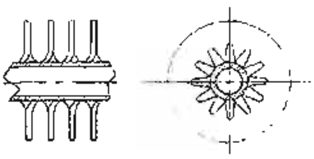

รูปที่ 2 ลักษณะของท่อครีบแบบเกลียวชนิดขอบหยัก

แต่อย่างไรก็ตาม รูปแบบของครีบที่ใช้ในอุตสาหกรรมมีลักษณะแตกต่างจากครีบวงกลม โดยมีลักษณะเป็นแบบครีบเกลียวชนิดขอบหยัก (Crimped Spiral Finned) แสดงดังรูปที่ 2 ทั้งนี้เนื่องจากง่ายต่อการผลิต จากการศึกษาของคณะผู้วิจัยพบว่าค่าสัมประสิทธิ์การถ่ายเทความร้อนระหว่างอากาศกับท่อครีบชนิดดังกล่าว มีความแตกต่างจากท่อครีบแบบวงกลมและปัจจุบันงานวิจัยที่เกี่ยวข้องกับการสมรรถนะของท่อครีบประเภทนี้ยังไม่แพร่หลายนัก ดังนั้นในงานวิจัยนี้จึงมุ่งเน้นที่จะศึกษาเพื่อหารูปแบบของสมการ สหสัมพันธ์เพื่อใช้คำนวณค่าสัมประสิทธิ์การถ่ายเทความร้อนของท่อครีบแบบเกลียวชนิดขอบหยัก โดยในบทความวิจัยนี้จะเป็นกรณีของการจัดเรียงท่อแบบเหลื่อมกัน ซึ่งรูปแบบสมการสหสัมพันธ์ที่ได้คาดว่าจะเป็นประโยชน์ต่อการออกแบบเครื่องแลกเปลี่ยนความร้อนที่ใช้ในอุตสาหกรรม

2. ทฤษฎี

อัตราการถ่ายเทความร้อนของเครื่องแลกเปลี่ยนความร้อนแบบไหลตามขวาง ซึ่งแลกเปลี่ยนความร้อนระหว่างน้ำซึ่งมีอุณหภูมิสูงและอากาศซึ่งมีอุณหภูมิต่ำกว่าแสดงดังรูปที่ 3 สามารถคำนวณได้จาก

$$Q = \dot{m}_a Cp_a \left(T_{ao} - T_{ai}\right) \qquad (1)$$

$$Q = \dot{m}_w Cp_w \left(T_{wi} - T_{wo}\right) \qquad (2)$$

โดยที่ Q คืออัตราการถ่ายเทความร้อน $\dot{m}$ คืออัตราการไหลเชิงมวล Cp คือค่าความจุความร้อนจำเพาะ และ T คืออุณหภูมิ

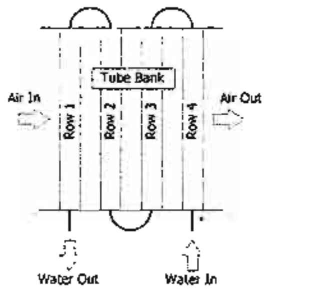

รูปที่ 3 การถ่ายเทความร้อนระหว่างน้ำและอากาศของเครื่องแลกเปลี่ยนความร้อนแบบไหลตามขวาง

ดัชนีที่ใช้บ่งบอกสมรรถนะที่นิยมใช้ในปัจจุบันคือค่าประสิทธิผล (Effectiveness) ซึ่งสามารถคำนวณได้จาก

$$\varepsilon = \frac{Q}{Q_{max}} \qquad (3)$$

$$\varepsilon = \frac{Q}{\left(\dot{m}Cp\right)_{min} \Delta T_{max}} \qquad (4)$$

โดยที่ ε คือค่าประสิทธิผล

ในการคำนวณค่าประสิทธิผลของเครื่องแลกเปลี่ยนความร้อน นิยมใช้ความสัมพันธ์ของ $\varepsilon - NTU$ ในการคำนวณ ซึ่งในกรณีของงานวิจัยนี้ เครื่องแลกเปลี่ยนความร้อนจัดอยู่ในประเภทไหลตามขวาง โดยมีจำนวนท่อ 4 แถว แลกเปลี่ยนความร้อนระหว่างน้ำร้อนซึ่งไหลภายในท่อ กับอากาศซึ่งไหลด้านนอกท่อ โดยกำหนดให้ค่า $\left(\dot{m}Cp\right)_{min}$ อยู่ด้านอากาศ สามารถแสดงความสัมพันธ์ของ $\varepsilon - NTU$ ในรูปของ

$$\varepsilon = \frac{1}{C^*}\left\{1 - e^{-4KC^*}\left[\begin{array}{l} 1 + C^* K^2\left(6 - 4K + K^2\right) \\ + 4\left(C^*\right)^2 K^4 \left(2 - K\right) \\ + \dfrac{8\left(C^*\right)^3 K^6}{3} \end{array}\right]\right\} \qquad (5)$$

$$K = 1 - e^{-NTU/4} \qquad (6)$$

$$NTU = \frac{UA}{\left(\dot{m}Cp\right)_{min}} \qquad (7)$$

$$C^* = \frac{\left(\dot{m}Cp\right)_{min}}{\left(\dot{m}Cp\right)_{max}} \qquad (8)$$

ค่าสัมประสิทธิ์การถ่ายเทความร้อนรวมพื้นที่ (UA) ของเครื่องแลกเปลี่ยนความร้อนที่ทำการศึกษาสามารถคำนวณได้จาก

$$\frac{1}{UA} = \frac{1}{\eta_o h_o A_o} + \frac{\ln\left(d_o / d_i\right)}{2\pi k L_t} + \frac{1}{h_i A_i} \qquad (9)$$

โดยที่ h_o และ h_i คือสัมประสิทธิ์การถ่ายเทความร้อนด้านนอกและในท่อตามลำดับ โดยที่ค่า h_i สามารถคำนวณได้จากสมการของ Gnielinski (6) คือ

$$h_i = \left(\frac{k}{d}\right)_i \frac{\left(Re_{Di} - 1000\right)Pr\left(f_i / 2\right)}{1 + 12.7\sqrt{f_i / 2}\left(Pr^{2/3} - 1\right)} \tag{10}$$

$$f_i = \left[1.58\ln\left(Re_{Di}\right) - 3.28\right]^{-2} \tag{11}$$

โดยที่ Re_{Di} คือค่า Reynolds Number ของการไหลภายในท่อ

จากสมการ (9) ค่า η_o นิยามว่าคือ อัตราการถ่ายเทความร้อนที่แท้จริงของครีบและท่อต่ออัตราการถ่ายเทความร้อนของครีบและท่อในกรณีที่อุณหภูมิของครีบและท่อมีค่าเท่ากันค่า η_o คำนวณได้จาก

$$\eta_o = 1 - \frac{A_f}{A_o}\left(1 - \eta\right) \tag{12}$$

$$A_o = A_f + A_b \tag{13}$$

$$A_o = \frac{nL\pi}{f_s + f_t}\left(0.5\left(d_f^{\,2} - d_o^{\,2}\right) + d_f f_t + d_o f_s\right) \tag{14}$$

$$A_f = \frac{nL\pi}{f_s + f_t}\left(0.5\left(d_f^{\,2} - d_o^{\,2}\right) + d_f f_t\right) \tag{15}$$

โดยที่ A_f, A_b คือพื้นที่ของครีบและพื้นที่ของท่อที่ไม่ถูกครีบบังตามลำดับ โดยในการวิจัยนี้ได้ประมาณพื้นที่ของท่อครีบที่ทดสอบว่ามีขนาดเท่ากับพื้นที่ของท่อครีบแบบวงกลม ค่าประสิทธิภาพของครีบ (η) สามารถคำนวณได้จากสมการของ Schmidt (5) ดังนี้

$$\eta = \frac{\tanh\left(mr\phi\right)}{mr\phi} \tag{16}$$

$$m = \sqrt{\frac{2h_o}{k_f \delta_f}} \tag{17}$$

$$\phi = \left(\frac{R_{eq}}{r} - 1\right)\left[1 + 0.35\ln\left(\frac{R_{eq}}{r}\right)\right] \tag{18}$$

$$\frac{R_{eq}}{r} = 1.27\frac{X_M}{r}\left(\frac{X_L}{X_M} - 0.3\right)^{1/2} \tag{19}$$

$$X_M = \frac{S_t}{2} \tag{20}$$

$$X_L = \frac{\sqrt{\left(0.5S_t\right)^2 + \left(S_l\right)^2}}{2} \tag{21}$$

จากสมการข้างต้น และผลการทดสอบสมรรถนะของเครื่องแลกเปลี่ยนความร้อน สามารถนำมาใช้ในการคำนวณค่าสัมประสิทธิ์การถ่ายเทความร้อนระหว่างอากาศกับกลุ่มท่อ (h_o) อนึ่งในกรณีของความดันตกคร่อมเครื่องแลกเปลี่ยนความร้อน สามารถจัดอยู่ในรูปของ Friction Factor ซึ่งมีนิยามดังนี้

$$f = \frac{A_c \rho_i}{A_o \rho_m}\left[\frac{2\rho_i \Delta P}{G_c^{\,2}} - \left(1 + \sigma^2\right)\left(\frac{\rho_i}{\rho_o} - 1\right)\right] \tag{22}$$

โดยที่ A_c คือ Minimum Flow Area σ คือ Contraction Ratio ของเครื่องแลกเปลี่ยนความร้อน G_c คือ Mass Flux ของอากาศซึ่งคำนวณจาก Minimum Flow Area และ Subscripts i, o, m คือสภาวะด้านเข้า ออก และเฉลี่ยตามลำดับ

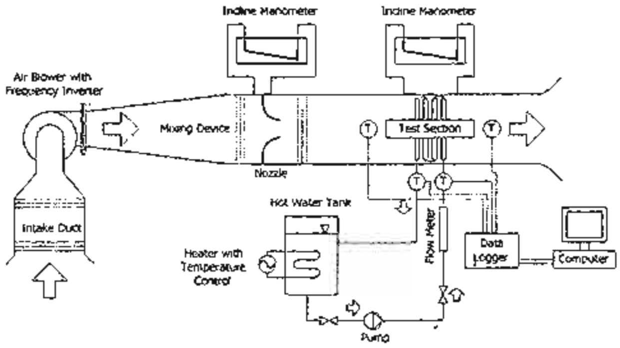

รูปที่ 4 ลักษณะของอุปกรณ์การวิจัย

3. อุปกรณ์และวิธีการวิจัย

รูปที่ 4 แสดงอุปกรณ์การวิจัยซึ่งประกอบด้วยอุปกรณ์หลัก คือ ท่อส่งอากาศขนาดหน้าตัด 0.5x0.5 m โดยมี Air Blower ขนาด 2 hp ทำหน้าที่ส่งอากาศอุณหภูมิห้องเข้าไปแลกเปลี่ยนความร้อนที่กลุ่มท่อ โดยลักษณะของท่อที่ทดสอบแสดงดังตารางที่ 1 และอัตราการไหลของอากาศจะถูกวัดโดย Standard Nozzle และ Incline Manometer โดยในการวิจัยนี้อัตราการไหลของอากาศจะอยู่ในช่วง 0.2-0.5 kg/s โดยที่อุณหภูมิของอากาศด้านเข้ากลุ่มท่อมีค่าประมาณ 25 °C

น้ำร้อนอุณหภูมิ 65 °C อัตราการไหล 8 l/min จะถูกส่งจากถังน้ำร้อนเข้าไปไหลเวียนภายในกลุ่มท่อเพื่อแลกเปลี่ยนความร้อนกับอากาศ ทำการวัดอุณหภูมิของอากาศและน้ำด้านเข้าและออกจากกลุ่มท่อ โดยใช้ Thermocouple ชนิด K และ ความดันตกคร่อมกลุ่มท่อโดยใช้ Incline Manometer

ตารางที่ 1 ลักษณะของกลุ่มท่อที่ใช้ทดสอบ

d_o (mm)	d_i (mm)	f_s (mm)	f_h (mm)	f_t (mm)	S_t (mm)	S_l (mm)	n_r	n_t
21.7	16.5	6.10	10.0	0.4	72.0	36.0	4	6
21.7	16.5	3.85	10.0	0.4	72.0	36.0	4	6
21.7	16.5	2.85	10.0	0.4	72.0	36.0	4	6
21.7	16.5	6.10	10.0	0.4	84.0	24.2	4	5
21.7	16.5	3.85	10.0	0.4	84.0	24.2	4	5
21.7	16.5	2.85	10.0	0.4	84.0	24.2	4	5
21.7	16.5	6.10	10.0	0.4	50.0	43.3	4	9
21.7	16.5	3.85	10.0	0.4	50.0	43.3	4	9
21.7	16.5	2.85	10.0	0.4	50.0	43.3	4	9
21.7	16.5	6.10	10.0	0.4	55.6	48.2	4	8
21.7	16.5	3.85	10.0	0.4	55.6	48.2	4	8
21.7	16.5	2.85	10.0	0.4	55.6	48.2	4	8
21.7	16.5	3.85	15.0	0.4	55.6	48.2	4	8
27.2	21.6	3.85	10.0	0.4	50.0	43.3	4	9

จากการทดลองเพื่อหาค่าอัตราการถ่ายเทความร้อนของเครื่องแลกเปลี่ยนความร้อนแบบไหลตามขวาง นำข้อมูลที่ได้มาคำนวณ

หาค่าสัมประสิทธิ์การถ่ายเทความร้อนระหว่างอากาศกับกลุ่มท่อ (h_o) และค่า Friction Factor (f) ของอากาศที่ไหลผ่านกลุ่มท่อ นอกจากนี้ยังทำการสร้างสมการสหสัมพันธ์เพื่อใช้ในการคำนวณค่าดังกล่าว โดยแสดงผลของพารามิเตอร์ต่างๆ ในสมการที่สร้างขึ้น

4. ผลการทดลองและการวิเคราะห์

รูปที่ 5 แสดงผลของขนาดท่อที่มีต่อค่าสัมประสิทธิ์การถ่ายเทความร้อนและค่าความดันอากาศตกคร่อมกลุ่มท่อ ซึ่งพบว่าค่าดังกล่าวจะแปรผันตามความเร็วของอากาศ ซึ่งเป็นคุณลักษณะของเครื่องแลกเปลี่ยนความร้อน อย่างไรก็ตามจากการทดลองพบว่า ท่อขนาดเล็กมีค่าสัมประสิทธิ์การถ่ายเทความร้อนสูงกว่าท่อขนาดใหญ่ ทั้งนี้เนื่องจากว่าในกรณีของท่อขนาดใหญ่มีโอกาสที่จะการหมุนวนของอากาศด้านหลังท่อ (Re-circulation) ของอากาศด้านหลังท่อมากกว่าในกรณีของท่อขนาดเล็ก ซึ่งปรากฏการณ์ดังกล่าวส่งผลให้พื้นที่ในการถ่ายเทความร้อนส่วนหนึ่งสูญเสียไป ทำให้สัมประสิทธิ์การถ่ายเทความร้อนลดต่ำลง Wang et al. [7] ได้ทำการทดลองโดยการฉีดสี เข้าไปในบริเวณกลุ่มท่อ พบว่ามีการเกิด Re-circulation ของอากาศด้านหลังท่อ โดยเฉพาะท่อขนาดใหญ่ ทำให้ค่าสัมประสิทธิ์การถ่ายเทความร้อนลดลง ซึ่งข้อมูลดังกล่าวได้สอดคล้องกับผลการทดลองที่ได้รับ

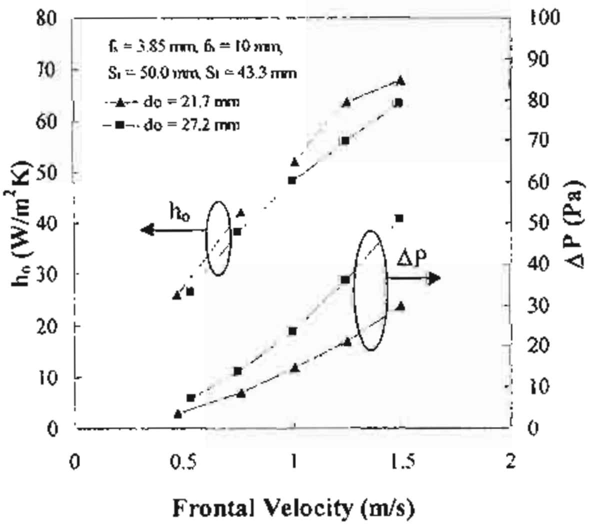

รูปที่ 5 ผลของขนาดท่อต่อค่า h_o และ ΔP

ในกรณีของความดันอากาศตกคร่อมกลุ่มท่อ พบว่าท่อขนาดใหญ่จะมีความดันตกคร่อมมากกว่าท่อขนาดเล็ก ซึ่งเป็นปรากฏการณ์ปกติของเครื่องแลกเปลี่ยนความร้อน

ผลของความสูงของครีบแสดงดังรูปที่ 6 ซึ่งพบว่าความสูงของครีบไม่มีผลต่อความดันอากาศตกคร่อมกลุ่มท่อมากนัก โดยเฉพาะอย่างยิ่ง ในกรณีของความความเร็วอากาศต่ำ พบว่าความดันตกคร่อมไม่มีความแตกต่างกันในกรณีของความสูงครีบเท่ากับ 10 และ 15 mm อย่างไรก็ตาม ในกรณีที่ความเร็วของอากาศเพิ่มมากขึ้น ความแตกต่างของค่าความดันอากาศตกคร่อมจะเด่นชัดขึ้น นอกจากนี้จากรูปดังกล่าวยังพบว่า ขนาดความสูงของครีบเท่ากับ 10 mm ให้ค่าสัมประสิทธิ์การถ่ายเทความร้อนสูงกว่าครีบขนาดความสูง 15 mm ผลการทดลองดังกล่าวสามารถอธิบายได้ดังนี้

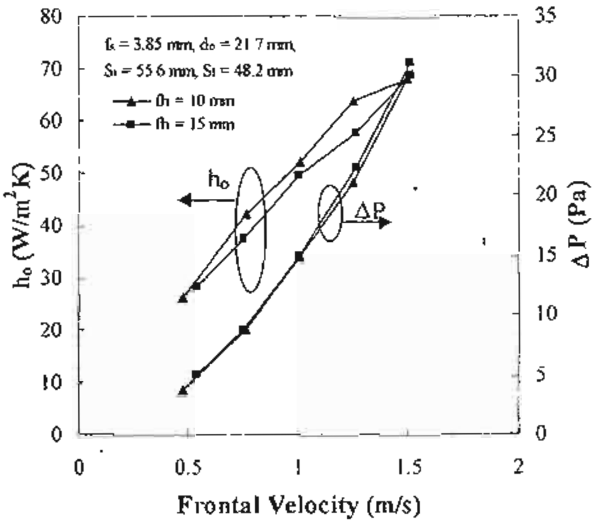

รูปที่ 6 ผลของความสูงของครีบต่อค่า h_o และ ΔP

ในกรณีครีบที่มีความสูงมาก ค่าความต้านทานการไหลของอากาศรอบๆ ท่อครีบจะสูงกว่าในกรณีของครีบที่มีความสูงต่ำกว่า ดังนั้นอากาศส่วนใหญ่จึงไม่ไหลเข้าไปแลกเปลี่ยนความร้อนกับพื้นผิวของท่อครีบ แต่จะไหลผ่านไปในช่องว่างระหว่างท่อ ทำให้ประสิทธิภาพในการแลกเปลี่ยนความร้อนลดต่ำลง ส่งผลให้ค่าสัมประสิทธิ์การถ่ายเทความร้อนลดลง

รูปที่ 7 แสดงผลของผลของการจัดเรียงท่อและ ระยะห่างระหว่างครีบต่อค่าสัมประสิทธิ์การถ่ายเทความร้อน และค่าความดันอากาศตกคร่อม พบว่าค่าความดันอากาศตกคร่อมเครื่องแลกเปลี่ยนความร้อนจะแปรผกผันกับระยะห่างระหว่างท่อในแถวเดียวกันและระยะห่างระหว่างครีบ ซึ่งปรากฏการณ์ดังกล่าว เป็นคุณลักษณะที่พบได้ในเครื่องแลกเปลี่ยนความร้อนประเภทนี้

ในกรณีของค่าสัมประสิทธิ์การถ่ายเทความร้อน พบว่ากรณีระยะห่างระหว่างท่อ 50 mm อิทธิพลของระยะห่างระหว่างครีบมีค่าต่ำ ซึ่งผลดังกล่าวจะสอดคล้องกับการทดลองของ Rich [8] และ Wang et al. [9] แต่อย่างไรก็ตามในกรณีของระยะห่างระหว่างท่อเท่ากับ 84 mm พบว่าค่าสัมประสิทธิ์การถ่ายเทความร้อนจะลดลงเมื่อระยะห่างระหว่างครีบลดลง ทั้งนี้เนื่องจากว่าในกรณีนี้ อากาศส่วนใหญ่จะไหลผ่านช่องว่างระหว่างท่อดังนั้นในกรณีของระยะห่างระหว่างครีบน้อยซึ่งก่อให้เกิดความต้านทานการไหลบริเวณกลุ่มท่อมาก จะมีค่าสัมประสิทธิ์การถ่ายเทความร้อนลดลง อย่างไรก็ตามการถ่ายเทความร้อนในกลุ่มท่อครีบปรากฏการณ์ที่เกิดขึ้นมีความซับซ้อนมาก ซึ่งยังต้องอาศัยการวิจัยในระดับต่อไป

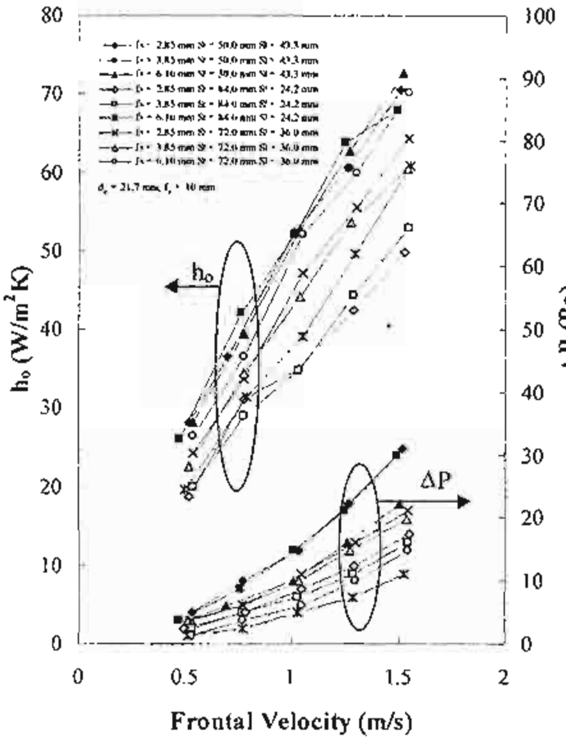

รูปที่ 7 ผลของการจัดเรียงท่อและ ระยะห่างระหว่างครีบต่อค่า h_o และ ΔP

งานวิจัยนี้ได้ทำการพัฒนาแบบจำลองสำหรับคำนวณค่าสัมประสิทธิ์การถ่ายเทความร้อน และค่าความดันอากาศตกคร่อมกลุ่มท่อ โดยได้รวบรวมปัจจัยที่เกี่ยวข้องต่างๆ เข้าไว้ด้วยกัน โดยแบบจำลองที่พัฒนาขึ้น แสดงในสมการที่ 23-24 โดยที่ ค่าสัมประสิทธิ์การถ่ายเทความร้อนจะแสดงในรูปของ Nusselt Number (Nu) และค่าความดันอากาศตกคร่อมจะแสดงในรูปของ Friction Factor (f)

$$Nu = 0.0276\,Re_D^{\,0.8834}\left(\frac{f_t}{f_s}\right)^{-0.1430}\left(\frac{S_l}{S_t}\right)^{1.1866}\left(\frac{S_t}{d_o}\right)^{0.7815}\left(\frac{d_f}{d_o}\right)^{-0.1250} \quad (23)$$

$$f = 2.1768\,Re_D^{\,-0.2679}\left(\frac{f_t}{f_s}\right)^{-0.2468}\left(\frac{S_l}{S_t}\right)^{1.8680}\left(\frac{S_t}{d_o}\right)^{0.3011}\left(\frac{d_f}{d_o}\right)^{-0.4470} \quad (24)$$

รูปที่ 8-9 แสดงการเปรียบเทียบค่า Nu และ f จากการทดลองและ Correlation ที่ได้พัฒนาขึ้น โดยพบว่าสมการที่ 23 สามารถทำนายข้อมูลได้ 98.6% ในช่วง ±15% และสมการที่ 24 สามารถทำนายผลการทดลองได้ 91.3% ในช่วง ±20%

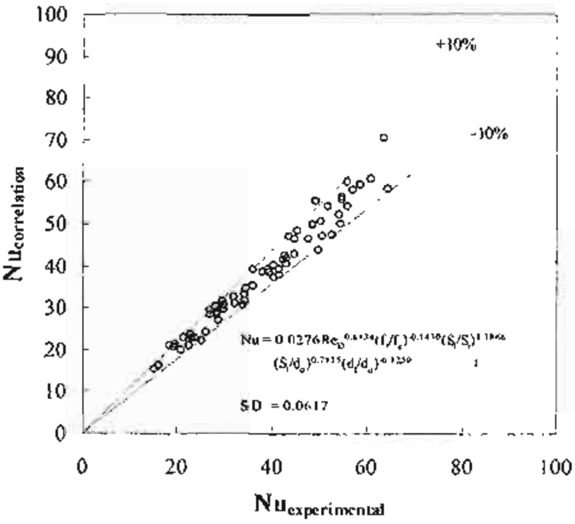

รูปที่ 8 การเปรียบเทียบ Nu จากการทดลองและ Correlation

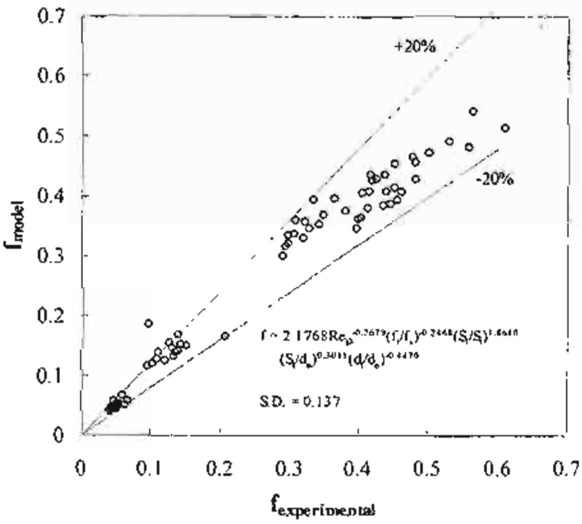

รูปที่ 9 การเปรียบเทียบ f จากการทดลองและ Correlation

5. สรุป

จากการทดลองสามารถสรุปผลได้ดังนี้

5.1 ค่าสัมประสิทธิ์การถ่ายเทความร้อนจะแปรผกผันกับขนาดท่อครีบเนื่องจากการเกิด Re-circulation บริเวณด้านหลังท่อ และในขณะเดียวกันจะแปรผกผันกับความสูงของครีบทั้งนี้เนื่องจากครีบขนาดความสูงมากจะเกิดความต้านทานการไหลของอากาศที่เข้ามาแลกเปลี่ยนความร้อน

5.2 ระยะห่างระหว่างท่อส่งผลต่อค่าสัมประสิทธิ์การถ่ายเทความร้อนคือในกรณีของระยะห่างมาก ค่าสัมประสิทธิ์การถ่ายเทความร้อนจะลดต่ำลง เนื่องจากอากาศส่วนใหญ่จะไหลผ่านช่องว่างระหว่างท่อ และในขณะเดียวกัน ระยะห่างดังกล่าวยังส่งผลเกี่ยวเนื่องกับระยะห่างระหว่างครีบด้วย คือ ในกรณีของระยะห่างระหว่างท่อน้อย ผลของระยะห่าง

ระหว่างครีบจะไม่เด่นชัดนัก และในทางกลับกันกรณีของระยะห่างระหว่างท่อมาก ผลของระยะห่างระหว่างครีบจะชัดเจนขึ้น

5.3 ความดันอากาศตกคร่อมกลุ่มท่อจะแปรผันกับขนาดท่อ ความสูงของครีบ และแปรผกผันกับระยะห่างระหว่างท่อ และระยะห่างระหว่างครีบ

5.4 สมการสหสัมพันธ์ที่พัฒนาขึ้นเพื่อใช้คำนวณค่าสัมประสิทธิ์การถ่ายเทความร้อนและค่าความดันตกคร่อม สามารถใช้ทำนายผลการทดลองได้เป็นอย่างดี

6. กิตติกรรมประกาศ

คณะผู้วิจัยขอขอบพระคุณสำนักงานกองทุนสนับสนุนการวิจัยที่ให้ทุนอุดหนุนในการทำวิจัยครั้งนี้

เอกสารอ้างอิง

1. Briggs D.E. and Young E.H., "Convective Heat Transfer and Pressure Drop of Air Flowing Across Triangular Pitch Banks of Finned Tubes", Chemical Engineering Progress Symposium Series, 1963, Vol.59, No. 41, pp.1-10.
2. Robinson K.K. and Briggs D.E., "Pressure Drop of Air Flowing Across Triangular Pitch Banks of Finned Tubes", Chemical Engineering Progress Symposium Series, 1966, Vol.62, No.64, pp.177-184.
3. Rabas T.J., Eckels P.W. and Sabatino R.A., "The Effect of Fin Density on the Heat Transfer and Pressure Drop Performance of Low Finned Tube Banks", Chemical Engineering Comunications, 1981, Vol.10, No.2, pp.127-147.
4. Rabas T.J. and Huber F.V., "Row Number Effects on the Heat Transfer Performance of Inline Finned Tube Banks", Heat Transfer Engineering, 1989, Vol.10, No.4, pp.19-29.
5. Schmidt, Th.E., "Heat Transfer Calculation for Extended Surfaces", Refrigeration Engineering, 1949, pp. 351-357.
6. Gnielinski V., "New Equation for Heat and Mass Transfer in Turbulent Pipe and Channel Flow", Int. Chem. Engng, 1976, Vol.16, pp. 359-368.
7. Wang, C.C., Lou, J., Lin, Y.T. and Wei, C.S., "Flow Visualization of Annular and Delta Winlet Vortex Generators in Fin-and-tube Heat Exchanger Application", Int. J. of Heat and Mass Transfer, 2002, Vol.45, pp. 3803-3815.
8. Rich, D.G. , ASHRAE Transactions, 1973, Vol.79, No. 2, pp. 137-145.
9. Wang, C.C., Chang, Y.J., Hsieh, Y.J. and Lin, Y.T., "Sensible heat and friction characteristics of plate fin-and-tube heat exchangers having plane fins", Int. J. of Refrigeration, 1996, Vol.19, No. 4, pp. 223-230

Nomenclature

A	Area (m^2)
Cp	Specific heat (J/kgK)
d_f	Outside diameter of finned tube (mm)
d_i	Inside diameter of bare tube (mm)
d_o	Outside diameter of bare tube (mm)
f	Friction factor
f_h	Fin height (mm)
f_s	Fin Spacing (mm)
f_t	Fin thickness (mm)
G_c	Mass flux of air base on minimum flow area (kg/sm^2)
h	Heat transfer coefficient (W/m^2K)
k	Thermal conductivity (W/mK)
L	Length (m)
L_t	Total Length (m)
$\dot{m}$	Mass flow rate (kg/s)
n	Total number of tube
n_r	Number of tube rows
n_l	Number of tubes in row
NTU	Number of transfer unit
Nu	Nusselt Number
P	Pressure (Pa)
Q	Heat transfer rate (W)
Re_D	Reynolds number
S_t	Transverse pitch (mm)
S_l	Longitudinal pitch (mm)
S_{min}	Minimum flow area (m^2)
T	Temperature (^{o}C)
U	Overall heat transfer coefficient (W/m^2K)
V_{max}	Maximum velocity (m/s)

Greek symbols

ε	Effectiveness
η	Efficiency
μ	Dynamic viscosity (Pas)
ρ	Density (kg/m^3)
σ	Contraction ratio of cross sectional area

Subscripts

a	Air
b	Bare tube
f	Fin
i	Inlet, tube side
o	Outlet, air side
w	Water

Air-Side Heat Transfer Coefficient of Thermosyphon Heat Pipe with Crimped Spiral Fins: A Case Study of Staggered Arrangement

A. Nuntaphan
South East Asia Center for Training in Energy for Development
Electricity Generating Authority of Thailand
Mae Moh, Lampang 52220
Tel. 6654-256938
Fax. 6654-256907
email: mnmatp@egat.or.th

T. Kiatsiriroat
Department of Mechanical Engineering
Faculty of Engineering Chiang Mai University
Chiang Mai 50200
Tel. 6653-944144
Fax. 6653-944145
email:
tanong@dome.eng.cmu.ac.th

ABSTRACT

This research work studies the air-side heat transfer coefficient of thermosyphon heat pipe in case of staggered-arrangement tubes bank. Normally, the air-side heat transfer coefficient is the lowest and it controls the overall heat transfer of the system. To enhance the overall performance, extended surface is used at the air-side and the crimped spiral finned tube is normally selected in case of thermosyphon heat pipe. In this research work, the heat transfer coefficient of the thermosyphon heat pipe with crimped spiral fins is investigated. The parameters affecting the performance of heat exchanger such as tube diameter, fin spacing, fin height and tube spacing have been studied. Moreover the empirical correlation for evaluating the air-side heat transfer coefficient is also developed in this work.

Keywords: air-side heat transfer coefficient, thermosyphon heat pipe, crimped spiral fins, heat transfer model

1. INTRODUCTION

Many types of heat exchangers are used as industrial waste heat recovery units such as cross flow, rotary, run around coil, and especially thermosyphon heat exchanger which has high performance and low operating cost. The thermosyphon heat exchanger is used to recover heat from flue gas of the boiler or furnace and transfer this energy to increase the temperature of combustion air (air-preheater) or boiler feed water (economizer).

The thermosyphon heat exchanger composes of a set of thermosyphon heat pipes with in-line or staggered arrangement. In case of air-preheater, The effective method to improve the performance is to increase the air-side surface area with extended surface. The circular finned is normally designed for the thermosyphon and many correlations are developed for calculating the air-side heat transfer performance of this finned tube [1-3]. However, the process to construct the real circular finned tube is quite complicated with high cost. Thus the crimped spiral fins is used in practice and Figure 1 shows the shape of the finned tube.

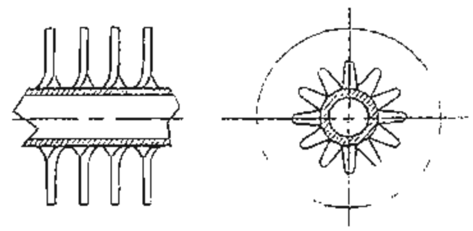

Figure 1. The shape of crimped spiral fins.

In Thailand, there are a few factories construct this kind of fin and no available heat transfer performance data. Therefore, in this study, the performance of the thermosyphon heat exchanger using crimped spiral fins is investigated and the correlation for evaluating the heat transfer performance of the finned tube is also formulated.

This work can be divided in to two parts. The first part is to test the performance of the crimped spiral fins and correlate the heat transfer data. The second part is to find out the performance of the thermosyphon heat exchanger using this kind of finned tubes by using the data from Nuntaphan[4].

2. PERFORMANCE TEST OF CRIMPED SPIRAL FIN

2-1 Theory

This research work follows the ANSI/ARI standard [5] for testing the performance of the finned tubes. The air-side heat transfer coefficient of the crimped spiral fins can be evaluated by arranging it as a cross flow heat exchanger shown in Figure 2. Hot water is flowing inside the tube bank and transfers heat to the cross flow air stream. The heat transfer rate (Q) of heat exchanger can be calculated as

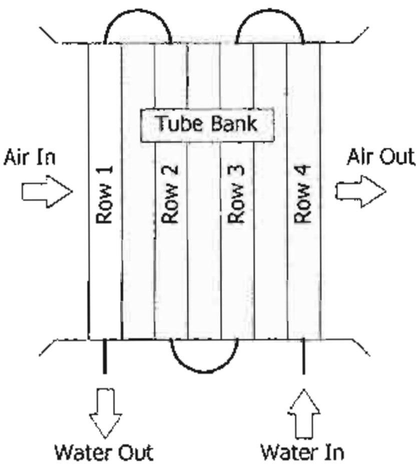

Figure 2. Cross flow heat exchanger.

$$Q = \dot{m}_a Cp_a (T_{ao} - T_{ai}) \quad (1)$$

$$Q = \dot{m}_w Cp_w (T_{wi} - T_{wo}) \quad (2)$$

where $\dot{m}_a$ is the mass flow rate of air, $\dot{m}_w$ is the mass flow rate of water, T_{ai}, T_{ao} are inlet and outlet temperatures of air stream, T_{wi}, T_{wo} are inlet and outlet temperature of water and Cp_a, Cp_w are specific heats of air and water respectively.

The performance indicator of heat exchanger is the effectiveness which is defined as

$$\varepsilon = \frac{Q}{Q_{max}} \quad (3)$$

$$\varepsilon = \frac{Q}{(\dot{m}Cp)_{min} \Delta T_{max}} \quad (4)$$

where ε is the effectiveness. The relation between the effectiveness and the air side heat transfer coefficient in case of 4 tube rows is as follow

$$\varepsilon = \frac{1}{C^*}\left\{1 - e^{-4KC^*}\left[\begin{array}{l} 1 + C^*K^2(6 - 4K + K^2) \\ + 4(C^*)^2K^4(2 - K) \\ + \frac{8(C^*)^3K^6}{3} \end{array}\right]\right\} \quad (5)$$

$$K = 1 - e^{-NTU/4} \quad (6)$$

$$NTU = \frac{UA}{(\dot{m}Cp)_{min}} \quad (7)$$

$$C^* = \frac{(\dot{m}Cp)_{min}}{(\dot{m}Cp)_{max}} \quad (8)$$

$$\frac{1}{UA} = \frac{1}{\eta_o h_o A_o} + \frac{\ln(d_o / d_i)}{2\pi kL} + \frac{1}{h_i A_i} \quad (9)$$

where h is the heat transfer coefficient, A is area, d is tube diameter, L is tube length, k is thermal conductivity of tube material, η_o is surface efficiency of the airside and subscripts o, i are defined as the air side and the tube side respectively.

The tube side heat transfer coefficient can be calculated from Gnielinski correlation [6] as

$$h_i = \left(\frac{k}{d}\right)_i \frac{(Re_{Di} - 1000)Pr(f_i / 2)}{1 + 12.7\sqrt{f_i / 2}(Pr^{2/3} - 1)} \quad (10)$$

$$f_i = [1.58 \ln(Re_{Di}) - 3.28]^{-2} \quad (11)$$

where Re_{Di} is the tube-side Reynolds number. The surface efficiency from equation (9) can be estimated from

$$\eta_o = 1 - \frac{A_f}{A_o}(1 - \eta) \quad (12)$$

$$A_o = A_f + A_b \quad (13)$$

where A_o is the total surface area of finned tube, A_f is surface area of fin, A_b is surface area of bare tube and η is fin efficiency which can be calculated from Schmidt approximation [7] as follows:

$$\eta = \frac{\tanh(mr\phi)}{mr\phi} \quad (14)$$

$$m = \sqrt{\frac{2h_o}{k_f f_t}} \tag{15}$$

$$\phi = \left(\frac{R_{eq}}{r} - 1\right)\left[1 + 0.35\ln\left(\frac{R_{eq}}{r}\right)\right] \tag{16}$$

$$\frac{R_{eq}}{r} = 1.27\frac{X_M}{r}\left(\frac{X_L}{X_M} - 0.3\right)^{1/2} \tag{17}$$

$$X_L = \frac{\sqrt{(S_t/2)^2 + S_l}}{2} \tag{18}$$

$$X_M = 0.5S_t \tag{19}$$

where k_f is thermal conductivity of fin material, S_t and S_l are transverse and longitudinal pitches of tube bank respectively and f_t is fin thickness.

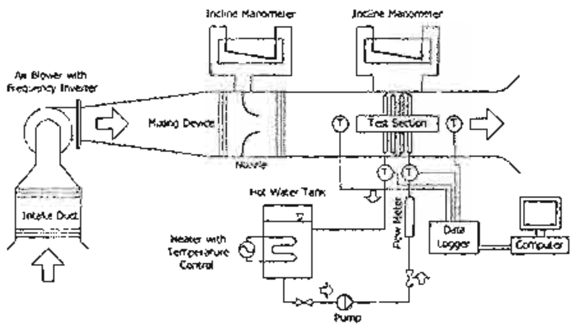

Figure 3. Schematic sketch of experimental setup.

2-2 The experimental setup

Figure 3 shows the experimental setup. The air stream at room temperature is fed through the tube bank while the hot water is flowing inside the tube. The water flow rate is kept constant at 8 l/min and the inlet temperature is at 65°C. The mass flow rate of air is varied in the range of 0.1-0.5 kg/s. By measuring the inlet and the outlet temperatures of the water and the air streams including the mass flow rate of each side, the air side heat transfer coefficient could be calculated.

Table 1 shows dimensions of the finned tubes and their arrangement. The effect on the heat transfer performance of the parameters such as tube diameter, fin height, fin spacing, fin thickness and tube arrangement are studied. Moreover the empirical model including these parameters is formulated for calculating the air side heat transfer coefficient

Table 1 Dimensions of various type of heat exchanger.

d_o	d_i	f_s	f_h	f_t	S_t	S_l	n_r	n_t
21.7	16.5	6.10	10.0	0.4	72.0	36.0	4	6
21.7	16.5	3.85	10.0	0.4	72.0	36.0	4	6
21.7	16.5	2.85	10.0	0.4	72 0	36.0	4	6
21.7	16.5	6.10	10.0	0.4	84.0	24.2	4	5
21.7	16.5	3.85	10.0	0.4	84.0	24.2	4	5
21.7	16.5	2.85	10.0	0.4	84.0	24.2	4	5
21.7	16.5	6.10	10.0	0.4	50.0	43.3	4	9
21.7	16.5	3.85	10.0	0.4	50.0	43.3	4	9
21.7	16.5	2.85	10.0	0.4	50.0	43.3	4	9
21.7	16.5	6.10	10.0	0.4	55.6	48.2	4	8
21.7	16.5	3.85	10.0	0.4	55.6	48.2	4	8
21.7	16.5	2.85	10.0	0.4	55.6	48.2	4	8
21.7	16.5	3.85	15.0	0.4	55.6	48.2	4	8
27.2	21.6	3.85	10.0	0.4	50.0	43.3	4	9

Note: All dimensions are in millimeter.

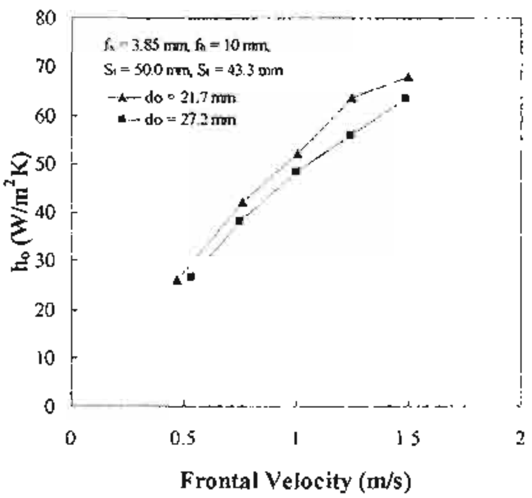

Figure 4. Effect of tube diameter on air-side heat transfer coefficient.

2-3 Results and Discussion

Figures 4-6 shows the relation of the air-side heat transfer coefficient and the mass flow rate of air stream. All of the mentioned Figures give the same undoubted results that higher the mass flow rate of air stream results in higher the heat transfer coefficient. From Figure 4, it is found that smaller diameter of tube gives higher heat transfer coefficient. This result comes from the re-circulation of air stream behind the tube that increases with the tube diameter. This affect pronounces the ineffective area of tube and it brings to get lower heat transfer coefficient. Wang et al. [8] also found this phenomena by using flow visualization.

Figure 5 shows the effect of fin spacing, and S_t on the airside heat transfer coefficients. The tube diameter is 21.7 mm and the fin height is 10 mm. For a smaller transverse tube pitch

(S_t = 50 mm), one can see the effect of fin spacing on the heat transfer coefficients is negligible. This result is analogous to that of continuous fin geometry as reported by Rich [9] and Wang et al. [10]. However, for a larger transverse pitch of 84 mm, the heat transfer coefficients decrease with the decrease of fin spacing. This phenomenon may arise from the influence of airflow bypass effect. As is known, the corresponding pressure drop rises with the decrease fin spacing. As a consequence, although the airflow is directed by the tube row, the airflow is prone to flowing the portion where the flow resistance is smaller. For a very large of transverse tube pitch of 84 mm, part of the directed airflow just bypass the tube row and fin without effective contribution to the heat transfer, thereby causing a drop of heat transfer coefficients at smaller fin spacing. This flow bypass phenomenon becomes much where the transverse tube pitch is increased. Therefore, one can see no appreciable change of heat transfer coefficients for S_t = 50 mm.

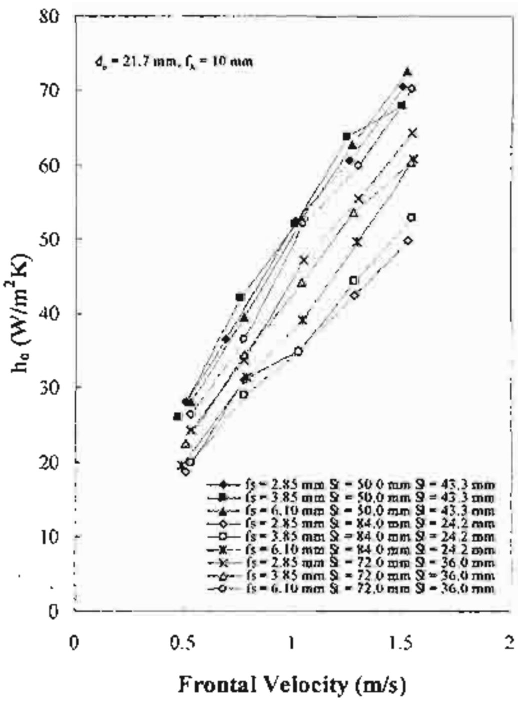

Figure 5. Effect of fin spacing and tube arrangement on the air-side heat transfer coefficient.

The effect of fin height on the airside performance is shown in Figure 6. It is found that the heat transfer coefficients of f_h = 10 mm are higher than that of f_h = 15 mm and the explanation is as follow. In case of f_h = 15 mm, the airflow resistance around fin tube is larger than f_h = 10 mm. Therefore, part of the directed airflow just bypass the tube row without effective contribution to the heat transfer and lower heat transfer coefficient is obtained.

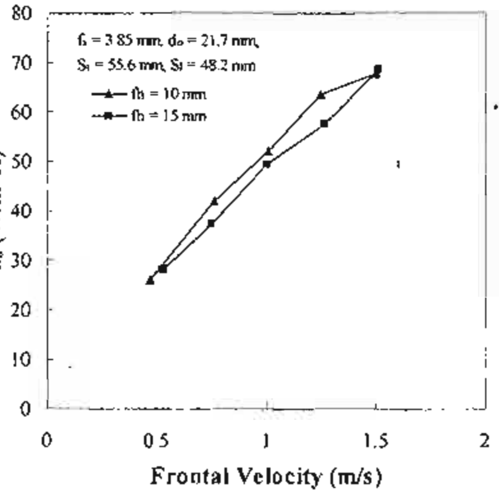

Figure 6. Effect of fin height on air-side heat transfer coefficient.

In this research work, the empirical model for predicting the heat transfer coefficient for various types of the finned tubes is also developed. The empirical model is as follow.

$$Nu = 0.0276\, Re_D^{\,0.8834} \left(\frac{f_t}{f_s}\right)^{-0.1430} \left(\frac{S_l}{S_t}\right)^{1.1866} \left(\frac{S_t}{d_o}\right)^{0.7835} \left(\frac{d_f}{d_o}\right)^{-0.1250} \qquad (20)$$

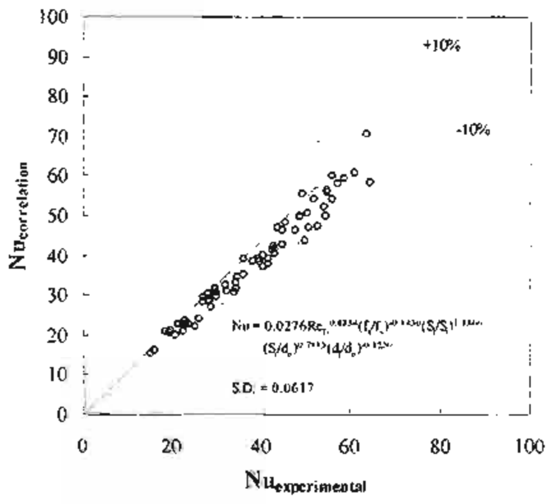

Figure 7. Comparison of Nu from the experimental data and the model.

Figure 7 shows the comparison of Nu from the experimental data and the model. It is found that the model can predict 98.6% of the experimental data with in ±15% error.

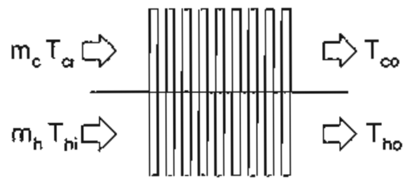

a. Parallel flow arrangement

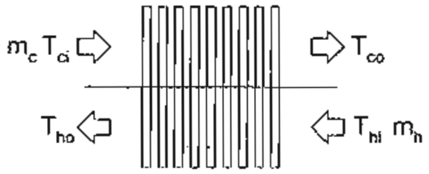

b. Counter flow arrangement

Figure 8. Thermosyphon heat exchanger. Water is working fluid inside.

3. PERFORMANCE OF THERMOSYPHON HEAT EXCHANGER USING CRIMPED SPIRAL FIN

In this part, the crimped spiral fin tube is used as in the air-to-air thermosyphon heat exchanger as shown in Figure 8.The heat transfer rate of the thermosyphon heat exchanger can be calculated as follows:

$$\begin{aligned} Q &= \dot{m}_h Cp_h (T_{hi} - T_{ho}) \\ &= \dot{m}_c Cp_c (T_{co} - T_{ci}) \\ &= (UA)\Delta T_{lmtd} \end{aligned} \quad (21)$$

where UA is the product of overall heat transfer coefficient-area of the thermosyphon heat exchanger. In this research work, the simulation program for calculating the performance of thermosyphon heat exchanger developed by Nuntaphan [4] is selected for evaluating the performance. Figures 9-12 show the simulation results at various conditions.

From the Figures, it is found that the performance of the system depends on the mass flow rate of air and the inlet temperature of hot gas. Note that in this part the mass flow rate of the hot gas equals to the mass flow rate of the cold gas. Moreover, it is also found that the counter flow gives higher performance than the parallel flow.

Figure 9 shows the effect of tube arrangement on the performance of thermosyphon heat exchanger. It is found that triangular arrangement gives the highest heat transfer rate because of its highest air-side heat transfer coefficient.

Figures 10-11 show the effect of fin spacing and fin height on the heat transfer rate. The outputs show the same results as those described in the previous section.

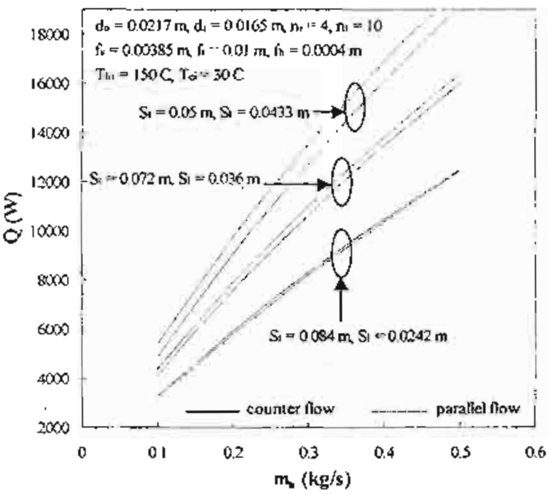

Figure 9. Effect of tube arrangement on the performance of thermosyphon heat exchanger.

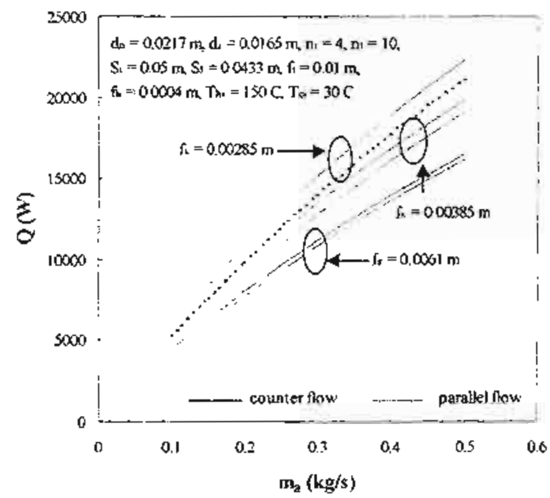

Figure 10. Effect of fin spacing on the performance of thermosyphon heat exchanger.

Figure 12 shows the effect of the inlet hot gas temperature on the heat rate. Higher the temperature difference between the heat source and heat sink results in higher heat transfer rate.

Anyway, the temperature must be controlled not to exceed the critical heat flux condition.

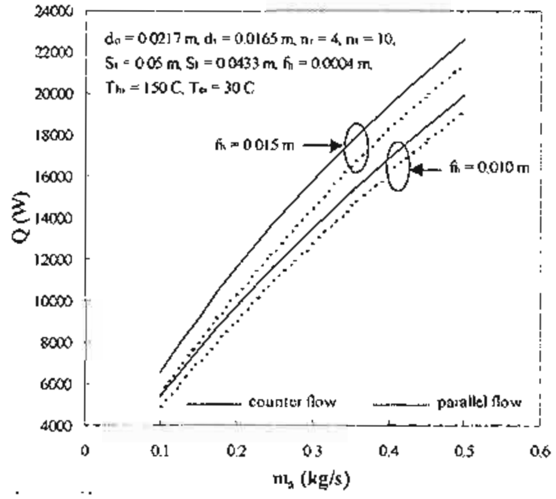

Figure 11. Effect of fin height on the performance of thermosyphon heat exchanger.

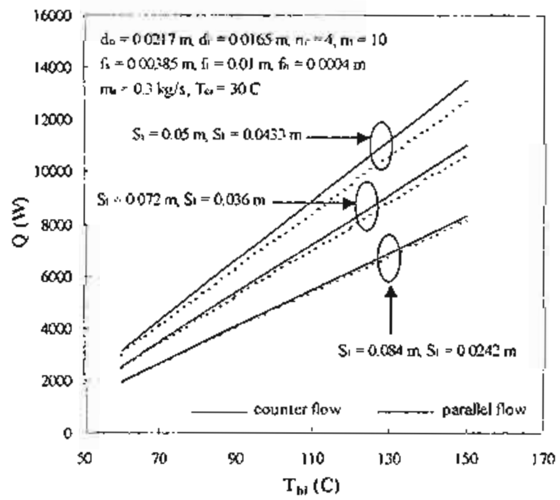

Figure 12. Effect of hot gas temperature on the performance of thermosyphon heat exchanger.

4. CONCLUSION

This work studies the performance of crimped spiral fin at various conditions such as fin spacing, fin height, tube arrangement, mass flow rate and temperature of air. The empirical model for predicting the air-side heat transfer coefficient is also developed and it can predicts the results quite well. This research also studies the performance of thermosyphon heat exchanger using crimped spiral fin. It is found that fin spacing, fin height, tube arrangement, mass flow rate and temperature of air and the direction of air streams give high effect to the heat transfer rate of heat exchanger.

5. ACKNOWLEDGEMENT

The authors gratefully acknowledge the support provided by the Thailand Research Fund for carrying out this study.

NOMENCLATURES

A	Area (m^2)
Cp	Specific heat (J/kgK)
d_f	Outside diameter of finned tube (mm)
d_i	Inside diameter of bare tube (mm)
d_o	Outside diameter of bare tube (mm)
f_h	Fin height (mm)
f_s	Fin Spacing (mm)
f_t	Fin thickness (mm)
h	Heat transfer coefficient (W/m^2K)
k	Thermal conductivity (W/mK)
L	Length (m)
$\dot{m}$	Mass flow rate (kg/s)
n_r	Number of tube rows
n_t	Number of tubes in row
NTU	Number of transfer unit
Nu	Nusselt Number
Pr	Prandtl number
Q	Heat transfer rate (W)
Re_D	Reynolds number
S_t	Transverse pitch (mm)
S_l	Longitudinal pitch (mm)
T	Temperature (°C)
U	Overall heat transfer coefficient (W/m^2K)

Greek symbols

ε	Effectiveness
η	Efficiency

Subscripts

a	Air
b	Bare tube
f	Fin
i	Inlet, tube side
o	Outlet, air side
w	Water

REFERENCES

1. Briggs D.E. and Young E.H., 1963, Convective Heat Transfer and Pressure Drop of Air Flowing Across Triangular Pitch Banks of Finned Tubes, Chemical

Engineering Progress Symposium Series, Vol.59, No. 41, pp.1-10.

2. Robinson K.K. and Briggs D.E., 1966. Pressure Drop of Air Flowing Across Triangular Pitch Banks of Finned Tubes Chemical Engineering Progress Symposium Series, Vol.62, No.64, pp.177-184.
3. Rabas T.J., Eckels P.W. and Sabatino R.A., 1981, The Effect of Fin Density on the Heat Transfer and Pressure Drop Performance of Low Finned Tube Banks, Chemical Engineering Comunications, Vol.10, No.2, pp.127-147.
4. Nuntaphan A., 2000, Performance of Heat Pipe Heat Exchanger Using Binary Working Fluids, Ph.D. Thesis, King Mongkut's University of Technology Thonburi, Thailand
5. ANSI/ARI 410-81, 1981, Standard for Forced Circulation Air Cooling and Air Heating Coils.
6. Gnielinski V., 1976, New Equation for Heat and Mass Transfer in Turbulent Pipe and Channel Flow, Int. Chem. Engng, Vol.16, pp. 359-368.
7. Schmidt Th.E., 1949, Heat Transfer Calculation for Extended Surfaces, Refrigeration Engineering, pp. 351-357.
8. Wang, C.C., Lou, J., Lin, Y.T. and Wei, C.S., 2002, Flow Visualization of Annular and Delta Winlet Vortex Generators in Fin-and-tube Heat Exchanger Application, Int. J. of Heat and Mass Transfer, Vol.45, pp. 3803-3815.
9. Rich, D.G., 1973, ASHRAE Transactions, vol. 79, No.2, pp.137-145.
10. Wang, C.C., Chang, Y.J., Hsieh, Y.J. and Lin, Y.T., 1996, Int. J. of Refrigeration, Vol. 19, pp. 223-230.